Title
The Embryonic Origins of Primate Encephalization

Author
Halley, Andrew Christopher

Publication Date
2016

Peer reviewed|Thesis/dissertation

The Embryonic Origins of Primate Encephalization

By

Andrew Christopher Halley

A dissertation submitted in partial satisfaction of the

requirements for the degree of

Doctor of Philosophy

in

Biological Anthropology

in the

Graduate Division

of the

University of California, Berkeley

Committee in charge:

Professor Terrence W. Deacon
Professor Sabrina Agarwal
Professor Lucia Jacobs

Spring 2016

Abstract

The Embryonic Origins of Primate Encephalization

by

Andrew Christopher Halley

Doctor of Philosophy in Biological Anthropology

University of California, Berkeley

Professor Terrence W. Deacon, Chair

Encephalization is one of the defining characteristics of the primate Order. Unlike other mammalian radiations, primates exhibit exceptionally high relative brain sizes at birth and across prenatal development. This indicates that the shared degree of adult encephalization in primates is the developmental product of changes to early brain or body growth that have never been fully characterized. This dissertation examines brain and body growth relationships across prenatal ontogeny in a wide range of primate and non-primate mammals in order to reexamine the developmental origins of primate relative brain size.

A review of allometric brain/body growth over fetal development shows that primate prenatal encephalization is shared by all primate radiations but not the closest out-groups, and begins during embryonic development. Fetal rates of exponential brain growth acceleration in primates are within the range of eutherian values; species with larger adult brains or isocortical proportions do not exhibit faster fetal brain growth. Neither allometric nor acceleration data support theories proposing faster fetal brain growth in mammals according to physiological or life history variables. Rates of fetal body and visceral organ growth acceleration are exceptionally slow in primates, consistent with slow postnatal body growth rates and life history schedules. Embryonic development is characterized by high brain/body proportions in many non-primate mammals; however, only primates retain this high allometric proportion into later fetal stages of development. This novel feature of primate growth is likely a consequence of slower postcranial body growth, rather than any particular feature of primate brain growth and development.

This study provides developmental evidence that increases in relative brain size at the origin of the primate Order may have been a consequence of body size reduction, possibly as an adaptation to locomotion within an arboreal niche.

For my parents.

TABLE OF CONTENTS

LIST OF FIGURES

LIST OF TABLES

ACKNOWLEDGMENTS

My PhD advisor, Terrence Deacon, has been so central to my intellectual development that it will take me years to sort through what he's taught me. Terry, thank you for your generosity, your encouragement, and your consistent curiosity about how things work. Thanks also to the other members of my dissertation and qualifying exam committees for their unique contributions to my education and research: Sabrina Agarwal, Lucia Jacobs, Bill Hanks, and Alexei Yurchak.

To my family, my first and best teachers – you have never stopped supporting every step of my education, and for that I'll be eternally grateful. To my undergraduate advisors, who taught me the most by treating me as a peer: Mark Shriver, Richard Doyle, Erich Schienke, Sam Richards, Laurie Mulvey. Thanks to Matthew Kirkcaldie and Dalton Hance for entertaining my frequent pleas for feedback and advice, both of which were given in generous portions. Barb Finlay, Leah Krubitzer, Georg Striedter, Chet Sherwood, and Christine Charvet have all improved these efforts with their feedback and inspiration from their own research.

The museum work which generated the embryonic dataset for this dissertation would have been impossible without the help of my many hosts. Eileen Westwig at the American Museum of Natural History warmly accommodated my frequent visits and helped translate obscure biological terms from German. Peter Giere at the Museum für Naturkunde hosted me for a month, teaching me alternatively about comparative embryology and the history of Cold War Berlin. Liz Lockett at the National Museum of Health and Medicine picked me up from the bus station on rainy days and fetched embryos from the warehouse. Blythe Williams, Richard Kay, and Kathleen Smith at Duke University opened their departments' collections to my research despite the summer lull. And Drew Noden at the Cornell Veterinary School was terribly kind – picking me up from the airport, lending me a bicycle and helmet, and offering me full access (and necessary guidance) to their beautiful comparative embryo collection.

I am also deeply indebted to my many gracious friends who opened their homes across the East Coast to me and my microscope, *pro bono*: Andrew O'Reilly, Christian Capasso, John Quinn, Damien Charles-Singh, Erin Welsh, Grover Seestedt, Brittany Harris, Ryan Griffin, Mark Kleeb & DBA, Peter & Erica, Kate Vivenzio, Jamie and McKenzie Jones-Rounds, Brad Martin, and Alyssa Cozzo.

Thanks to the staff of the Anthropology department, and particularly Ned Garrett, Kathleen Van Sickle, and Tom Bottomley – you have been great friends through often-difficult times, and it has made a world of difference.

Thanks to Emily, of course, for everything. We both know the *real* title of this dissertation.

This research was generously supported by funding from the National Science Foundation Graduate Research Fellowship Program, a L.S.B. Leakey Foundation Research Grant, a German Academic Exchange Service (Deutscher Akademischer Austausch Dientst [DAAD]) Short Term Research Grant, a National High Magnetic Field Laboratory (NHMFL) pilot research grant, UC Berkeley Graduate Division Summer Research Grants (2011, 2015), the Robert H. Lowie Grant (2011, 2014, 2015), and the UC Berkeley Institute of Cognitive and Brain Sciences Research Grant (2013).

Andrew C. Halley
CURRICULUM VITAE

Department of Anthropology
University of California, Berkeley
232 Kroeber Hall
Berkeley, CA 94720

Phone: 610 620 4293
Fax: 510 643 8557
email: achalley@berkeley.edu

EDUCATION

2016	PhD	Biological Anthropology	University of California, Berkeley
	Advisor:	Terrence W. Deacon	
2008	BS	Psychology (Neuroscience)	Pennsylvania State University
	Honors	Biological Anthropology	Schreyer Honors College
	Advisor:	Mark D. Shriver	
	Minor	Philosophy	

PAPERS

2015 — A.C. Halley, M. Boretsky, D. Puts, M. Shriver. Self-reported sexual behavioral interests and polymorphisms in the dopamine receptor D4 (DRD4) exon III VNTR in heterosexual young adults. *Archives of Sexual Behavior*. In press, available online.

In Review — A.C. Halley. Prenatal brain/body allometry across mammals. *Brain Behavior & Evolution*, in review.

In Preparation — A.C. Halley, T. W. Deacon. Primate encephalization: Allometric and growth relationships across ontogeny. In *Evolution of Nervous Systems 2nd Edition* (Jon Kaas, editor). In prep.

ABSTRACTS

2016 — A.C. Halley, T.W. Deacon. "The embryonic origins of primate encephalization: allometric and growth analyses." American Association of Physical Anthropologists, 85th Annual Meeting (Atlanta, GA). [Paper]. Aleš Hrdlička Prize.

2015 — A.C. Halley. "Meta-analysis of ontogenetic brain/body allometry across mammals: Implications for primate encephalization and fetal growth theories of relative brain size." J.B. Johnston Club for Evolutionary Neuroscience Annual Meeting (Chicago, IL). [Paper]

2014 — A.C. Halley, T.W. Deacon. "Relative acceleration of embryonic brain

development in mouse and rat compared with other mammalian species." Society for Neuroscience, 44th Annual Meeting (Washington, D.C.). [Poster]

2014 A.C. Halley. "Evolutionary changes in temporal schedules of embryonic neural development across mammalian species." UC Berkeley Annual Neuroscience Conference (Watsonville, CA). [Paper]

2014 A.C. Halley. "Meta-analysis of ontogenetic brain/body growth in primates and non-primate mammals." American Association of Physical Anthropologists, 83rd Annual Meeting (Calgary, Canada). [Poster]

2013 A.C. Halley, M. Boretsky, D. Puts, M. Shriver. "Human sexual behavioral preferences and polymorphisms in the dopamine receptor D4 (DRD4) exon 3 VNTR." International Society for Human Ethology (ISHE) 2014 Summer Institute (Ann Arbor, Michigan). [Poster] 1st Place – Poster Competition.

2012 A.C. Halley. "Politicizing neuroethics: reframing the cognitive enhancement debate." University of Pennsylvania Fellowship in Neuroscience and Society (Philadelphia, Pennsylvania). [Paper]

2008 A.C. Halley. "Human sexual behavior, personality traits, and the dopamine D4 receptor gene." Departmental Lecture (University Park, Pennsylvania). [Paper]

FELLOWSHIPS & AWARDS

2016	Aleš Hrdlička Prize - AAPA 2016 Student Presentations [Paper]
2014 – 2015	UC Berkeley Dean's Normative Time Fellowship
2014	Allen Institute for Brain Science: Course in Molecular Neuroanatomy (Selected Participant). Okinawa, Japan.
2011 – 2014	National Science Foundation Graduate Research Fellowship
2013	First Prize [Poster] International Society for Human Ethology Summer Institute 2013
2012	University of Pennsylvania Center for Neuroscience & Society Fellowship in Neuroscience and Society (Neuroethics)
2003 – 2007	Schreyer Honors College Academic Excellence Scholarship

EXTERNAL RESEARCH SUPPORT

2014 – 2016	The L.S.B. Leakey Foundation; Research Grant
2015	German Academic Exchange Service (Deutscher Akademischer Austausch Dientst [DAAD]) Short Term Research Grant
2013 – 2015	National High Magnetic Field Laboratory (NHMFL)

	Pilot Research Grant
2013	Travel Grant – Course in Molecular Neuroanatomy Okinawa Institute of Science and Technology

RESEARCH SUPPORT – UNIVERSITY OF CALIFORNIA, BERKELEY

2011, 2015	UC Berkeley Graduate Division Summer Research Grant
2011, 2014, 2015	Robert H. Lowie Grant
2014	UC Berkeley Graduate Division Travel Grant
2013	UC Berkeley Institute of Cognitive and Brain Sciences Summer Research Grant

RESEARCH SUPPORT – PENNSYLVANIA STATE UNIVERSITY

2007	Summer Research Scholarship; Schreyer Honors College
2007	Catherine Schultz Rein Trustee Scholarship College of the Liberal Arts, Pennsylvania State University

TEACHING & MENTORSHIP

Graduate Student Instructor (UC Berkeley)

2011; 2015	Human Brain Evolution
2011-13; 2016	Introduction to Biological Anthropology
2015	*Head GSI*
2013	Introduction to Skeletal Biology & Bioarchaeology
2010	Primate Behavioral Ecology

Course Reader *(UC Berkeley)*

2012	The Evolution of Sex Differences
2010	Evolution of the Brain and Language
2009	Evolution and Social Behavior

Guest Lectures *(UC Berkeley)*

2016	Introduction to Biological Anthropology; *Human brain evolution*.
2015	Human Brain Evolution; *Genes and early brain development*.
2015	Psychological Anthropology; *Emotion, rationality, and the brain*.
2015	Introduction to Biological Anthropology; *Evolution of late Homo*.
2014	Evolution of the Human Brain; *Homology & brain development*.
2013	Primate Behavior; *The evolution of primate brain development*.

Teaching Assistant *(Penn State)*

2004	Race and Ethnic Relations

Undergraduate Mentorship

2014 – 2016	Research supervisor, Anjana Krishnamurthy

UC Berkeley - Senior thesis in Integrative Biology

PROFESSIONAL SERVICE

2010 – 2013	Editorial Board Kroeber Anthropological Society Papers University of California, Berkeley

Grants Secured for the Kroeber Anthropological Society (UC Berkeley)

2012	Graduate Assembly Publications Grant
2011, 2012	Townsend Center for the Humanities Working Group Grant

PUBLIC SERVICE

Public Science Lectures

2014	NerdNite – San Francisco CA
2013	Bay Area Wonderfest – San Francisco CA
2013	Science Envoy – Bay Area Wonderfest Public science education workshop

Volunteer Educator – Mind & Brain Night

2014	East Oakland Pride Academy	Oakland, CA
2014	Frick Middle School	Oakland, CA
2012	Oakland Children's Hospital	Oakland, CA
2011	Willard Middle School	Berkeley, CA
2010	Willard Middle School	Berkeley, CA

PROFESSIONAL TRAINING

2013	Course in Molecular Neuroanatomy; Allen Institute for Brain Science / Okinawa Institute of Science and Technology
2013	Bay Area Wonderfest Science Envoy Program Workshop in public science education
2012	Allen Brain Atlas training; Berkeley, CA

CHAPTER 1. Introduction

Allometry in context

Students of brain evolution have long sought to understand how brain size and related measures correspond to something like interspecies "intelligence" [Striedter, 2005]. This enterprise has, perhaps not surprisingly, involved the search for some metric that distinguishes our own species, *Homo sapiens,* from "lower" animals. It has long been recognized that humans are dwarfed in absolute brain size by a range of species, such as elephants and cetaceans. Recognizing this, Darwin described in *Descent of Man* "the large proportion which the size of man's brain bears to his body" as "closely connected with his mental powers." Relative brain size, however, is again size-dependent – the largest brain/body ratios are those of the smallest mammals, many of which surpass the human proportion of ~2.5%. Finally, a number of measures describing residual variation around this interspecies trend – most notably, Jerison's [1976] encephalization quotient (EQ) – offered a measure that not only distinguished our species, but others we believe to be relatively intelligent within the mammalian order.

While encephalization has persisted as a proxy for general intelligence, the tools of comparative neuroscience have largely surpassed such crude mass comparisons. Contemporary methods allow mammalian brains to be compared according to functional, architectural, cellular, genetic, and systems levels undreamed of by Darwin and his contemporaries. Measures of general species intelligence have also been deconstructed into more domain-specific cognitive and behavioral capacities that can be linked to particular neurological features. Given this methodological sophistication, what can measures like allometry and encephalization still tell us about the evolution of primates? Yes, primates are highly encephalized relative to other mammals – but don't we learn more from describing their exceptionally large isocortices, reduced olfactory systems, expanded visual areas specialized for binocularity, additional somatosensory and motor fields for precise movement, and the appearance of granular prefrontal cortex for executive control?

At least since D'Arcy Thompson's *On Growth and Form* [1915], allometry has led a second life within biological sciences – namely, the description of relative growth relationships in comparative ontogeny. Growth is an exceptionally difficult variable to compare across species, as it is nonlinear, proceeds at different rates in different organs in different species, and is regularly agnostic to linear measures of time. This introduces the problem of selecting a meaningful temporal anchor at which comparisons can be made across dynamic processes, such as adulthood, birth, or stages of similar morphology. Amid these difficulties, allometric growth represents a critical tool for understanding phenotypic diversity, linking genetic and epigenetic mechanisms to alterations in growth patterns that generate variation across ontogeny.

This dissertation examines ontogenetic brain/body allometry in primates to better understand how and when during development our Order begins to exhibit exceptionally large brains. My principal focus is not the cognitive or behavioral correlates of encephalization, a body of scholarship that is beyond the scope of summary or critique here [cf. Lefebvre, 2012]. Instead, I focus on trying to unpack the embryonic and fetal growth patterns that produce primate encephalization later in ontogeny. This largely anatomical project attempts to explain an observation first made by Count [1947] nearly seventy years ago, and one which has resisted characterization since that time – why are primates uniquely encephalized across prenatal development?

Primate encephalization and "isocorticalization"

On average, primates exhibit roughly twice the brain size that we should expect for mammals of their body size (i.e. encephalization quotient; [Jerison, 1973]). However, primate radiations are encephalized to different degrees (Fig. 1.1A), and the deviation of brain size in different primate clades from allometric expectations depends on which outgroups we compare them to. For example, prosimian brain size is only marginally higher than mammalian allometric trends, but this comparison lumps together phylogenetically diverse mammals (rather than closely related clades), and is also affected by the inclusion of highly encephalized primates in calculating the mammalian average (note that this Chapter will employ the paraphyletic term "prosimian" rather than the cladistic group "strepsirrhine," as tarsiers follow streprsirrhine trends in encephalization, and evolutionary changes to brain size in the root anthropoid are of central concern). If we compare primates and tree shrews relative to glires (rodents and lagomorphs), the shared degree of encephalization since the LCA to Euarchontoglires becomes more apparent (Fig. 1.1A).

In general, mammalian brain structures scale in highly predictable ways as size increases (concerted evolution; [Stephan et al., 1981]) suggesting developmental regularities to how brains evolve [Finlay & Darlington, 1995]. However, in addition to being highly encephalized, primates are also "isocorticalized" as an Order, exhibiting larger isocortices than would be expected from interbrain allometric trends [Barton & Harvey, 2000](Fig. 1.1B). Whether or not we consider this deviation in isocortical proportions true "mosaic evolution" [Barton & Harvey, 2000; Finlay et al., 2001; Striedter, 2005; Reep et al., 2007], primate neocortex size does appear to be an outlier to allometric trends that describe brain structure scaling according to whole brain size [Stephan et al.,

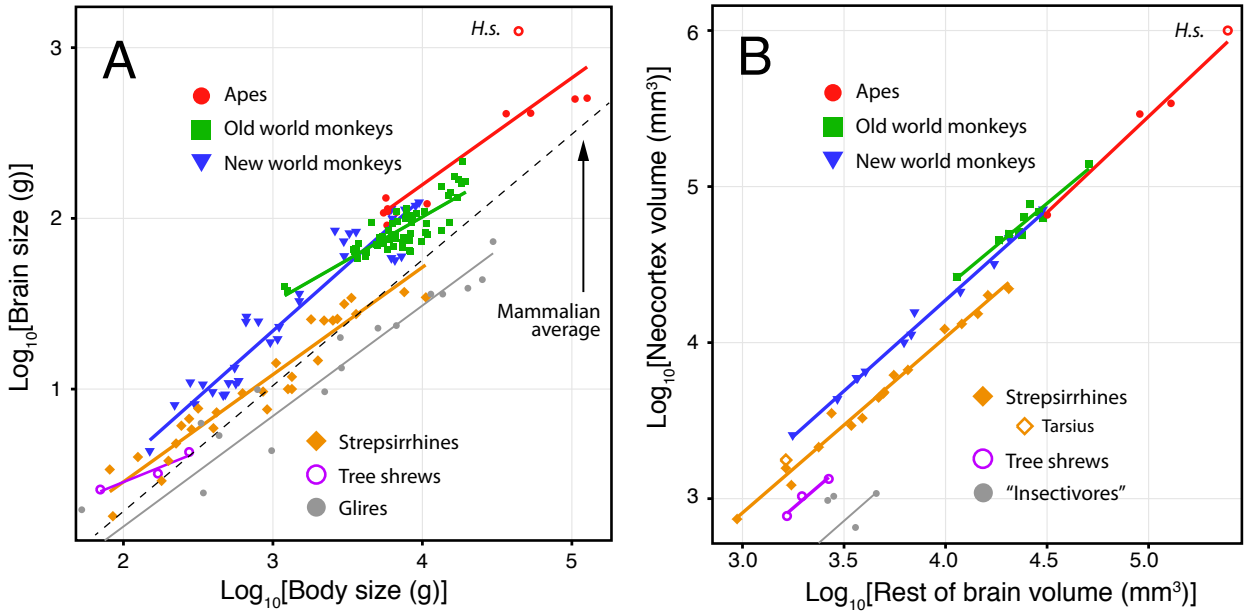

Figure 1.1. Primate encephalization and "isocorticalization". (A) Log-log transformed brain and body size in apes, old and new world monkeys, strepsirrhines, and tree shrews relative to the average mammalian regression for 1174 species (dotted line) [Van Dongen, 1998] and glires (rodents and rabbits; grey line). (B) Log-log transformed isocortex volume relative to the rest of the brain in each major primate radiation, relative to tree shrews and "insectivores" (*Eulopotyphla* and *Afrosoricidae*). Differences in primate encephalization are in part mirrored by relative increases in isocortical proportion. Data from (A) Sacher & Staffeldt [1974], Harvey & Clutton-Brock [1985]; (B) Stephan et al. [1981].

1981].

As in relative brain size, anthropoids have proportionally more isocortex than do prosimians, although all primates appear to exhibit degrees of this allometric shift relative to tree shrews or "insectivores" (a defunct taxon comprising primarily *Eulopotyphla* and *Afrosoricidae*, but a useful comparison point from Stephan et al.'s [1981] dataset on interbrain allometry). In addition to disproportionately large isocortices, primates exhibit a reduction in "limbic structures" (i.e. a variety of di- and telencephalic structures related to olfaction and expressing LAMP protein [Levitt, 1984; Levitt et al., 1997]). This observation has suggested that primates share a shift in early prosomeric boundaries [Puelles & Rubenstein, 2003], simultaneously increasing isocortical founder pools and shrinking LAMP-associated di- and telencephalic structures [Finlay et al., 2001; Reep et al., 2007]. Additional data on allometric growth of brain structures during embryonic development (as applied to birds in Striedter & Charvet [2008]) is sorely needed to clarify the developmental emergence of these adult differences.

Isocortical expansion is an attractive hypothesis to explain trends in primate encephalization for several reasons. Setting aside the overlap in tree shrew and prosimian relative brain size, two grade shifts in encephalization within the primate Order correspond to increases in relative isocortical proportion. First, prosimians are more highly encephalized than the out-group glires, and also have relatively large isocortices relative to "insectivores" (interbrain allometric data is unavailable for glires). Second, haplorhines are both more encephalized and have larger isocortices than strepsirrhines do. Whether humans deviate from the interbrain allometric trends of haplorhines (e.g. exhibit disproportionately large isocortices) depends largely on which brain structures we use as the basis of comparison [Deacon, 1988], but several analyses have found human isocortical proportions to be within the range of expected values [Finlay & Darlington, 1995; Barton & Harvey, 2000], and a preferential expansion should not be assumed *a priori* [Finlay & Workman, 2013].

Primate body growth and life history

While brain/body allometry has often been used as a proxy to describe evolutionary changes in brain size, changes to body size also play a central role [Smaers et al., 2012] and are particularly important for understanding fetal growth patterns. For example, the mammalian variation in rates of body growth during prenatal development is much higher that of brain growth [Sacher & Staffeldt, 1974] and most authors agree that larger brains – or brains with disproportionately large isocortices – are grown over longer *durations*, rather than by accelerating the rate of brain growth [Passingham, 1985; Deacon, 1990].

There are a number of reasons to suspect that as an Order, primate body size has been reduced. First, primates exhibit slow life histories relative to other mammals, exhibiting slow postnatal body growth [Leigh, 2001; Vinicius, 2005], juvenile and adolescent phases of development, and delayed sexual maturity [Charnov & Berrigan, 1993]. Sacher & Staffeldt's [1974] analysis of neonatal brain and body size vs. gestation length also indicates that primates exhibit abnormally slow body growth rates, while primate brain growth rates fall within the range of eutherian variation. Primate prenatal encephalization may reflect an Order-shared reduction in body size to accommodate challenges association with the occupation of an arboreal niche, such as locomotion or the need to carry young [Deacon, 1997].

Prenatal growth and birth timing

While the primary focus of this research is to characterize the origin of primate prenatal encephalization, its concern with prenatal growth rates allows us to test several theories that suggest faster fetal brain growth rates according to physiological and life history variables. These include relative basal metabolic rate [Martin, 1981; 1996], placental morphology [Elliot & Crespi, 2008], and altriciality/precociality [Barton & Capellini, 2011], and are described in more detail throughout the text. Chapter 2 examines these hypotheses according to allometric growth; Chapter 3 examines them according to species differences in rates of brain growth acceleration over time.

Large neonatal datasets on brain size, body size, and gestation length [Sacher & Staffeldt, 1974; Harvey & Clutton-Brock, 1985] have informed theories of altriciality/precociality, brain and body growth rates, and metabolic constraints on prenatal growth. This dissertation work provides interspecies characterization of birth timing relative to ontogenetic brain/body allometric trajectories (Chapter 2) and growth velocity curves (Chapter 3). These comparisons help to contextualize previous authors' observations about neonatal trends – analyses which have used diverse methods and statistical techniques – by showing how systematic differences exist in birth timing according to variables such as litter size.

Embryonic allometry

Comparative embryology has played a central and complicated role in the history of evolutionary theory [Gould, 1977; Richards, 1997], from Haeckel's "biogenetic law" to modern evolutionary developmental ("evo-devo") biology. Throughout this period, embryological research has been primarily qualitative, describing the emergence of species-unique characters during embryonic development and differences in the timing of developmental events (e.g. Butler & Juurlink, 1987). One of the most valuable resources emerging from this tradition has been the development of embryonic staging techniques (e.g. Carnegie Staging [cf. O'Rahilly & Müller, 2006]). Staging aligns embryos at similar developmental stages rather than according to age post conception, which is highly variable between and within species, and is often unknown in embryos available for study.

However, stages are generally applied to the whole embryo and are defined by developmental markers in different tissues over embryogenesis (e.g. neurulation during Carnegie Stages 8-9, pharyngeal arch formation during CS 10-12, upper limb digit formation in later stages). This limits their utility in characterizing species' differences in the timing of tissue growth and development (i.e. heterochrony [Gould, 1977]) which generate adult phenotypes later in ontogeny. Recent efforts to model neurodevelopmental events in different mammalian species [Workman et al., 2013] are a promising direction for comparative ontogeny, and similar efforts to describe schedules of tissue development elsewhere in the developing embryo might provide the basis for understanding how exactly evolution alters embryonic development to generate new forms.

Relatively little quantitative data (e.g. relative volumetric growth of organs and tissues) has been available to measure the emergence of species-unique phenotypes during embryonic development [but see e.g. Goedbloed, 1976; Striedter & Charvet, 2008]. In an effort to expand these efforts, my dissertation research has included the generation of a dataset of over 150 whole mammalian embryos digitized by microscopic photography and analyzed according to principles

of volumetric reconstruction (presented in Chapter 4). The current project utilizes this dataset to study the embryonic emergence of primate encephalization from brain and body growth patterns; however, this database should provide a resource for the further quantification of tissue and organ growth over embryonic development, and can be applied to many questions of relative growth in the future.

Dissertation structure

The research into primate encephalization is presented here as three complementary chapters. In Chapter 2, a comprehensive review of ontogenetic brain/body allometry is presented in a large sample of diverse mammalian species. This chapter aims to characterize the phylogenetic distribution and characteristics of primate prenatal brain/body proportions first described by Count [1947] and reexamined using a much larger dataset here. Chapter 3 examines fetal brain, body, and visceral organ growth acceleration in a smaller sample of species for which data of known post-conception age are available in the literature. Chapter 4 presents allometric data on brain and body growth over embryonic development collected and analyzed over the course of my dissertation research. Finally, Chapter 5 summarizes the findings of this study in relation to primate evolution and patterns of encephalization.

References

Barton RA, Capellini I (2011): Maternal investment, life histories and brain growth in mammals. Proc Natl Acad Sci USA 108:6169–6174.

Barton RA, Harvey PH (2000): Mosaic evolution of brain structure in mammals. Nature 405:1055–1058.

Butler H, Juurlink BHJ (1987): An Atlas for Staging Mammalian and Chick Embryos. Boca Raton, CRC Press.

Charnov EL, Berrigan D (1993): Why do female primates have such long lifespans and so few babies? or Life in the slow lane. Evol Anthrol 1:191–194.

Count EW (1947): Brain and body weight in man: their antecedents in growth and evolution. Ann N Y Acad Sci 46:993–1122.

Deacon TW (1988): Human brain evolution: II. Embryology and brain allometry. In Jerison HJ, Jerison I (eds): Intelligence and Evolutionary Biology. Berlin, Springer, pp 383–415.

Deacon TW (1990): Problems of ontogeny and phylogeny in brain-size evolution. Int J Primatol 11:237–282.

Deacon TW (1997): The Symbolic Species. New York, WW Norton & Co.

Elliot MG, Crespi BJ (2008): Placental invasiveness and brain-body allometry in eutherian mam-

mals. J Evol Biol 21:1763–1778.

Finlay BL, Darlington RB (1995): Linked regularities in the development and evolution of mammalian brains. Science 268:1578–1584.

Finlay BL, Workman AD (2013): Human exceptionalism. Trends Cog Sci 17:199–201.

Finlay BL, Darlington RB, Nicastro N (2001): Developmental structure in brain evolution. Behav Brain Sci 24:263–308.

Goedbloed JF (1976): Embryonic and postnatal growth of rat and mouse. IV. Prenatal growth of organs and tissues: age determination, and general growth pattern. Acta Anat 95:8–33.

Gould SJ (1977): Ontogeny and Phylogeny. Cambridge, Harvard University Press.

Harvey PH, Clutton-Brock TH (1985): Life history variation in primates. Evolution 39:559–581.

Jerison HJ (1973): Evolution of the Brain and Intelligence. New York, Academic Press.

Lefebvre L (2012): Primate encephalization. Prog Brain Res 195:393–412.

Leigh SR (2001): Evolution of human growth. Evol Anthropol 10:223–236.

Levitt P (1984): A monoclonal antibody to limbic system neurons. Science 223:229–301.

Levitt P, Barbe MF, Eagleson KL (1997): Patterning and specification of the cerebral cortex. Annu Rev Neurosci 20:1–24.

Martin RD (1981): Relative brain size and basal metabolic rate in terrestrial vertebrates. Nature 293:57–60.

Martin RD (1996): Scaling of the mammalian brain: the maternal energy hypothesis. Physiology 11:149–156.

O'Rahilly RR, Müller F (2006): The Embryonic Human Brain: An Atlas Of Developmental Stages. Hoboken, Wiley.

Passingham RE (1985) Rates of brain development in mammals including man. Brain Behav Evol 26:167–175.

Puelles L, Rubenstein LR (2003): Forebrain gene expression domains and the evolving prosomeric model. Trends Neurosci 26: 469–476.

Reep RL, Finlay BL, Darlington RB (2007): The limbic system in mammalian evolution. Brain Behav Evol 70:57–70.

Richards RJ (1992): The Meaning of Evolution: The Morphological Construction and Ideological Reconstruction of Darwin's Theory. Chicago, University of Chicago Press.

Sacher GA, Staffeldt EF (1974): Relation of gestation time to brain weight for placental mammals: implications for the theory of vertebrate growth. Am Nat 108:593–615.

Smaers JB, Dechmann DKN, Goswami A, Soligo C, Safi K (2012): Comparative analyses of evolutionary rates reveal different pathways to encephalization in bats, carnivorans, and primates. Proc Natl Acad Sci USA 109:18006–18011.

Stephan H, Frahm H, Baron G (1981): New and revised data on volumes of brain structures in insectivores and primates. Folia Primatol 35:1–29.

Striedter GF (2005): Principles of Brain Evolution. Sunderland, Sinauer Associates.

Striedter GF, Charvet CJ (2008): Developmental origins of species differences in telencephalon and tectum size: morphometric comparisons between a parakeet (Melopsittacus undulates) and a quail (Colinus virgianus). J Comp Neurol 507:1663–1675.

Thompson DW (1915): On Growth and Form. Cambridge, Cambridge University Press.

Vinicius L (2005): Human encephalization and developmental timing. J Hum Evol 49:762–776.

CHAPTER 2. Prenatal brain/body allometry in mammals

Abstract

Variation in relative brain size among adult mammals is produced by different patterns of brain and body growth across ontogeny. Fetal development plays a central role in generating this diversity, and aspects of prenatal physiology such as maternal relative metabolic rate, altriciality, and placental morphology have been proposed to explain allometric differences in neonates and adults. Primates are also uniquely encephalized across fetal development, but it remains unclear when this pattern emerges during development and whether it is common to all primate radiations. To reexamine these questions across a wider range of mammalian radiations, data on the primarily fetal rapid growth phase (RGP) of ontogenetic brain/body allometry was compiled for diverse primate (n_p=12) and non-primate (n_{np}=16) mammalian species, and was complemented by later ontogenetic data in sixteen additional species (n_p=9; n_{np}=7) as well as neonatal proportions in a much larger sample (n_p=38; n_{np}=83). Relative BMR, litter size, altriciality, and placental morphology fail to predict RGP slopes as would be expected if physiological and life history variables constrained fetal brain growth, but are associated with differences in birth timing along allometric trajectories. Prenatal encephalization is shared by all primate radiations, is unique to the primate Order, and is characterized by (1) a robust change in early embryonic brain/body proportions, and (2) higher average RGP allometric slopes due slower fetal body growth. While high slopes are observed in several non-primate species, primates alone exhibit an intercept shift at 1g body size. This suggests that primate prenatal encephalization is a consequence of early changes to embryonic neural and somatic tissue growth in primates that remain poorly understood.

Introduction

Theories of brain evolution have long aimed to link behavioral and cognitive complexity in animals to relative brain size and its allometrically corrected residual, the encephalization quotient (EQ)[Jerison, 1973]. However, the role of encephalization in predicting species' "intelligence" remains a matter of debate, and different aspects of brain variation and morphology, such as gross size [MacLean et al., 2014], isocortical proportions [Stephan & Andy, 1970], and neuron number [Herculano-Houzel et al., 2007] have been proposed as alternatives. Nevertheless, encephalization remains a central theoretical tool in evolutionary neuroscience – not least of all because it marks our own species, and several species we consider highly intelligent (e.g. non-human primates, odontocete cetaceans), as exceptional. Less is known about how brain and body growth during prenatal ontogeny contribute to patterns of encephalization later in life.

Primates are encephalized relative to other mammalian clades, exhibiting approximately twice the expected brain size on average [van Dongen, 1998]. However, unlike other highly encephalized species, primates exhibit exceptionally high relative brain size across every observed stage of prenatal development [Count, 1947; Holt et al., 1975; Sacher, 1982; Martin, 1983; Deacon, 1990]. This unique allometric growth pattern is robust, giving primates fetal brain/body

ratios approximately twice those of non-primates, and is conserved across species despite differences in encephalization between primate radiations (e.g. strepsirrhines vs. haplorhines)[Sacher, 1982]. Unfortunately, most aspects of this major shift in fetal brain/body proportions – e.g. when it emerges during ontogeny, and what causes it – remain poorly understood, despite the fact that increased relative brain size is one of the defining characteristics of the primate Order.

Comparing brain/body growth patterns across ontogeny can also help to answer a related question: why are some species more encephalized at birth than others? Higher neonatal brain/body proportions are often interpreted as consequences of faster brain growth *in utero*, and have been linked to a range of physiological and life history variables (see below). However, species become more or less encephalized by evolutionary changes to both brain and body size [Smaers et al., 2012] and fetal body growth rates are more variable across species than brain growth rates are [Sacher & Staffeldt, 1974]. Birth timing may also be variable along allometric growth trajectories, just as it is variable relative to whole brain growth [Dobbing & Sands, 1979] and neurodevelopment event sequences [Workman et al., 2013]. Comparing species' brain/body growth during fetal development can help to shed light on the variation observed in neonatal mammals, and allow us to test theories that predict faster fetal brain growth in certain species.

Sources of primate prenatal encephalization. Three phases of logarithmic brain/body growth can be distinguished across ontogeny in any given species (fig. 2.1A). First, a period of rapid brain and body growth with a high allometric slope is observed which originates early in embryonic development; second, data enter a deceleration phase as slope decreases; and third, a slow growth phase exhibits a shallow slope and ends in adult proportions. The timing of birth during this trajectory is variable across species, and may occur during either of the first two phases (fig. 2.1A). For this reason we here adopt Renfree et al.'s [1982] term "rapid growth phase" (RGP) instead of "fetal" or "prenatal" phase for the initial period of high allometric slope.

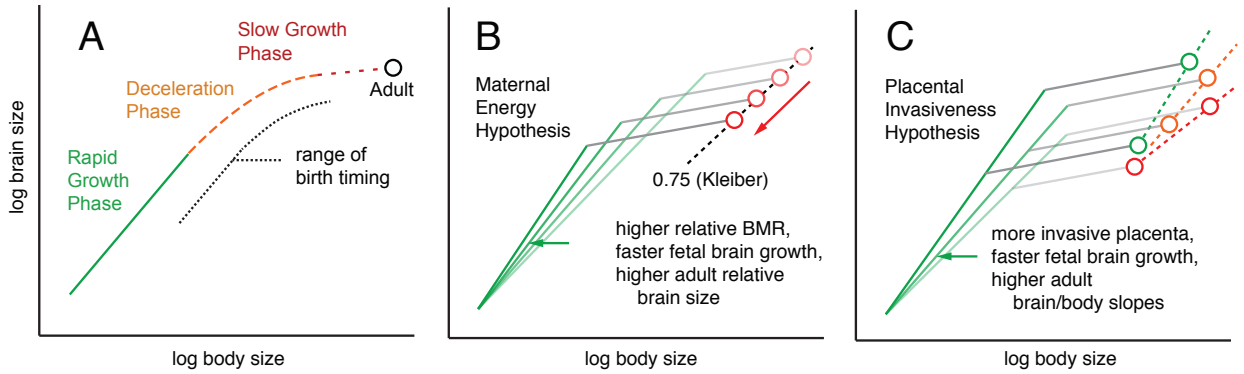

Figure 2.1. Basic models of ontogenetic allometry. Allometric brain/body growth across ontogeny exhibits a characteristic shape across all species available to study, described here in terms of three phases. (A) First, a largely prenatal rapid growth phase (RGP) exhibits a high allometric slope as both brain and body grow exponentially. Second, a deceleration phase reflects the slowing of brain growth relative to body growth. Third, a slow growth phase characterized by minimal brain growth ends in adult brain/body proportions. (B) Martin's [1996] maternal energy hypothesis predicts that smaller species with a relatively higher maternal basal metabolic rate (BMR) exhibit faster prenatal brain growth; this should increase RGP slope in smaller species, producing higher relative brain sizes in adults. (C) Elliott & Crespi [2008] suggest that more invasive forms of placenta are responsible for faster prenatal brain growth; this should increase RGP slope in species with more invasive forms of placenta, producing higher neonatal and adult allometric slopes in those species.

Most authors agree that primates exhibit a shared increase in relative brain size across fetal development when compared with other mammals [Count, 1947; Holt et al., 1975, 1981; Gould, 1977; Sacher, 1982; Martin, 1983; Deacon, 1990, 1997; but see Vinicius, 2005] – an increase observable at birth [Sacher, 1982; Martin, 1983] – but the evolutionary and developmental origins of this allometric effect remain obscure. Two features of the primate RGP have been highlighted in earlier studies, and have generated different theories to explain them. I will here introduce these features as provisional hypotheses based on previous studies, and will revisit them below in light of the larger sample of species analyzed here.

First, primates appear to exhibit an intercept shift in RGP regression models. The intercept of log-log RGP regression models has a precise interpretation: predicted brain size at 1g body size. Despite differences in the length of the embryonic period [Butler & Juurlink, 1987], most species transition from embryonic to fetal development (marked by the onset of marrow formation in the humerus [Streeter, 1949]) between 0.3g and 3g body size [unpublished observations], or approximately -0.5 and 0.5 in log-log plots. This makes the RGP intercept an approximate measure of relative brain size at the end of embryonic and beginning of fetal development. Sacher [1982] proposed that embryonic somatic tissue was reduced by half in the last common ancestor to primates in order to lower maternal investment, allow longer gestation, and produce more precocial young. This was based on Leuteneggar's [1973, 1979] observation that haplorhines have litter weights that are approximately double those of strepsirrhines, while small non-primate mammals (analyzed under the earlier taxon "insectivores") are intermediate.

Second, primates appear to have relatively high RGP slopes (approximately isometric) compared to negative allometric slopes common in other mammals. Slope changes can be introduced by changes to the fetal growth rates of either brain or body [Striedter, 2005]. Most evidence suggests that high primate RGP slopes are a consequence of slow fetal body growth [Holt et al., 1981; Martin, 1983] as shown in studies of comparative growth modeling [e.g. Payne & Wheeler, 1968; Sacher & Staffeldt, 1974; see below]. Primates also have slow postnatal rates of somatic growth [Charnov & Berrigan, 1993; Leigh, 2001; Vinicius, 2005] as part of their slow life histories, and have recently been shown to exhibit half the expected total energy expenditure (TEE) for mammals of their size [Pontzer et al., 2014]. Holt et al. [1981] proposed that slower fetal somatic growth in primates (producing higher RGP slopes) is a strategy to funnel limited fetal resources to brain growth.

Theories of accelerated fetal brain growth. Do species differ in rates of fetal brain growth according to physiological or life history variables? This is a difficult question to answer, as whole brain growth follows a sigmoid curve over ontogeny [Laird, 1967], species are born along different portions of this curve [Dobbing & Sands, 1979], and growth "rate" (i.e. velocity in grams per day) changes as brains increase in size. Most evidence for differential rates of fetal brain growth has come from studies examining large datasets of neonatal brain size, body size, and gestation length [e.g. Sacher & Staffeldt, 1974; Harvey & Clutton-Brock, 1985], but methods differ considerably across studies and often integrate different combinations of variables into multiple regression models. This study will focus on several theories that implicate faster prenatal brain growth as the proximate cause of later mammalian variation in neonatal or adult brain/body proportions, as these theories make testable predictions about the slope of RGP data over prenatal ontogeny.

First, the maternal energy hypothesis [Martin, 1996] argues that maternal basal metabolic

rate (BMR), relative to body size, constrains the rate of fetal brain growth. Accordingly, smaller species with relatively higher BMR (i.e. Kleiber's law)[Kleiber, 1961] have relatively larger brains because of faster brain growth in utero (Fig. 2.1B). Support for this argument comes from a shared 0.75 exponent in (a) adult mammalian brain/body allometry, and (b) maternal BMR ($\propto$ mass$^{3/4}$) vs. neonatal brain size, correcting for altriciality [Martin, 1981]. Second, Elliot & Crespi [2008] proposed that more invasive placental morphologies increase the efficiency of fatty acid transfer, promoting faster rates of fetal brain growth. Allometric evidence comes from higher neonatal and adult brain/body slopes in species with more invasive placenta (adult slopes diagrammed in fig. 2.1C). Finally, several life history studies have suggested faster fetal brain growth in precocial species relative to altricial species following correction for different allometric and life history variables, such as adult and neonatal body size, litter size, and gestation duration [cf. Pagel & Harvey, 1988; Barton & Capellini, 2011].

This paper reexamines ontogenetic brain/body allometry in a larger sample of primate and non-primate mammalian species than has previously been assembled from the literature (to my knowledge, Martin's [1983] examination of 6 primate and 10 non-primate species was the largest; this study collects fetal data in 12 primates and 16 non-primate mammals, and incorporates later postnatal data in an additional 9 and 7 species, respectively). Allometric growth data is an important complement to studies of brain and body size vs. post-conception age [e.g. Cheek, 1975; Widdowson, 1981] because it is more widely available in a larger number of species. In addition, the theories of fetal brain growth discussed above are based on differences in neonatal brain/body allometry (not fetal brain growth directly), and so their predictions can be tested against fetal allometric data. This comparative dataset is used here to revisit two central questions in the evolution of relative brain size. (1) When do primates become more encephalized during prenatal development, what causes this change in allometric growth, and is it shared across the primate Order? (2) Do prenatal allometric growth patterns support theories describing faster fetal brain growth according to physiological or life history variables? RGP regression slopes are used to test whether relative BMR, placental invasiveness, developmental state at birth (i.e. altriciality) or litter size preferentially affect fetal brain growth rates.

Materials & Methods

Data on ontogenetic brain/body size across a range of primate and non-primate mammalian species was collected from literature sources. Both individual and averaged data is included. When only figures were available for species data unavailable elsewhere, data points were reconstructed digitally from figures using image analysis software (Photoshop CC) by measuring x- and y-axis distances of individual data points. When available, original regression model parameters were used in statistical tests; models of reconstructed data were used to plot data.

RGP data was assembled in 28 mammalian species (n=1091) for which it was unambiguously available; this data was utilized to produce RGP regression models of both individual primate and non-primate species, as well as average models for both groups. Cutoffs for RGP dataset inclusion near the deceleration phase were determined by visual inspection of entire ontogenetic plots. Twelve primate species are represented (n=285), including five new world monkeys (*Callithrix jacchus, Sapajus apella, Aotus azarae, Saimiri boliviensis, Saimiri sciureus*), six old world monkeys (*Trachypithecus cristatus, Macaca mulatta, Macaca nemestrina, Macaca radiata, Macaca fascicularis, Papio* ssp.), and one hominoid (*Homo sapiens*). *Papio* species

are combined, as RGP data overlap. Sixteen non-primate mammalian species are represented (n=627), including three rodents (*Mus musculus, Rattus rattus, Mesocricetus auratus*), one lagomorph (*Oryctolagus cuniculus*), one bat (*Artibeus jamaicensis*), two carnivores (*Felis catus, Canis familiaris*), five ungulates (*Sus scrofa, Ovis aries, Bos taurus, Camelus dromedarius, Bubalus bubalis*), one odontocete cetacean (*Stenella coeruleoalba*), and three marsupials (*Macropus giganteus, Macropus eugenii, Monodelphis domestica*). Data for miniature and domestic pig are combined, as RGP data in both breeds overlap.

The RGP dataset was then supplemented with loess models (span=1.2) of both deceleration and slow growth phase data in (a) 22/28 species listed above for which data was available from later phases, and (b) an additional 16 species for which unambiguous RGP data was unavailable, but later data exists (fig. 2.2). In the former case, the largest data point in RGP data was duplicated as the first data point in the later loess series to provide visual continuity between the models. Primate species added (n=9) include the new world monkey *Ateles geoffroyi,* old world monkeys *Trachypithecus obscurus, Papio hamadryas, Papio anubis,* and *Papio papio,* and hominoids *Gorilla gorilla, Hylobates lar, Pan troglodytes,* and *Pongo* ssp. As above, *Papio* data are combined. Non-primate mammals added (n=7) include the rodent *Cavia porcellus*, xenarthrans *Dasypus novemcinctus* and *Bradypus* sp., the ungulate *Equus ferus caballus*, odontocete cetaceans *Phocoena phocoena* and *Tursiops truncatus*, and the proboscid *Loxodonta africanus*. Data for chicken (*Gallus gallus domesticus*) are also included for comparison. The total sample here includes 21 primate (n=1005) and 23 non-primate (n=1637) species.

Data on neonatal and adult brain/body proportions [Sacher & Staffeldt, 1974; Harvey & Clutton-Brock, 1985] were superimposed on regression models from the RGP (fig. 2.3). This dataset includes 38 primate species (5 apes, 12 new world monkeys, 11 old world monkeys, and 10 prosimians; n=76) and 82 non-primate (n=164) mammals. For each species, a single line connects neonatal and adult data points; the slopes of these lines are used as proxies for the relative position of birth along ontogenetic trajectories, with steeper slopes representing earlier parturition on average.

Finally, in primate (n=34) and non-primate species (n=77) for which gestation length is available, cube root transformed neonatal data are used as proxies of fetal growth rates [cf. Sacher & Staffeldt, 1974] to examine how brain and body rates differ in primates and non-primate mammals (fig. 2.4).

Statistical Models & Tests. Regression analysis of the RGP poses a number of unique statistical problems. RGP data are of limited availability in many species, and are often unevenly distributed – late fetal data predominates, while embryonic data is rare. These extremes are also most likely to exhibit nonlinear properties, as embryonic relative brain size deviates from linearity considerably [c.f. Wingert, 1969; Goedbloed, 1976; personal observations], and the onset of deceleration is often difficult to determine without earlier data for comparison. This is especially important because allometric analyses are sensitive to high and low values [Gould, 1975; Deacon, 1990; Striedter, 2005]. Finally, literature data are regularly reported as averages (rather than individual data points); this collapses natural variation, making it difficult to compare linear models even when data is readily available across a wide range of body sizes.

Ordinary least squares (OLS) regression models of log-transformed RGP brain and body size (g) were fit to 28 species (Table 1), as well as to the aggregate datasets for primates and non-primates (dotted lines in figs. 2.2, 2.3). OLS regression is used here to allow comparison

with previous research; reduced major axis regression models are included in Supplementary Information. Two primate species (*Macaca radiata* and *Saimiri sciureus*) were excluded in statistical tests, as RGP data in these species is clustered and produces biologically unlikely estimates (e.g. 0.7% and 52% brain/body ratios at the intercept, respectively); they are retained in Fig. 2.2A to demonstrate their alignment with other primate RGP trajectories. In order to test whether primate RGP models differ from those of non-primate species in the remaining sample of 10 primate and 16 non-primate species, an analysis of covariance (ANCOVA) was performed predicting brain size from body size, including dummy-coded primate/non-primate and species as covariates. However, because RGP models include averaged data (i.e. violate the homoscedasticity assumption of ANCOVA) and sample sizes differ across species, more conservative independent-samples t-tests were performed comparing slope and intercept between primate and non-primate regression models.

A simple sorting test was used to determine how well RGP models for primate and non-primate species fit to neonatal proportions. As neonatal values are prevalent during the deceleration phase (i.e. when trajectories curve to the right), horizontal displacement (rather than vertical or perpendicular distance) of neonatal values from the primate and non-primate models was calculated by measuring the distance between observed and predicted body size at given brain sizes. Absolute values of horizontal distance produced by each model were used to sort species according to their most proximate model (i.e. primate vs. non-primate).

Relative BMR (cal/kg/day) was estimated from a form of Kleiber's [1947] equation: cal/day = $70*mass^{0.75}$. Litter size averages, developmental state at birth (eyes open = precocial; eyes closed = altricial), placental morphology (epitheliochorial, endotheliochorial, hemochorial), and gestation length were drawn from previous studies [Sacher & Staffeldt, 1974; Harvey & Clutton-Brock, 1985]. Degree of placental invasiveness and developmental state were dummy coded for inclusion in regression models.

Linear regression models were performed predicting RGP slope from relative BMR, developmental state at birth, litter size, and placental morphology. Relative BMR and litter size tests were performed within primates, within non-primate mammals, and in the combined samples. Placental type and developmental state tests were performed in non-primate mammals and the combined sample; differences within primates cannot be tested without RGP data for epitheliochorial strepsirrhines, which is unavailable, and all sample primates are precocial at birth. Phylogenetic generalized least squares (PGLS) models of these tests were also performed and are included in Supplementary Information; the results of this study are unchanged by phylogenetic correction.

Slope between neonatal and adult brain/body values were calculated in log-log coordinates to obtain a relative measure of parturition along the entire trajectory. OLS linear regression models were performed to determine whether relative BMR, developmental state at birth, litter size, or placental invasiveness predict neonatal-adult slope. Marsupials were omitted from all neonatal-adult slope analyses. Finally, a multiple regression model incorporated litter size, BMR, and placental invasiveness to predict neonatal-adult slope. Each test was performed on the total sample, as well as the primate and non-primate subsamples.

Results

RGP Analysis. OLS regression models of RGP data in all species are presented in Table 2.1

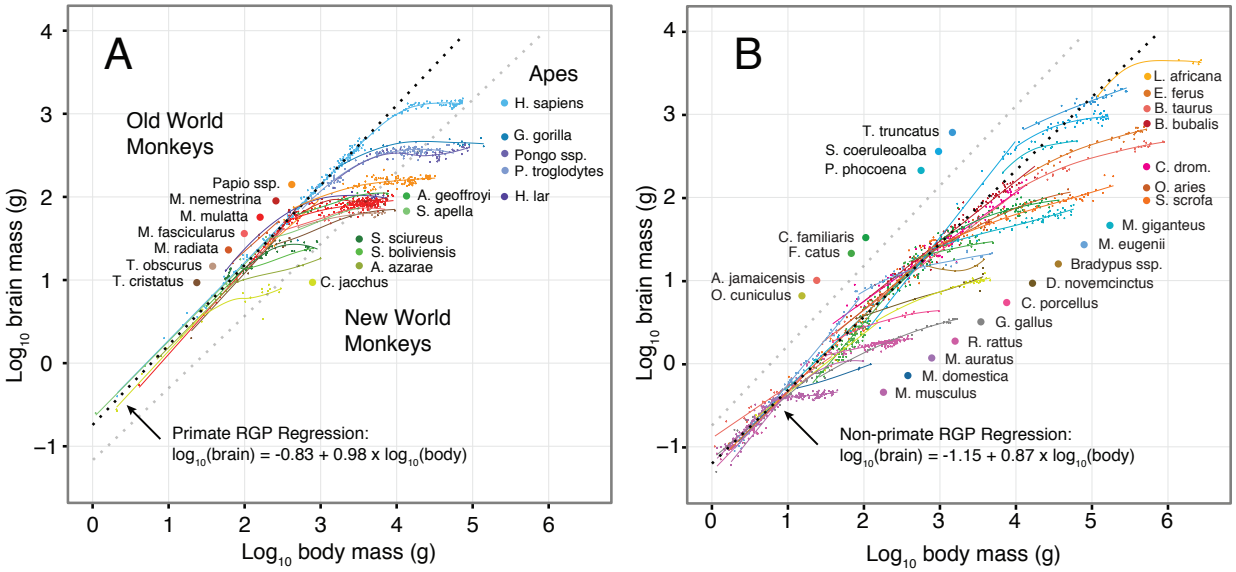

Figure 2.2. Ontogenetic allometry plots. Partial or complete ontogenetic allometric plots in (A) 21 primate species and (B) 23 non-primate mammals (including two marsupials) as well as one bird. RGP regression models are fit to 12 primate and 16 non-primate mammals for which data was available; dotted lines indicate average RGP regression parameter models from species models in primates and nonprimates ($Total_{species}$ in Table 2.1). Regression equations are listed for each average model. Individual species RGP ordinary least squares (OLS) regression parameters are listed in Table 1. RGP data are supplemented with later ontogenetic trajectories in an additional 9 primate and 7 non-primate species. On average, primates exhibit a higher intercept (-0.83 vs. -1.15) than non-primates, indicating early alterations to relative brain size during embryogenesis.

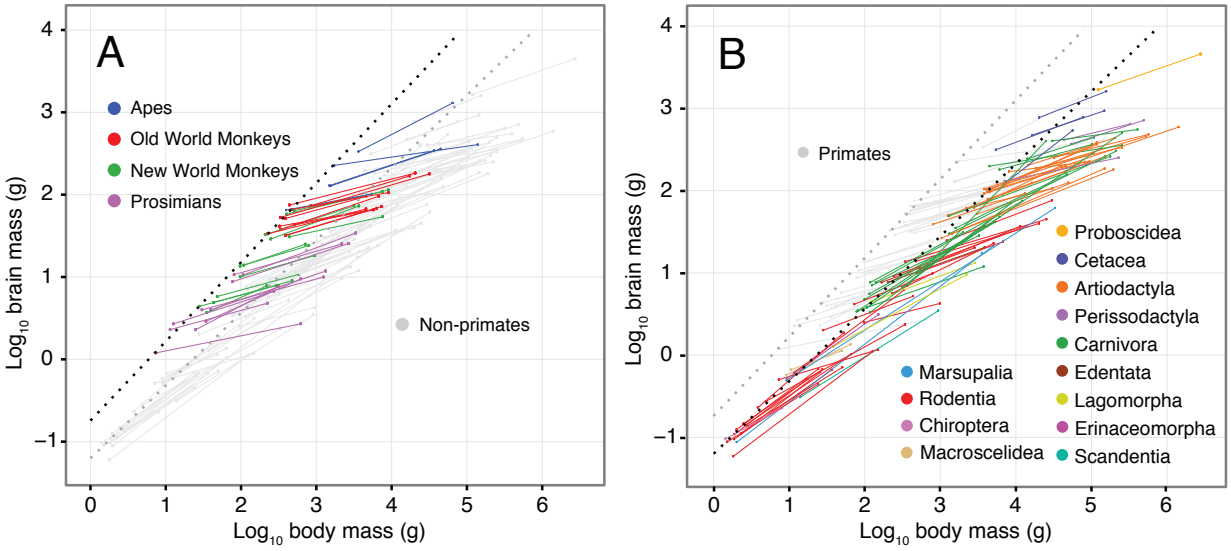

Figure 2.3. Neonatal-adult slopes compared with RGP average regression models. Neonatal and adult brain/body proportions relative to rapid growth phase (RGP) average regression models in (A) 38 primate and (B) 82 non-primate mammalian species. A single line connects neonatal and adult values for each species; higher slopes indicate species born earlier along ontogenetic trajectories (e.g. rodents and marsupials). Primate neonatal values for this expanded dataset, including those of prosimians, conform well to the primate average RGP slope produced from twelve species (see Methods), while the only species of tree shrew - *Tupaia glis* - conforms to the non-primate trend.

(RMA model results are presented in Supplementary Information). Two average models for primate and non-primate subsamples describe (1) OLS regression models fit through all of each subsample data points ("$Total_{indiv}$"), and (2) average slope and intercept values from each species' individual model ("$Total_{species}$").

An ANCOVA (between-model factors: dummy-coded primate/non-primate [pnp] and species; covariate: logbody) found main effects of pnp ($F[1, 884]=46{,}887.0$, $p<0.001$) and the interaction term pnp*logbody ($F[1, 884]=191.2$, $p<0.001$). Independent samples t-tests comparing species-level regression model coefficients found that differences in RGP slopes between primate (0.976; n=10) and non-primate (0.874; n=16) subsamples are not significant ($t=-1.83$; $p=0.080$); the difference in average RGP intercept between primate (-0.825; n=10) and non-primate (-1.147; n=16) subsamples was significant ($t=-2.59$; $p=0.016$), indicating a predicted brain/body ratio of 14.9% and 7.1% at 1g body size in primates and non-primates, respectively.

Sorting neonatal values for the larger dataset (fig. 2.3) according to the most proximate model correctly categorized 119 mammalian species as primates or non-primates; one odontocete cetacean (*Stenella attenuata graffmani*) was closer to the primate model.

Relative BMR (cal/kg/day) failed to predict RGP slope in the total sample ($t=0.356$, $p=0.725$; n=26), the non-primate subsample ($t=0.520$, $p=0.611$; n=16), and the primate subsample ($t=-0.105$, $p=0.919$; n=10). Litter size failed to predict RGP slope in the total sample ($t=-0.262$, $p=0.795$; n=26), the non-primate subsample ($t=1.132$, $p=0.277$; n=16), and the primate subsample ($t=0.099$, $p=0.924$; n=10). Developmental state at birth failed to predict RGP slope in the total sample ($t=-0.067$; $p= 0.947$; n=26) or the non-primate subsample ($t=-1.09$; $p=0.294$; n=10). No predictor was significant when marsupials were excluded. Finally, placental type failed to predict RGP slope in the total eutherian sample ($t=1.994$, $p=0.059$; n=23) and the non-primate subsample ($t=0.792$, $p=0.445$; n=13). No test was significant when phylogenetic generalized least squares (PGLS) models were incorporated to test for the effects of phylogeny (see Supplementary Information).

Neonatal-Adult Analysis. Relative BMR positively predicted neonatal-adult slope in the total eutherian sample ($t=5.724$, $p<0.001$; n=118) and non-primate subsample ($t=5.611$, $p<0.001$; n=80). Litter size positively predicted neonatal-adult slope in the total eutherian sample ($t=7.149$, $p<0.001$; n=118) and the non-primate subsample ($t=4.832$, $p<0.001$; n=80); both relationships remained significant when strictly uniparous species were excluded. Uniparous mammals alone exhibited lower slope variance (0.011; n=55) than did the entire sample (0.028; n=117). Precociality negatively predicted neonatal-adult slope in the total eutherian sample ($t=-11.33$; $p<0.001$; n=103) and the non-primate subsample ($t=-9.126$; $p<0.001$; n=83). Placental invasiveness positively predicted neonatal-adult slope in the non-primate subsample alone ($t=3.618$; $p=0.001$; n=80). A multiple regression model using litter size, BMR, and placental invasiveness to predict neonatal-adult slope showed positive significant results for litter size and relative BMR in the total sample (BMR: $t=5.416$, $p<0.001$; litter: $t=3.771$, $p<0.001$; n=118) and the non-primate subsample (BMR: $t=3.442$, $p=0.001$; litter: $t=2.713$, $p=0.008$; n=80). No variable predicted neonatal-adult slope in the primate subsample in any test.

Discussion

RGP Allometry in Primates and Other Mammals. Fetal data in twelve primate and sixteen

non-primate mammals indicates that by the end of embryonic development (i.e. at the intercept of ~1g body size), primates already exhibit ~2x the brain/body proportions of non-primate mammals (fig. 2.2; table 2.1)[Sacher, 1982; Deacon, 1990; Striedter, 2005]. Neonatal data representing a much broader sample of primate species (Fig. 2.3) suggest that this feature is also observed in strepsirrhine species for which RGP data is unavailable. Despite the fact that tree shrews exhibit adult relative brain sizes comparable to strepsirrhines [Striedter, 2005], the one species included here – *Tupaia glis* – exhibits neonatal values close to the non-primate mammalian average, suggesting the shift is not observed in the closest available out-group [Sacher & Staffeldt, 1974; Sacher, 1982; Martin, 1983]. Neonatal values had previously suggested that odontocete cetaceans shared the primate embryonic shift [Sacher, 1982; Martin, 1983; Deacon, 1990]; however, fetal data from *Stenella coeruleoalba* suggests that the relatively high neonatal brain/body ratios of odontocetes are a consequence of high slopes, rather than differential em-

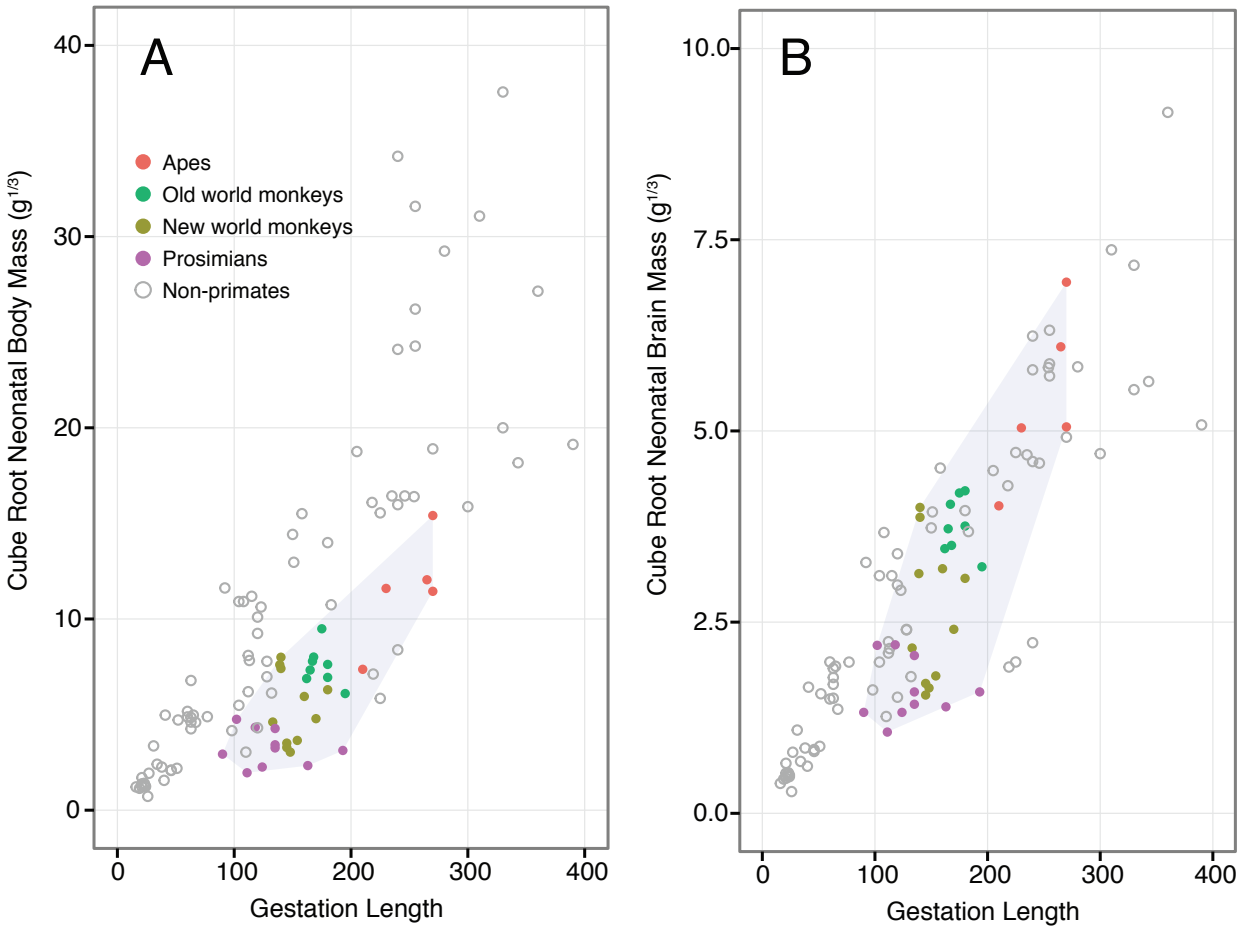

Figure 2.4. Estimated brain and body growth rates from neonatal values. Neonatal brain size, body size, and gestation length can be used as proxies for exponential growth during fetal development. Following Sacher & Staffeldt [1974], cube root transformed values for (A) body size and (B) brain size are plotted against average length of gestation in 34 primate and 77 non-primate mammalian species. Polygons are fit to primate subsamples. (A) Primate fetal body growth rates fall below the range of non-primate mammals, while (B) primate fetal brain growth rates are within the range of mammalian values. This suggests that high RGP allometric slopes in primates are likely due to slower fetal body growth rather than faster fetal brain growth.

Table 2.1. RGP Regression Models. Results of ordinary least squares (OLS) regression models of rapid growth phase (RGP) data in 12 primates, 16 non-primate mammals, and one bird. Reduced major axis results are presented in Supplementary Information. Caution should be exercised in interpreting slope and intercept values for individual species, as data availability significantly affects regression model fits. $Total_{indiv}$ indicates regression models of entire primate and non-primate samples; $Total_{species}$ indicates average intercept and slope values of species models.

	Intercept	b	r^2	p-value	n
Callithrix jacchus	-0.841	0.987	0.987	0.000	9
Sapajus apella	-0.664	0.928	0.994	0.000	11
Aotus arizae	-0.722	0.908	0.995	0.000	9
Saimiri boliviensis	-0.712	0.927	0.994	0.003	4
*Saimiri sciureus**	-2.111	1.778	0.839	0.001	8
Trachypithecus cristatus	-0.904	0.993	0.985	0.000	8
Macaca mulatta	-0.920	1.026	0.997	0.000	19
Macaca nemestrina	-1.432	1.230	0.803	0.006	7
*Macaca radiata**	-0.277	0.812	0.978	0.001	5
Macaca fascicularis	-0.912	1.007	0.999	0.016	3
Papio ssp.	-0.474	0.817	0.924	0.001	7
Homo sapiens	-0.673	0.940	0.996	0.000	195
$Total_{indiv}$	-0.744	0.962	0.994	0.000	285
$Total_{species}$	-0.825	0.976	NA	NA	(12)
Artibeus jamaicensis	-0.895	0.624	0.918	0.000	17
Bos taurus	-0.769	0.707	0.992	0.000	17
Bubalus bubalis[1]	-0.617	0.704	NA	NA	100
Camelus dromedarius[1]	-0.487	0.640	NA	NA	100
Canis familiaris[2]	-1.214	0.882	0.677	0.000	30
Felis catus[2]	-1.663	1.079	0.869	0.000	119
*Gallus gallus**	-1.210	0.830	0.962	0.000	35
Macropus eugenii[1]	-1.352	1.098	0.997	NA	93
Macropus giganteus[1] **	-1.140	0.866	NA	NA	43
Mesocricetus auratus	-1.465	1.128	0.976	0.000	18
Mus musculus[2]	-1.203	0.937	0.938	0.000	103
Monodelphis domestica	-1.270	0.966	1.000	NA	2
Oryctolagus cuniculus	-1.067	0.715	0.976	0.000	8
Ovis aries	-0.864	0.758	0.969	0.000	24
Rattus rattus[3]	-1.195	0.835	0.941	0.000	50
Stenella coeruleoalba	-1.974	1.164	0.987	0.000	15
Sus scrofa[3]	-1.183	0.885	0.983	0.000	67
$Total_{indiv}$	-1.201	0.882	0.982	0.000	806
$Total_{species}$	-1.147	0.874	NA	NA	(16)

1. OLS regression parameters given in original papers, rather than reconstructed data models.

2. OLS models are from entirely from reconstructed data, as original analyses were unavailable from source literature.

3. Data was reconstructed for some sources, but not in others.

* Slope and intercept values for these species are excluded from $Total_{species}$ averages; see Methods.

** Slope and intercept are averages of male and female model parameters in original paper.

bryonic proportions. The shared intercept shift does not mean that the RGP in primate species is perfectly uniform [e.g. Vinicius, 2005]; however, these differences are minimal relative to the shared primate increase when compared to other mammalian lineages.

Primates also exhibit relatively higher slopes (approximately isometric) during the fetal period of brain/body growth. However, this effect is less pronounced than the intercept shift (as reflected in conflicting ANCOVA and t-test results), as diverse eutherians (e.g. golden hamster [*Mesocricetus auratus*], striped dolphin [*Stenella coeruleoalba*], and cat [*Felis catus*]) also exhibit RGP slopes at or above isometry. Interestingly, several marsupial species which exhibit exceptionally slow brain and body growth during pouch life [e.g. Renfree et al., 1982] also exhibit high allometric slopes during this period (e.g. Tammar wallaby [*Macropus eugenii*] and short-tailed opossum [*Monodelphis domestica*]). This emphasizes how allometric data, which contain no direct information about growth over time, can obscure important underlying differences in brain and body growth rates. Finally, exceptionally low allometric slopes (near or below 0.7) are observed in large ungulates during later stages of fetal development (e.g. ox [*Bos taurus*], camel [*Camelus dromedarius*], and water buffalo [*Bubalus bubalis*]).

The higher RGP slopes observed in primates are mostly likely the product of slower somatic fetal growth [Payne & Wheeler, 1968; Holt et al., 1981; Martin, 1983], as cube-root models of neonatal body size are lower than expected for given gestation lengths (fig. 2.4A) while brain size is within the range of non-primate species (fig. 2.4B). Alterations to primate embryonic development (i.e. the intercept shift) cannot be fully characterized without comparative data across this period, as available datasets suggest that brain/body proportions shift rapidly during embryonic stages of development [c.f. Wingert, 1969; Goedbloed, 1976]. It is also worth noting that the primate prenatal trend – shared across diverse radiations – is unrelated to differences in adult brain size or isocortical proportions (e.g. between strepsirrhines and haplorhines; [Barton & Harvey, 2000], Fig. 2.3A), and may instead reflect changes to embryonic somatic development [Sacher, 1982].

Physiological Theories of Fetal Growth. The present analysis failed to find support for theories implicating relative BMR [Martin, 1983], placental invasiveness [Elliot & Crespi, 2008], or altriciality [Pagel & Harvey, 1988; Barton & Capellini, 2011] in rates of fetal brain growth, as measured by RGP slope. It remains possible that the sample size in this study is too small to measure these effects, that incorporation of gestational metabolic rate rather than BMR might yield different results, or that the present focus on individual ontogenetic trajectories (rather than total litter brain or body weights) may account for these conflicting results. However, differences in birth timing along ontogenetic trajectories (see below) suggest an alternative explanation for variation in neonatal brain and body size, variables central to theories that species differ in fetal brain growth rates.

Using the slope between neonatal and adult values (fig. 2.3) as a proxy for the timing of birth along ontogenetic trajectories, we found evidence that high relative BMR (i.e. small body size), large litter size, altriciality, and more invasive placenta are associated with earlier birth. Because relative brain size decreases over ontogeny in most species, small mammals with large litters and altricial young (e.g. hemochorial rodents) will always exhibit higher neonatal relative brain size – not necessarily because fetal brain growth rates are different, but because birth occurs earlier along allometric trajectories (see also Clauss et al. [2014]). This interpretation agrees with the well-documented variability of parturition relative to sigmoid brain growth and velocity

curves [Dobbing & Sands, 1979] and neurodevelopmental stages [Workman et al., 2013]. Finally, primates exhibit higher relative brain size at birth [Sacher, 1982; Martin, 1983], a direct consequence of their novel prenatal allometric growth trajectory; as such, they should not be combined with non-primate species in studies of neonatal allometry.

If previously proposed physiological factors do not selectively increase rates of prenatal brain growth, what accounts for the observed variation in RGP slope within our sample? Preliminary analysis on a smaller number of species for which aged brain and body measurements are available (Chapter 3) indicates that RGP slope variation is driven almost entirely by rates of fetal body growth, with faster-growing species (e.g. rabbit) exhibiting lower RGP slopes, and slower-growing species (e.g. primates) exhibiting higher slopes. Brain growth rates, by contrast, exhibit minimal variation and do not positively predict RGP slope [Chapter 3; see also Sacher & Staffeldt, 1974; Fig. 2.4]. Primates' low total energy expenditure (TEE) relative to body size may underlie their slow somatic growth rates [Pontzer et al., 2014], producing near-isometric RGP slopes across prenatal development. These finding highlights the central role that changes to body size play in generating the observed adult variation in relative brain size across mammalian lineages [e.g. Smaers et al., 2012].

Limitations. Prenatal allometric data are particularly useful for identifying broad alterations to fetal growth patterns, such as the shared primate encephalization trends across fetal development. However, several issues limit their interpretation, particularly at lower taxonomic levels. Differences in data availability and distribution can produce different RGP model parameters, even when comparing different datasets of a single species. While most analyses of the RGP have presumed it to be linear, several studies have suggested either multiphasic linear or curvilinear relationships in certain species (e.g. cat [Count, 1947]; mouse [Forbes & Lopez, 1989]). This is likely the case in several ungulates described here with low slopes and high intercepts (e.g. camel, buffalo, ox). This phenomenon remains poorly understood, and likely reflects differential timing of peak brain growth velocity [Dobbing & Sands, 1979] relative to body growth, which remains exponential across prenatal development. In short, the RGP models described in this study – and their application to fetal growth theories – should be interpreted with caution and respect to data distribution and sample size.

Conclusions

Count's [1947] original observation that primates exhibit exceptionally high prenatal brain/body proportions is supported by a greatly expanded pool of mammalian species; it consists of relatively high average RGP slope (shared with several other mammalian species) and an evolutionarily novel intercept shift not observed in any non-primate mammal, including the closest out-groups. Its presence at the species-shared size boundary of embryonic and fetal development (i.e. the log-log intercept) indicates that alterations to embryonic neural and somatic cell populations may be responsible for primate encephalization generally. Ontogenetic allometric evidence does not support previous findings that relative BMR, placental morphology, or precociality play a role in fetal brain growth rates. Similarly, litter size does not affect RGP slopes. Large litter size, high relative BMR, altriciality, and invasive placentation are all associated with earlier birth along ontogenetic allometric trajectories, but causal interpretations are complicated by the phylogenetic overlap of these traits (e.g. in rodents).

Whereas relative brain size has traditionally been studied in relation to species differences in intelligence [e.g. Jerison, 1973], less attention has been paid to its role in establishing functional connectivity early in ontogeny [but see Deacon, 1990]. Changes to peripheral systems during early neurodevelopment have been shown to induce dramatic changes to cortical organization and connectivity [e.g. Krubitzer & Dooley, 2013]. Both the degree and early emergence of primate prenatal encephalization make it a good candidate for such epigenetic changes, though it remains unclear which if any of the differences in primate brain connectivity (e.g. cortical organization [reviewed in Preuss, 2007]) might correspond to this shared alteration to relative brain size across fetal growth.

Allometric datasets represent an important complement to growth data of known age post-conception, which are limited to a few model species. Combining these analyses in the future may help to clarify deviations from allometric linearity as well as the underlying source of species differences in RGP slope. Further research extending allometric and growth analysis into embryonic stages of ontogeny [as in Goedbloed, 1976; Striedter & Charvet, 2008] should help to clarify when and how primate prenatal encephalization – the "extraordinary evolutionary event" at the origin of the primate order [Sacher, 1982] – emerges during embryonic development.

References

Agrawal HC, Davis JM, Himwich WA (1967): Water content of developing kitten brain. J Neurochem 14:179–181.

Agrawal HC, Davis JM, Himwich WA (1968): Water content of dog brain parts in relation to maturation of the brain. Am J Physiol 215:846–848.

Bailey P, Bonin GV, McCulloch WS (1950): The Isocortex of the Chimpanzee. Urbana, University of Illinois Press.

Barry L (1920): The effects of inanition on the pregnant albino rat, with special reference to the changes in the relative weights of the various parts, systems, and organs of the offspring. Contrib Embryol 53:91–136.

Barton RA, Capellini I (2011): Maternal investment, life histories and brain growth in mammals. Proc Natl Acad Sci USA 108:6169–6174.

Bell AW, Battaglia FC, Meschia G (1987): Relation between metabolic rate and body size in the ovine fetus. J Nutr 117:1181–1186.

Benveniste H, Fowler JS, Rooney W, Ding Y-S, Baumann AL, Moller DH, Du C, Backus W, Logan J, Carter P, Coplan JD, Biegon A, Rosenblum L, Scharf B, Gatley JS, Volkow ND (2005): Maternal and fetal 11C-cocaine uptake and kinetics measured in vivo by combined PET and MRI in pregnant nonhuman primates. J Nucl Med Off Publ Soc Nucl Med 46:312–320.

Blinkov SM, Glezer II (1968): The Human Brain in Figures and Tables: A Quantitative Handbook. New York, Basic Books.

Bolter DR (2011): A comparative study of growth patterns in crested langurs and vervet monkeys. Anat Res Int 2011:e948671, pp 1–12.

Brizzee K, Dunlap W (1986): Growth; in Dukelow, WR, Erwin J (eds): Comparative Primate Biology Volume 3: Reproduction and Development. New York: Alan R. Liss, pp 363–413.

Butler H, Juurlink BHJ (1987): An Atlas for Staging Mammalian and Chick Embryos. Boca Raton, CRC Press.

Capellini I, Venditti C, Barton RA (2011): Placentation and maternal investment in mammals. Am Nat 177:86–98.

Chambers PL, Hearn JP (1985): Embryonic, foetal and placental development in the Common marmoset monkey (Callithrix jacchus). J Zool 207:545–561.

Cheek DB (1975). Appendix II: Data on normal fetal and postnatal Macaca mulatta; in Cheek DB (ed): Fetal and Postnatal Cellular Growth. Hoboken, Wiley, pp. 521–534.

Chellman GJ, Bussiere JL, Makori N, Martin PL, Ooshima Y, Weinbauer GF (2009): Developmental and reproductive toxicology studies in nonhuman primates. Birth Defects Res B Dev Reprod Toxicol 86:446–462.

Clauss M, Dittmann MT, Müller DWH, Zerbe P, Cadron D (2014): Low scaling of a life history variable: analysing eutherian gestation periods with and without phylogeny-informed statistics. Mamm Biol 79:9–16.

Connolly CJ (1950): External Morphology of the Primate Brain. Springfield, Charles C Thomas.

Count EW (1947): Brain and body weight in man: their antecedents in growth and evolution. Ann N Y Acad Sci 46:993–1122.

Crile G, Quiring DP (1940): A record of the body weight and certain organ and gland weights of 3690 animals. Ohio J Sci 40:219–260.

Cukierski MA, Prahalada S, Zacchei AG, Peter CP, Rodgers JD, Hess DL, Cukierski MJ, Tarantal AF, Nyland T, Robertson RT, Hendrickx AG (1989): Embryotoxicity studies of norfloxacin in cynomolgus monkeys: I. Teratology studies and norfloxacin plasma concentration in pregnant and nonpregnant monkeys. Teratology 39:39–52.

de Souza SW, Dobbing J (1971): Cerebral edema in developing brain: I. Normal water and cation content in developing rat brain and postmortem changes. Exp Neurol 32:431–438.

Deacon TW (1990): Problems of ontogeny and phylogeny in brain-size evolution. Int J Primatol 11:237–282.

Deacon TW (1997): The Symbolic Species. New York, WW Norton & Co.

Deacon TW (2000): Heterochrony in brain evolution: cellular versus morphological analyses; in Parker ST, Langer J, McKinney ML (eds): Biology, Brains, and Behavior : The Evolution of Human Development. Santa Fe, SAR Press, pp. 41–88.

Dekaban AS, Sadowsky D (1978): Changes in brain weights during the span of human life: relation of brain weights to body heights and body weights. Ann Neurol 4:345–356.

DeSilva J, Lesnik J (2006): Chimpanzee neonatal brain size: implications for brain growth in Homo erectus. J Hum Evol 51:207–212.

DeVito J, Graham J, Schultz G, Sundsten J, Prothero J (1986): Morphology of the developing brain in Macaca nemestrina; in Lee PC, Else JG (eds): Primate Ontogeny, Cognition, and Social Behavior. Cambridge, Cambridge University Press, pp. 131–139.

Dhéré C, Lapicque L (1899): Relation entre la forme du cerveau et la grandeur du sujet chez le chien; in Voorst JV (ed): The Zoological Record: Being Records of Zoological Literature, pp 783–785.

Dickerson JWT, Dobbing J (1967): Prenatal and postnatal growth and development of the central nervous system of the pig. Proc R Soc Lond B Biol Sci 166:384–395.

Dobbing J, Sands J (1970): Growth and development of the brain and spinal cord of the guinea pig. Brain Res 17:115–123.

Dobbing J, Sands J (1979): Comparative aspects of the brain growth spurt. Early Hum Dev 3:79–83.

Donaldson HH (1908): A comparison of the albino rat with man in respect to the growth of the brain and of the spinal cord. J Comp Neurol Psychol 18:345–392.

Donaldson HH (1924): The Rat: Data and Reference Tables for the Albino Rat (Mus norvegicus albinus) and the Norway Rat (Mus norvegicus). Philadelphia, Wistar Institute for Anatomy & Biology.

Edwards MJ (1969): Congenital defects in guinea pigs: prenatal retardation of brain growth of guinea pigs following hyperthermia during gestation. Teratology 2:329–336.

Elliot MG, Crespi BJ (2008): Placental invasiveness and brain-body allometry in eutherian mammals. J Evol Biol 21:1763–1778.

Finlay BL, Franco ECS, Yamada ES, Crowley JC, Parsons M, Muniz JAPC, Silveira LCL (2008): Number and topography of cones, rods and optic nerve axons in New and Old World

primates. Vis Neurosci 25:289–299.

Forbes TL, Lopez GR (1989): Determination of critical periods in ontogenetic trajectories. Funct Ecol 3:625–632.

Fox MW (1966): Brain to body relationships in ontogeny of canine brain. Experientia 22:111–112.

Frasch MG, Müller T, Wicher C, Weiss C, Löhle M, Schwab K, Schubert H, Nathanielsz PW, Witte OW, Schwab M (2007): Fetal body weight and the development of the control of the cardiovascular system in fetal sheep. J Physiol 579:893–907.

Friedman L, Gaines DW, Newell RF, Smith MC, Braunberg RC, Flynn TJ, O'Donnell MW (1995): Growth patterns in selected organs of the miniature swine as determined by gross macromolecular composition. J Anim Sci 73:1340–1350.

Garden AS, Roberts N (1996): Fetal and fetal organ volume estimations with magnetic resonance imaging. Am J Obstet Gynecol 175:442–448.

Gest TR, Siegel MI (1983): The relationship between organ weights and body weights, facial dimensions, and dental dimensions in a population of olive baboons (Papio cynocephalus anubis). Am J Phys Anthropol 61:189–196.

Gihr M, Pilleri G (1969): On the anatomy and biometry of Stenella styx Gray and Delphinus delphis L. (Cetacea, Delphinidae) of the western Mediterranean. Investig Cetacea 1:15–16.

Goedbloed JF (1976): Embryonic and postnatal growth of rat and mouse. IV. Prenatal growth of organs and tissues: age determination, and general growth pattern. Acta Anat 95:8–33.

Gould S (1975): Allometry in primates, with emphasis on scaling and the evolution of the brain. Contrib Primatol 5:244–292.

Gould SJ (1977): Ontogeny and Phylogeny. Cambridge, Harvard University Press.

Le Gros Clark WE (1927): Description of the cerebral hemispheres of the brain of a gorilla. J Anat 61:467–475.

Guihard-Costa A-M, Ménez F, Delezoide A-L (2002): Organ weights in human fetuses after formalin fixation: standards by gestational age and body weight. Pediatr Dev Pathol 5:559–578.

Halley AC (2015): Meta-analysis of ontogenetic brain/body allometry in mammals: implications for primate encephalization and fetal growth theories of relative brain size. The 35th Annual Meeting of the J.B. Johnston Club for Evolutionary Neuroscience and the 27th Annual Karger Workshop in Evolutionary Neuroscience: Abstracts. Brain Behav Evol 85:287–293.

Hansen K, Sung CJ, Huang C, Pinar H, Singer DB, Oyer CE (2003): Reference values for second trimester fetal and neonatal organ weights and measurements. Pediatr Dev Pathol 6:160–167.

Harel S, Watanabe K, Linke I, Schain RJ (1972): Growth and development of the rabbit brain. Biol Neonate 21:381–399.

Hartwig WC (1996): Perinatal life history traits in New World monkeys. Am J Primatol 40:99–130.

Harvey PH, Clutton-Brock TH (1985): Life history variation in primates. Evolution 39:559–581.

Hendrickx AG, Cukierski M, Prahalada S, Janos G, Rowland J (1985): Evaluation of bendectin embryotoxicity in nonhuman primates: I. Ventricular septal defects in prenatal macaques and baboon. Teratology 32:179–189.

Herculano-Houzel S, Collins CE, Wong P, Kaas JH (2007): Cellular scaling rules for primate brains. Proc Natl Acad Sci USA 104:3562–3567.

Herndon JG, Tigges J, Anderson DC, Klumpp SA, McClure HM (1999): Brain weight throughout the life span of the chimpanzee. J Comp Neurol 409:567–572.

Holt AB, Cheek DB, Mellits ED, Hill DE (1975): Brain size and the relation of the primate to the nonprimate; in Cheek DB (ed): Fetal and Postnatal Cellular Growth: Hormones and Nutrition. Hoboken, Wiley, pp 23–44.

Holt AB, Renfree M, Cheek D (1981): Comparative aspects of brain growth: a critical evaluation of mammalian species used in brain growth research with emphasis on the Tammar wallaby; in Hetzel BS, Smith RM (eds): Fetal Brain Disorders – Recent Approaches to the Problem of Mental Deficiency. Amsterdam, Elsevier/North-Holland Biomedical Press, pp. 17–43.

Hoskins ER (1916): The growth of the body and organs of the albino rat as affected by feeding various ductless glands (thyroid, thymus, hypophysis, and pineal). J Exp Zool 21:295–346.

Hrdlička A (1925): Weight of the brain and of the internal organs in American monkeys with data on brain weight in other apes. Am J Phys Anthropol 8:201–211.

Hubbert WT, Stalheim OH, Booth, GD (1972): Changes in organ weights and fluid volumes during growth of the bovine fetus. Growth 36:217–233.

Jackson CM (1909): On the prenatal growth of the human body and the relative growth of the various organs and parts. Am J Anat 9:119–165.

Jacobsen H, Schmidt M, Holm P, Sangild PT, Vajta G, Greve T, Callesen H (2000): Body dimensions and birth and organ weights of calves derived from in vitro produced embryos cultured with or without serum and oviduct epithelium cells. Theriogenology 53:1761–1769.

Jensen EC, Gallaher BW, Breier BH, Harding JE (2002): The effect of a chronic maternal cortisol infusion on the late-gestation fetal sheep. J Endocrinol 174:27–36.

Jerison HJ (1973): Evolution of the Brain and Intelligence. New York, Academic Press.

Jolicoeur P, Pirlot P (1988): Asymptotic growth and complex allometry of the brain and body in the white rat. Growth Dev Aging 52:3–9.

Keith A (1895): Growth of brain in men and monkeys, with a short criticism of the usual method of stating brain-ratios. J Anat Physiol 29:282–303.

Kennard MA, Willner MD (1941): Findings in 216 routine autopsies of Macaca mulatta. Endocrinology 28:955–966.

Kennard MA, Willner MD (1941): Findings at autopsies of seventy anthropoid apes. Endocrinology 28:967–976.

Kerr GR, Allen JR, Scheffler G, Couture J (1974): Fetal and postnatal growth of rhesus monkeys (M. mulatta). J Med Primatol 3:221–235.

King HD (1910): The effects of various fixatives on the brain of the albino rat, with an account of a method of preparing this material for a study of the cells in the cortex. Anat Rec 4:213–244.

Kleiber M (1961): The Fire of Life: An Introduction to Animal Energetics. Hoboken, Wiley.

Kobayashi T (1963): Brain-to-body ratios and time of maturation of the mouse brain. Am J Physiol 204:343–346.

Kozma C, Macklin W, Cummins L, Mauer R (1974): The anatomy, physiology, and the biochemistry of the rabbit; in Weisbroth S, Flatt R, Kraus A (eds): Biology of the Laboratory Rabbit. San Diego, Academic Press, pp 50–69.

Krubitzer, L (2007): The magnificent compromise: cortical field evolution in mammals. Neuron 56:201–208.

LaBorde JB, Terry KK, Howard PC, Chen JJ, Collins TFX, Shackelford ME, Hansen DK (1997): Lack of embryotoxicity of fumonisin b1 in New Zealand white rabbits. Toxicol Sci 40:120–128.

LaBorde JB, Hansen DK, Young JF, Sheehan DM, Holson RR (1992): Prenatal dexamethasone exposure in rats: effects of dose, age at exposure, and drug-induced hypophagia on malformations and fetal organ weights. Toxicol Sci 19:545–554.

Lafeber HN, Rolph TP, Jones CT (1984): Studies on the growth of the fetal guinea pig: the effects of ligation of the uterine artery on organ growth and development. J Dev Physiol 6:441–

459.

Latimer HB (1938): The prenatal growth of the cat. VII. The growth of the brain and of its parts, of the spinal cord and of the eyeballs. J Comp Neurol 68:381–394.

Latimer HB (1942): The weights of the brain and of its parts, and the weight and length of the spinal cord in the dog. Growth 6:39–57.

Leutenegger W (1973): Maternal-fetal weight relationships in primates. Folia Primatol 20:280–293.

Leutenegger W (1979): Evolution of litter size in primates. Am Nat 114:525–531.

Long NM, Vonnahme KA, Hess BW, Nathanielsz PW, Ford, SP (2009): Effects of early gestational undernutrition on fetal growth, organ development, and placentomal composition in the bovine. J Anim Sci 87:1950–1959.

Lowrey LG (1911): Prenatal growth of the pig. Am J Anat 12:107–138.

MacLean EL, Hare B, Nunn CL, Addessi E, Amici F, Anderson RC, Aureli F, Baker JM, Bania AE, Barnard AM, Boogert NJ, Brannon EM, Bray EE, Bray J, Brent LJN, Burkart JM, Call J, Cantlon JF, Cheke LG, Clayton NS, Delgado MM, DiVincenti LJ, Fujita K, Herrmann E, Hiramatsu C, Jacobs LF, Jordan kE, Laude JR, Leimgruber KL, Messer EJE, Moura AC de A, Ostojić L, Picard A, Platt ML, Plotnik JM, Range F, Reader SM, Reddy RB, Sandel AA, Santos LR, Schumann K, Seed AM, Sewall KB, Shaw RC, Slocombe KE, Su Y, Takimoto A, Tan J, Tao R, van Schaik CP, Virányi Z, Visalberghi E, Wade JC, Watanabe A, Widness J, Young JK, Zentall TR, Zhao Y (2014): The evolution of self-control. Proc Natl Acad Sci USA 111:E2140–E2148.

Mahaney MC, Leland MM, Williams-Blangero S, Marinez YN (1993): Cross-sectional growth standards for captive baboons: I. Organ weight by chronological age. J Med Primatol 22:400–414.

Mangold-Wirz K (1966): Cerebralisation und ontogenesemodus bei eutherien. Acta Anat 63:449–508.

Manocha SL (1979): Physical growth and brain development of captive-bred male and female squirrel monkeys, Saimiri sciureus. Experientia 35:96–98.

Marino L, Sudheimer K, Pabst DA, McLellan WA, Arshad S, Naini G, Johnson JI (2004): Anatomical description of an infant bottlenose dolphin (Tursiops truncatus) brain from magnetic resonance images. Aquatic Mammals 30:315–326.

Maroun LL, Graem N (2005): Autopsy standards of body parameters and fresh organ weights in nonmacerated and macerated human fetuses. Pediatr Dev Pathol Off J Soc Pediatr Pathol Paediatr Pathol Soc 8:204–217.

Martin RD (1981): Relative brain size and basal metabolic rate in terrestrial vertebrates. Nature 293:57–60.

Martin RD (1983): Human Brain Evolution in an Ecological Context. New York, American Museum of Natural History.

Martin RD (1996): Scaling of the mammalian brain: the maternal energy hypothesis. Physiology 11:149–156.

Martin RD (2008): Evolution of placentation in primates: implications of mammalian phylogeny. Evol Biol 35:125–145.

Matsuzawa T (1981): Changes in blood components and organ weights in growing White Leghorn chicks. Growth 45:188–197.

McCutcheon, IE, Metcalfe J, Metzenberg AB, Ettinger T (1982): Organ growth in hyperoxic and hypoxic chick embryos. Respir Physiol 50:153–163.

McLellan WA, Koopman HN, Rommel SA, Read AJ, Potter CW, Nicolas JR, Westgate AJ, Pabst DA (2002): Ontogenetic allometry and body composition of harbour porpoises (Phocoena phocoena, L.) from the western North Atlantic. J Zool 257:457–471.

Miyazaki N, Fujiyama T, Fujise Y (1981): Body and organ weight of striped and spotted dolphins off the Pacific coast of Japan. Sci Rep Whales Res Inst 33:27–67.

Morgane PJ, Jacobs MS (1972): Comparative anatomy of the cetacean nervous system; in Harrison RJ (ed): Functional Anatomy of Marine Mammals. London, Academic Press, pp 117–244.

Mustafa MS, Berg R, Taher el-S (1969): Prenatal growth of some organs in the camel (Camelus dromedarius). Relative between body weight and brain, thymus, stomach and oesophagus weights. Zbl Vet Med A 16:536–542.

Myers RE, Hill DE, Holt AB, Scott RE, Mellits ED, Cheek DB (1971). Fetal growth retardation produced by experimental placental insufficiency in the rhesus monkey. I. Body weight, organ size. Biol Neonate 18:379–394.

Nelson JE (1988): Growth of the brain; in Tyndale-Biscoe DCH, Janssens DPA (eds): The Developing Marsupial. Berlin/Heidelberg, Springer, pp 86–100.

O'Rahilly RR, Müller F (2006): The Embryonic Human Brain: An Atlas Of Developmental Stages. Hoboken, Wiley.

Ogawa T (1961): Evolution of the brain, with special remarks on primates and cetaceans. Primates 3:73–74.

Osgerby JC, Wathes DC, Howard D, Gadd TS (2002): The effect of maternal undernutrition on ovine fetal growth. J Endocrinol 173:131–141.

Pagel MD, Harvey PH (1988): How mammals produce large-brained offspring. Evolution 42:948–957.

Payne PR, Wheeler EF (1968): Comparative nutrition in pregnancy and lactation. Proc Nutr Soc 27:129–138.

Pilleri G, Gihr M (1970): The central nervous system of the mysticete and odontocete whales. Investig Cetacea 2:89–127.

Pirlot P, Bernier R (1974): Embryonic brain-growth in a fruit bat. Anat Embryol 146:193–208.

Pirlot P, Stephan H (1970): Encephalization in chiroptera. Can J Zool 48:433–444.

Pond WG, Boleman SL, Fiorotto ML, Ho H, Knabe DA, Mersmann HJ, Savell JW, Su DR (2000): Perinatal ontogeny of brain growth in the domestic pig. Exp Biol Med 223:102–108.

Pontzer H, Raichlen DA, Gordon AD, Schroepfer-Walker KK. Hare B, O'Neill MC, Muldoon KM, Dunsworth HM, Wood BM, Isler K, Burkart J, Irwin M, Schumaker RW, Lonsdorf EV, Ross SR (2014): Primate energy expenditure and life history. Proc Natl Acad Sci USA 111:1433–1437.

Portmann A (1962): Cerebralisation und ontogenese. Med Grundlangenforschung 4:1–62.

Preuss TM (2007): Evolutionary specializations of primate brain systems; in Ravosa MA, Dagosto M (eds): Primate Origins: Adaptations and Evolution. Boston, Springer US, pp 625–675.

Renfree MB, Holt AB, Green SW, Carr JP, Cheek DB (1982): Ontogeny of the brain in a marsupial (Macropus eugenii) throughout pouch life. Brain Behav Evol 20:57–71.

Riese W, Riese H, von Bonin G (1952): Investigations on the brain weight of the baboon (Papio papio Desm.). J Comp Neurol 96:127–137.

Rizzolatti G, Arbib MA (1998): Language within our grasp. Trends Neurosci 21:188–194.

Robinson PF (1971): The body weight-organ weight relationships of the immature hamster, Mesocricetus auratus, from birth to weaning. Growth 35:253–258.

Robinson JG, Redford KH (1986): Body size, diet, and population density of neotropical forest mammals. Am Nat 128:665–680.

Rosebrough RW, Steele NC, Frobish LT (1980): Effect of ketogenic diets in gestation on some

characteristics of carbohydrate metabolism in fetal pig brain and liver. Growth 45:42–57.

Sacher GA (1982): The role of brain maturation in the evolution of the primates; in Armstrong E, Falk D (eds): Primate Brain Evolution. New York, Springer, pp 97–112.

Sacher GA, Staffeldt EF (1974): Relation of gestation time to brain weight for placental mammals: implications for the theory of vertebrate growth. Am Nat 108:593–615.

Sangild PT, Schmidt M, Jacobsen H, Fowden AL, Forhead A, Avery B, Greve T (2000): Blood chemistry, nutrient metabolism, and organ weights in fetal and newborn calves derived from in vitro-produced bovine embryos. Biol Reprod 62:1495–1504.

Schleifenbaum C (1973): Untersuchungen zur postnatalen ontogenese des gehirns von groβpudeln und wölfen. Z Für Anat Entwicklungsgeschichte 141:179–205.

Schneidereit M (1985): Study of fetal organ growth in Wistar rats from day 17 to 21. Lab Anim 19:240–244.

Schultz AH (1941): The relative size of the cranial capacity in primates. Am J Phys Anthropol 28:273–287.

Schwartz JE, Kovach A, Meyer J, McConnell C, Iwamoto HS (1998): Brief, intermittent hypoxia restricts fetal growth in Sprague-Dawley rats. Neonatology 73:313–319.

Seelke AMH, Dooley JC, Krubitzer LA (2013): Differential changes in the cellular composition of the developing marsupial brain. J Comp Neurol 521:2602–2620.

Serres EA (1824): Anatomie Comparée Du Cerveau. Paris, Gabon.

Shek JW, Wen GY, Wisniewski HM (1985): Atlas of the Rabbit Brain and Spinal Cord. Basel, Karger.

Shepard TH, Shi M, Fellingham GW, Fujinaga M, Fitzsimmons JM, Fantel AG, Barr M (2009): Organ weight standards for human fetuses. Pediatr Pathol 8:513–524.

Sherwood CC, Stimpson CD, Raghanti MA, Wildman DE, Uddin M, Grossman LI, Goodman M, Redmond JC, Bonar CJ, Erwin JM, Hof PR (2006): Evolution of increased glia–neuron ratios in the human frontal cortex. Proc Natl Acad Sci USA 103:13606–13611.

Sikes SK (1971): Natural History of the African Elephant. London, Weidenfeld & Nicolson.

Sikov MR, Thomas JM (1970): Prenatal growth of the rat. Growth 34:1–14.

Singer D, Sung C, Wigglesworth J (1991): Fetal growth and maturation with standards for body and organ development. Textb Fetal Perinat Pathol 1:11–15.

Smaers JB, Dechmann DKN, Goswami A, Soligo C, Safi K (2012): Comparative analyses of evolutionary rates reveal different pathways to encephalization in bats, carnivorans, and primates. Proc Natl Acad Sci USA 109:18006–18011.

Stephan H, Andy, OJ (1970): The allocortex in primates; in Noback CR, Montagna W (eds): The Primate Brain. New York, Appleton-Century-Crofts, pp 109–135.

Stephan H, Bauchot R, Andy OJ (1970): Data on size of the brain and of various brain parts in insectivores and primates; in Noback CR, Montagna W (eds): The Primate Brain. Advances in Primatology Vol. 1. New York, Appleton Century Crofts, pp 289–297.

Stock MK, Francisco DL, Metcalfe J (1983): Organ growth in chick embryos incubated in 40% or 70% oxygen. Respir Physiol 52:1–11.

Streeter GL (1949): Developmental horizons in human embryos (fourth issue). A review of the histogenesis of cartilage and bone. Contrib Embryol 33:149–169.

Striedter GF (2005): Principles of Brain Evolution. Sunderland, Sinauer Associates.

Striedter GF, Charvet CJ (2008): Developmental origins of species differences in telencephalon and tectum size: morphometric comparisons between a parakeet (Melopsittacus undulates) and a quail (Colinus virgianus). J Comp Neurol 507:1663–1675.

Taher el-S, Moustafa MS, Berg R (1969): Prenatal growth of some organs in the Egyptian water buffalo (Bos/Bubalus/bubalis/L.). Relation between body weight and brain, thymus, stomach, and oesophagus weights. Zbl Vet Med A 16:529–535.

Tarantal AF, Hunter MK, Gargosky SE (1997): Direct administration of insulin-like growth factor to fetal rhesus monkeys (Macaca mulatta). Endocrinology 138:3349–3358.

Tarara R (1984): The effect of medroxyprogesterone acetate (Depo-provera) on prenatal development in the baboon (Papio anubis): a preliminary study. Teratology 30:181–185.

Thomas JM, Beamer JL (1971): Age-weight relationships of selected organs and body weight for miniature swine. Growth 35:259–272.

Town SC, Putman CT, Turchinsky NJ, Dixon WT, Foxcroft GR (2004): Number of conceptuses in utero affects porcine fetal muscle development. Reproduction 128:443–454.

Trieb G, Pappritz G, Lützen L (1976): Allometric analysis of organ weights. I. Rats. Toxicol Appl Pharmacol 35:531–542.

Tumbleson ME (1973): Brain weight, as a function of age, in miniature swine. Growth 37:13–17.

Vallet JL, Freking BA (2006): Changes in fetal organ weights during gestation after selection for ovulation rate and uterine capacity in swine. J Anim Sci 84:2338–2345.

van Dongen P (1998): Brain size in vertebrates; in Nieuwenhuys R, ten Donkelaar HJ, Nicholson C (eds): The Central Nervous System of Vertebrates. New York, Springer, pp 2099–2131.

van Golde J, Borm PJ, Wolfs M, Gerver W, Blanco CE (1998): The effect of hyperoxia on embryonic and organ mass in the developing chick embryo. Respir Physiol 113:75–82.

Vinicius L (2005): Human encephalization and developmental timing. J Hum Evol 49:762–776.

Wallace L (1945): The composition of sheep foetuses. J Physiol 104S:33P–34P.

Weil A (1943): The chemical growth of the brain of the white rat and its relation to sex. Growth 7:257–264.

Westergaard E (1969): The cerebral ventricles of the golden hamster during growth. Cells Tissues Organs 72:533–548.

Wildman DE, Chen C, Erez O, Grossman LI, Goodman M, Romero R (2006): Evolution of the mammalian placenta revealed by phylogenetic analysis. Proc Natl Acad Sci USA 103:3203–3208.

Wilson JG, Fradkin R, Hardman A (1970): Breeding and pregnancy in rhesus monkeys used for teratological testing. Teratology 3:59–71.

Wingert F (1969): Biometrische Analyse der Wachstumsfunktionen von Hirnteilen und Körpergewicht der Albinomaus. J Hirnforschungen 11:133–197.

Workman AD, Charvet CJ, Clancy B, Darlington RB, Finlay BL (2013): Modeling transformations of neurodevelopmental sequences across mammalian species. J Neurosci 33:7368–7383.

Zuckerman S, Fisher RB (1938): Growth of the brain in the rhesus monkey. Proc Zool Soc Lond B107:529–538.

Chapter 2: Supplementary information

Table S2.1. Rapid Growth Phase (RGP) Reduced Major Axis (RMA) Regression Models

Results of reduced major axis (RMA) regression models of rapid growth phase (RGP) data in 12 primate and 16 non-primate mammalian species. The major findings of this paper are unaffected by this alternative analysis.

	intercept	*b*	r^2	p-value
Callithrix jacchus	-0.848	0.994	0.987	0.000
Sapajus apella	-0.669	0.930	0.994	0.000
Aotus arizae	-0.725	0.910	0.995	0.000
Saimiri boliviensis	-0.717	0.930	0.994	0.003
Saimiri sciureus	-2.589	2.045	0.839	0.001
Trachypithecus cristatus	-0.919	1.001	0.985	0.000
Macaca mulatta	-0.923	1.028	0.997	0.000
Macaca nemestrina	-1.922	1.422	0.803	0.006
Macaca radiata	-0.293	0.819	0.978	0.001
Macaca fascicularis	-0.913	1.007	0.999	0.016
Papio ssp.	-0.543	0.845	0.924	0.001
Homo sapiens	-0.678	0.942	0.996	0.000
Total	-0.752	0.964	0.994	0.000
Artibeus jamaicensis	-0.906	0.640	0.918	0.000
Bos taurus	-0.774	0.709	0.992	0.000
Bubalus bubalis	-0.724	0.732	0.962	0.000
Camelus dromedarius	-0.589	0.665	0.959	0.000
Canis familiaris	-1.772	1.088	0.677	0.000
Felis catus	-1.831	1.169	0.869	0.000
Macropus eugenii	-1.353	1.103	0.993	0.000
Macropus giganteus	-1.170	0.875	0.985	0.000
Mesocricetus auratus	-1.479	1.143	0.976	0.000
Monodelphis domestica	-1.270	0.966	1.000	N/A
Mus musculus	-1.216	0.967	0.938	0.000
Oryctolagus cuniculus	-1.077	0.721	0.976	0.000
Ovis aries	-0.885	0.767	0.969	0.000
Rattus rattus	-1.210	0.856	0.941	0.000
Stenella coeruleoalba	-2.000	1.172	0.987	0.000
Sus scrofa	-1.197	0.892	0.983	0.000
Total	-1.214	0.887	0.982	0.000

Phylogenetic generalized least-squares (PGLS) analysis

Phylogenetic generalized least-squares (PGLS) models were used to determine whether incorporating phylogenetic information changes the results of this study. Tree topology and branch lengths are taken from Bininda-Emonds et al. [2008]. Analysis is performed using the ape, geiger, and phytools packages for R; PGLS was performed using the pgls tool in the caper package with lambda set to maximum likelihood.

PGLS models do not significant predict RGP slope in the entire sample from relative basal metabolic rate (cal/kilogram/day)($t=0.232$; $p=0.818$), dummy-coded placental invasiveness ($t=1.995$; $p=0.059$), or litter size ($t=0.584$; $p=0.565$).

Analyses within primate and non-primate subsamples used pruned trees reflecting these groupings. Within the primate subsample, RGP slope was not predicted by either litter size ($t=0.099$; $p=0.924$) or relative BMR ($t=-0.105$; $p=0.919$). Similarly, within the non-primate subsample, neither litter size ($t=1.132$; $p=0.277$) nor relative BMR ($t=0.520$; $p=0.611$) predicted RGP slope. Placental invasiveness did not predict RGP slope in the non-primate subsample ($t=0.792$; $p=0.443$); placental morphology is hemochorial in the entire primate subsample.

CHAPTER 3. Minimal variation in eutherian brain growth rates during fetal neurogenesis

Abstract

A central question in the evolution of brain development is whether species differ in rates of brain growth at similar age and mass during fetal neurogenesis. Studies of neonatal data have found allometric evidence for brain growth rate differences according to physiological variables such as relative metabolism and placental invasiveness, but these findings have not been tested against fetal data directly. Here, we examine rates of exponential brain growth in eight eutherian mammals, two marsupials, and two birds. Within eutherians, fetal brain growth rates exhibit minimal variation relative to body and visceral organ growth, vary independently of correlated growth patterns in other organs, and are unrelated to proposed physiological constraints such as metabolic rate or placental invasiveness. Brain growth rates in two birds overlap with eutherian variation, while marsupial brain growth is exceptionally slow. These findings suggest that limited fetal resources are preferentially allocated to neurodevelopment in eutherians, minimizing the variation in brain growth relative to visceral organ and whole body rates.

Introduction

Mammalian brains vary in size by five orders of magnitude, ranging from a fraction of a gram in some tree shrews [Naumann, 2015] to nearly 10kg in sperm whales [Kojima, 1951]. How has evolution altered neurodevelopment to produce brains of such different size? It is well established that larger brains are grown by lengthening the duration of brain development [Sacher & Staffeldt, 1974; Passingham, 1985; Pagel & Harvey, 1988], as reflected in extended neurodevelopmental schedules [Workman et al., 2013], longer periods of exponential growth [Dobbing & Sands, 1979], and later ages at which adult brain size is achieved. Nevertheless, species may also differ in rates of brain growth, particularly during fetal neurogenesis. Brain size at birth is not a simple function of gestation length [Sacher & Staffeldt, 1974], and differences in neonatal brain size have suggested faster brain growth in species with higher relative basal metabolism [Martin, 1981], more invasive placenta [Elliot & Crespi, 2008], and precociality at birth [Pagel & Harvey, 1988; Barton & Capellini, 2011]. At present, fetal brain growth data have never been directly compared across species to adequately test these hypotheses, or to characterize brain growth relative to other organs in the body.

Direct comparisons of brain growth velocity (i.e. "rate", mass/time) have been difficult because growth is nonlinear, following a sigmoid trajectory composed of an initial exponential phase, an inflection point, and a subsequent decay curve (Fig 3.1A, B)[Brody, 1945; Laird, 1967]. Velocity increases over the exponential phase as brains grow larger (Fig. 3.1C, D) until maximum velocity is reached. Species differ in the duration of the exponential period, the brain size at which peak growth velocity occurs, and the timing of birth relative to this inflection point (the "brain growth spurt" [Dobbing & Sands, 1979]). Species also differ in the time from conception to the onset and completion of neurulation, a period ranging from 9.5 days in mouse [Butler & Juurlink, 1987](40% gestation) to 29 days in human [O'Rahilly & Muller, 2006](11% gestation) and highly variable across species [Butler & Juurlink, 1987]. Brain size at birth – a

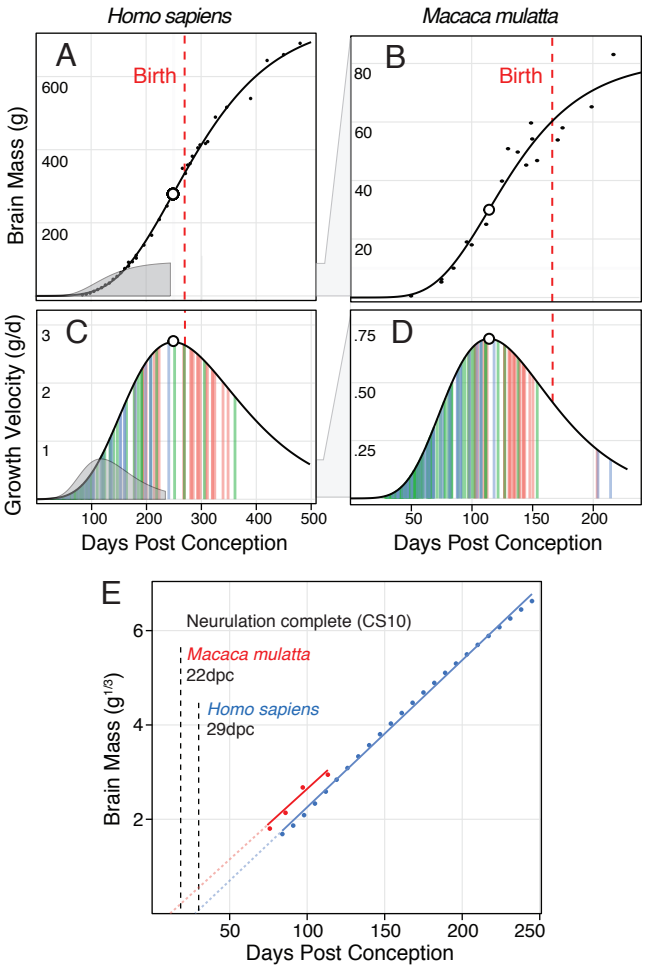

Figure 3.1. Methods for comparing brain growth. (A, B) Gompertz models fit to fetal and early postnatal brain growth data in human and rhesus monkey show differences in birth timing and the age and size of peak velocity (open circles). Rhesus function is superimposed on human curve (A: grey) to show earlier onset of exponential growth in rhesus. (C, D) Velocity curves (g/d) derived from gompertz functions for both species. Vertical color bars correspond to neurodevelopmental event estimates related to neurogenesis (green), tract formation (blue), and myelination (red)[Workman et al., 2013]. Brain growth accelerates through the neurogenic period prior to peak velocity (open circle). Again, rhesus velocity function is superimposed (C: grey) for comparison with human. (E) Exponential stages preceding peak velocity are fit with linear models of cube-root transformed brain mass to allow a comparison of growth acceleration (i.e. slope; figure S3.1), which is similar in both species; the intercept shift is an artifact of temporal differences in the completion of neurulation (Carnegie Stage 10).

common proxy for prenatal growth patterns – includes artifacts introduced by these differences in neurulation and birth timing, leading several authors to caution against its use as a temporal anchor in comparative neurodevelopment [Dobbing, 1973; Newell-Morris & Fahrenbruch, 1985].

Several methods allow the dynamic changes in growth velocity across species or organs to be compared. First, linear models of cube-root transformed data have been used to measure exponential growth using a single variable, slope, while keeping the exponent constant [Huggett & Widdas, 1951]. Cube-root slope measures the steepness of exponential curves (i.e. acceleration; fig. S3.1A, B) and corrects for artifacts introduced by the timing of neurulation by aligning data at the onset of exponential growth. Birth timing artifacts can be removed by identifying peak velocity (e.g. with Gompertz models) and comparing only the preceding exponential data; this also allows the incorporation of neurodevelopmental event models [Workman et al., 2013] into whole-brain growth and velocity curves. Second, instantaneous velocity can be measured between individual fetal measurements or averages; this method has several drawbacks (fig. S3.1C) but provides velocity estimates from raw observations that can be described according to increasing brain size. Together, these methods allow us to compare brain growth velocity as it increases over time and size in each species, and to compare brain with whole body and other organ growth patterns during fetal development.

This study directly examines rates of exponential brain growth collected from published studies (SI) in eight eutherian mammals (*Homo sapiens, Macaca mulatta, Sus scrofa, Ovis aries, Mus musculus, Rattus rattus, Cavia porcellus, Oryctolagus cuniculus*), two marsupials (*Macropus eugenii, Monodelphis domesticus*), and two birds (*Colinus virgianus, Melopsittacus undulates*). Gompertz growth models are used to calculate peak brain growth velocity (g/d) in the mammalian sample and isolate exponential phases of growth. Brain growth trajectories are compared to neurodevelopmental models [Workman et al., 2013], birth timing, and developmental state at birth (i.e. altricial/precocial). To determine if peak velocity improves on neonatal measures, tests predicting adult brain size are compared between (a) peak velocity age to total gestation length, and (b) peak velocity brain size to neonatal brain size. Linear models are fit to exponential cube-root data for brain, whole body, liver, heart, kidney, and lung; to mitigate variance in fetal age estimation across studies, model parameters are averaged in as many studies as possible (SI). Slopes are compared across organs and species to characterize relative growth rate variation and correlations in the eutherian sample. We test whether basal metabolic rate, placental structure, or precociality at birth predict cube-root brain slope, and whether slope predicts neonatal or adult brain size. Finally, we examine instantaneous brain growth velocities from raw data in the eutherian sample for comparison with cube-root results.

Materials and Methods

Data. Post-conception age (d) and weight (g) of fetal brain, body, heart, liver, lung (x2), and kidney (x2) were collected from published literature. When unique data was unavailable in the original paper, data were reconstructed from figures using Photoshop CC. Brain growth data preceding peak velocity were considered exponential and were included in cube root models. In species born earlier than peak velocity, all exponential data (including early postnatal data) were included in this analysis. Whole body growth data includes all fetal data in each species, as body growth peak velocity is always postnatal. Exponential growth data for liver, heart, lungs, and kid-

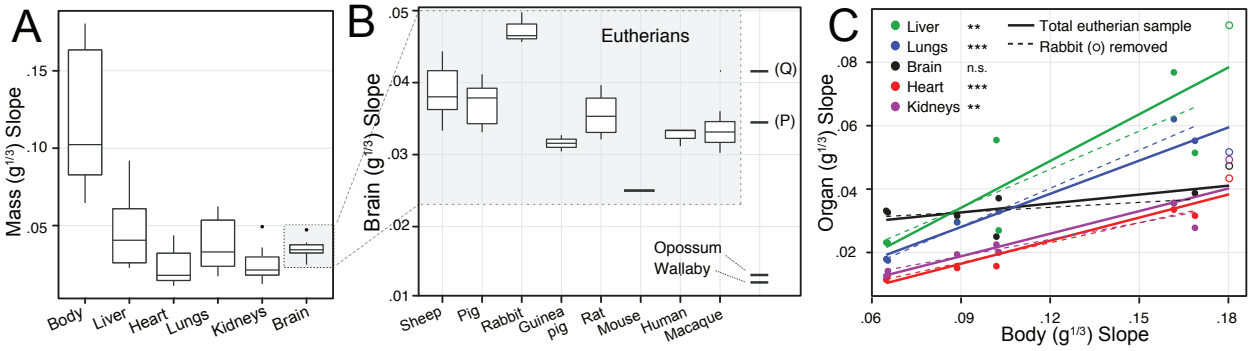

Figure 3.2. Cube-root slopes are averaged across available studies to produce robust measures of relative organ growth in eight eutherian species (Table S3.1). (A) Variation in average whole body and organ cube-root slopes across eight species; brain slopes exhibit the lowest degree of variation among the organs studied. (B) Brain cube-root slopes in eight eutherians, two marsupials, and two birds (Q: quail; P: parakeet). Eutherian ranges indicate variation in estimates from individual studies (SI). (C) Regression models predicting organ slopes from whole body slope in the eutherian sample (solid lines; n=8) and when rabbit is removed (dotted lines; n=7)(Table S3.1). In both cases, body slope significantly predicts organ slopes in every organ except the brain.

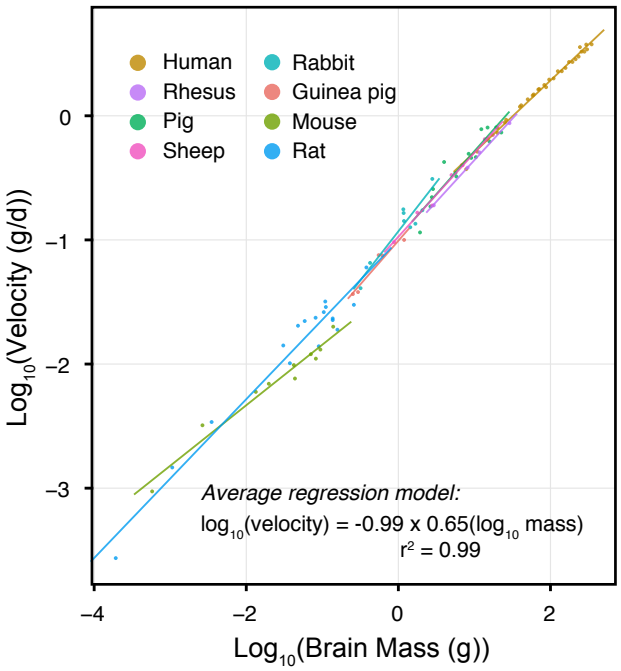

Figure 3.3. Instantaneous velocity (g/d) calculated from raw data scales with brain size at an approximately linear rate over six order of magnitude. Velocity is negatively allometric with increasing brain size. Velocities outside of a 95% CI were removed from species datasets prior to model fitting. See Fig. S3.1C for methods.

neys were isolated by visually inspecting cube-root data, determining a point of growth deceleration, and removing values older that.

Models. Gompertz models were fit to fetal, perinatal, and early postnatal brain growth data to calculate the age, brain size, and measure of peak velocity (g/d). First-order derivatives of gompertz equations were used to generate velocity curves, and model estimates of neurodevelopmental event timing [Workman et al., 2013] were applied to demonstrate neurogenic, tract formation, and myelination sequences in relation to velocity curves. Cube root models were calculated separately by data source for each organ and species to minimize artifacts introduced from differences in age estimation across studies (i.e. intercept shifts; cf. SI). Exponential data from each study was cube-root transformed, and ordinary least squares (OLS) models were fit predicting cube-root weight in grams from days post-conception. Model parameters were then averaged across available studies to produce a final slope estimate for statistical tests. Instantaneous velocities (fig. 3.3) were calculated by taking the slope between adjacent data points according to increasing age (SI: Methods). Statistical tests use OLS bivariate regression models, comparing log10 tranformed data where listed.

Statistical tests. Bivariate ordinary least squares (OLS) regression models were used in all statistical tests. Log-transformed data was used as described in Table S3.5.

Results and Discussion

Brain, body, and visceral organ growth rates. Eutherian brain growth slopes exhibit the lowest variation in the organs studied (Fig. 3.3A; Table S3.1). Brain slope variation is significantly lower than whole body ($F(7,7)=52.6$; $p<0.001$), liver ($F(7,7)=16.6$; $p<0.01$) and lungs ($F(6,7)=8.0$; $p<0.05$); heart and kidney variation are not significantly larger (Table S3.2). Whole body slope

significantly predicts the slope of liver ($p<0.01$; $r^2=0.77$), heart ($p<0.001$; $r^2=0.94$), lungs ($p<0.001$; $r^2=0.92$) and kidneys ($p<0.01$; $r^2=0.83$), but fails to predict brain slope ($p=0.083$; $r^2=0.46$)(Fig. 3.2C, solid lines). Rabbit exhibits exceptionally rapid growth in all organs, including brain; when removed from the sample, brain growth shows little association with body slope ($p=0.343$; $r^2=0.23$) while all visceral organs remain significant (Fig. 3.2C, dotted lines) (Table S3). Inter-organ correlations are shown in Table S3.4.

Cross-study variation in brain growth cube-root slopes for each species are shown in Figure 3.2B (see Figs. S3.4-S3.13). Rabbit exhibit the highest average slope (0.047) in our sample, a finding supported by three separate datasets; pig (0.037) and sheep (0.039) slopes are higher than overlapping values in rat (0.036), guinea pig (0.032), macaque (0.033), and human (0.033). Mouse exhibit the lowest slope (0.025) among eutherians. Data of exceptional quality on embryonic brain growth (1) reveal higher slopes between E9 to E12 in mouse (0.057) and between E12 to E15 in rat (0.076); as these slopes likely reflect symmetric proliferative cell division in the cortex (Fig. S3.3; [Caviness et al., 1995]), we have restricted our analyses to later neurogenic periods. Tammar wallaby, which undergo most neurogenesis postnatally during pouch life, have the lowest observed slope (0.012) despite undergoing similar neurodevelopmental events over this period. Limited data for short-tailed opossum (Fig. S3.13) suggest a similarly low slope (0.0133). Slopes in parakeet (0.035) and quail (0.042)(Fig. S3.13) fall within the range of eutherian values. Instantaneous brain growth rates (g/d) calculated from adjacent raw data points (SI: Methods) (Figs. 3.3; S3.1C) support the general observation of conservatism in brain growth rates, as brain growth velocity is primarily a function of fetal brain size at any given moment during eutherian neurogenesis. Deviations from this general allometric relationship (e.g. mouse, rabbit) correspond to differences in acceleration calculated from cube-root models.

Eutherian cube-root brain slopes in this sample fail to predict neonatal ($t=1.396$; $p=0.205$) or adult brain size ($t=0.534$; $p=0.610$), and are not predicted by relative BMR ($t=-1.69$; $p=0.142$), dummy-coded measures of placental invasiveness ($t=-0.68$; $p=0.524$), or dummy-coded precociality/altriciality at birth ($t=0.026$; $p=0.801$).

While the variation in eutherian brain growth acceleration is minimal relative to other organs (Fig. 3.2A) and largely overlapping across diverse eutherian species (Fig. 3.2B), these differences are nontrivial. For example, average models indicate that rabbit would increase brain size from 0.125g to 3.275 grams over a period of ~21 days; the corresponding increase would take 27 days in pig. By contrast, this increase would take 81 days in tammar wallaby. These extrapolations are limited by data availability over similar fetal brain sizes, and unfortunately obscure important differences in the growth patterns of major brain subdivisions. However, variation in eutherian acceleration rates in other organs is much higher. Coupled with weak correlation of brain with visceral organ and body growth slopes (Table S3.3), this indicates a surprising conservatism in eutherian exponential brain growth – shared with birds, but not with marsupials – during fetal neurogenesis.

This analysis clearly demonstrates that larger eutherian brains, with correspondingly large isocortices [Stephan et al., 1981], do not grow at faster acceleration *in utero*. We are unaware of any variable that corresponds to the observed variation in brain growth slopes measured here. However, while most species fall within a small range of variation, rapid growth in rabbit and slow growth in marsupials correspond to respective body growth rates in these outliers. One possibility is that most eutherians preferentially allocate oxygen and glucose to brain growth – a phenomenon observed in growth restriction studies (i.e. “brain sparing”; [Simmons et al., 1992;

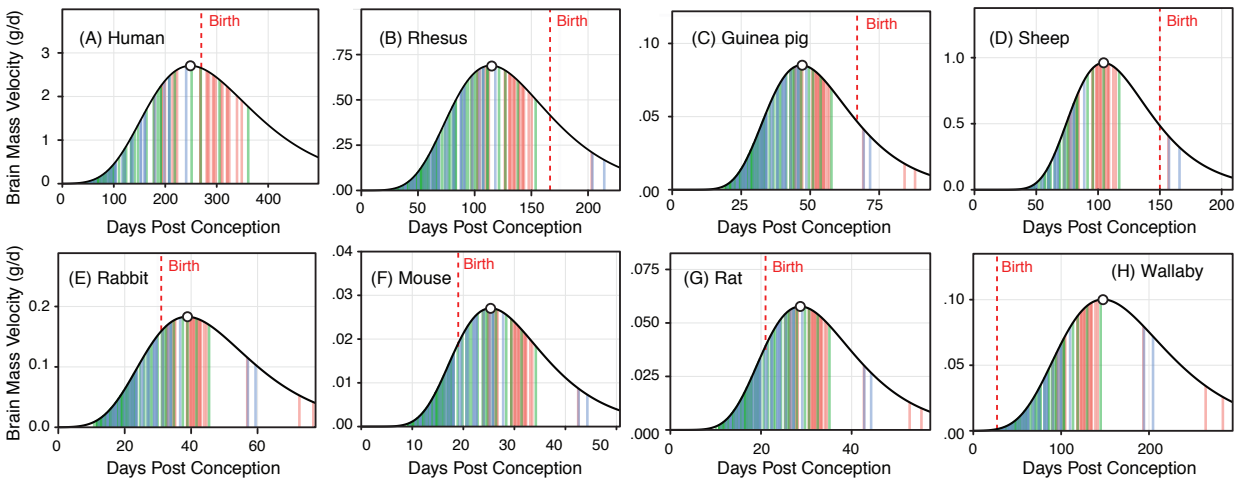

Figure 3.4. Velocity models of fetal and early postnatal brain growth in four altricial (A-D) and four precocial species (E-H). Color bars indicate model estimates for the age of events associated with neurogenesis (green), tract formation (blue), and myelination (red) taken from www.translatingtime.net (1). All of the precocial species in our sample are born following peak velocity. This may explain why precocial species have longer gestation lengths to grow neonatal brains of similar size as altricial species (2), and why altricial species have smaller neonatal brain size after correcting for gestation length (3,4).

McCutcheon et al., 1982; Tanaka et al., 1994]) – minimizing the brain growth rate variation across species, but producing exceptionally high or low brain growth rates in species with abnormal physiological conditions during early neurodevelopment.

Fetal Growth vs. Ontogenetic Brain/Body Allometry. Allometric data on fetal brain/body growth is more widely available in a larger number of species than aged growth data, and has recently been reviewed in 28 mammalian species [Chapter 2]. Fetal development is characterized by linear allometric brain/body growth (i.e. the "rapid growth phase" [Renfree et al., 1982]), with differences in slope and intercept producing variation in neonatal relative brain size. Are species with higher fetal allometric slopes – producing more encephalized neonates – exhibiting faster brain growth, or slower body growth?

Body coefficient negatively predicts RGP slope ($t=-6.09$, $p<0.01$; $r^2=0.88$) in seven of the eutherian species for which RGP slopes have been calculated. Surprisingly, brain growth coefficient *also* negatively predicts RGP slope ($t=-2.60$; $p=0.048$; $r^2=0.60$), implying a high brain/body slope in species with slower brain growth. However, rabbits exhibit both rapid brain and body growth, producing low allometric slopes during fetal development; when they are removed from the sample, body growth retains its significance ($t=-4.59$; $p<0.05$; $r^2=0.84$) while brain growth does not ($t=-1.44$; $p=0.22$; $r^2=0.34$)(Table S3.5). This provides strong evidence that fetal allometric brain/body slope differences, and corresponding variation in neonatal brain/body allometry, are the consequence of differential body growth.

Primates exhibit exceptionally high brain/body ontogenetic allometry during fetal development relative to other mammalian radiations [Count, 1947; Sacher, 1982; Deacon, 1990], a difference present as early as the embryonic period [Chapter 2]. The exceptionally slow somatic and visceral organ growth in primates shown here may help to explain primates' near-isometric brain/body growth during fetal development, and are consistent with other features of primate

life histories, such as slow postnatal somatic growth [Vinicius, 2005].

Brain growth velocity and birth timing. Peak growth velocity occurs prenatally in human, macaque, guinea pig, sheep, and pig, and postnatally in mouse, rat, rabbit, and tammar wallaby (Fig. 3.4). All of the species in our sample born before peak brain growth velocity are born with eyes closed (i.e. precocial), while species born after peak velocity are all born with eyes open (i.e. altricial). As we found no evidence that either altricial or precocial species have faster brain growth (Table S3.5), this systematic difference in birth timing may help to explain why altricial species have smaller neonatal brain size after gestation length is corrected for (implying faster growth in precocial species [Pagel & Harvey, 1988; Pagel & Harvey, 1990; Barton & Capellini, 2011]). Sacher & Staffeldt's [1974] apparently contradictory observation that altricial species achieve equivalent brain sizes over shorter gestation periods (suggesting faster altricial growth) is also what we should expect if precocial species are preferentially affected by the birth timing artifact described above. The variability in birth timing relative to brain growth trajectories, combined with the observation that whole body growth is much more variable across our sample, indicates that neonatal measurements (absolute or relative brain size) should be approached with caution as proxies for preceding fetal growth.

In the eutherian sample (n=8), peak velocity (g/d) positively predicts neonatal brain size ($p<0.001$; $r^2=0.95$) and adult brain size ($p<0.001$; $r^2=0.99$)(Fig. S3.2A). Age at peak velocity positively predicts peak velocity ($p<0.001$; $r^2=0.96$)(Fig. 3.2B) and predicts adult brain size ($p<0.001$; $r^2=0.95$) better than gestation length does ($p<0.001$; $r^2=0.87$)(Fig. S3.2C). Brain size at peak velocity also predicts adult brain size ($p<0.001$; $r^2=0.99$) better than neonatal brain size does ($p<0.001$; $r^2=0.94$)(Fig. 3.2D). Velocity curves fit well to neurodevelopmental event models (Fig. 3.4)[Workman et al., 2013] despite wide variability in peak velocity and birth timing (e.g. over tammar wallaby pouch life), with neurogenic events are generally constrained to exponential stages of growth. This indicates that peak velocity may be a better neurodevelopmental anchor than birth in species for which it can be calculated.

Conclusions

Our findings are limited by the small number of species for which aged growth data are available (most of which are domesticated), particularly during the exponential period of growth. Differences between published datasets for each species likely reflect the difficulties in determining time of conception, and individual differences in the timing of embryonic implantation (both reflected as intercept shifts). As most published data on fetal growth is averaged, natural variation within species is unavailable for statistical tests comparing growth coefficients. We have tried to mitigate these limitations by using average model parameters across datasets; accordingly, most of our findings exhibit strong statistical power despite a small sample size.

Removing artifacts associated with birth timing and neurulation show that fetal brain growth in eutherians is faster than estimates from neonatal datasets [Sacher & Staffeldt, 1974], exhibits the lowest degree of variation among the organs studied, and is generally independent of correlated growth patterns in visceral organ and whole body growth. The variation in brain growth acceleration described here supports previous reports of exceptionally slow growth in marsupials during postnatal pouch life [Renfree et al., 1982] and indicates rabbits may grow their brains at exceptionally high rates. Further research on mechanisms controlling absolute size

increase, such as cortical cell cycle duration, may help to elucidate how and why species deviate from broadly conserved brain growth patterns described here.

References

Barton RA, Capellini I (2011): Maternal investment, life histories and brain growth in mammals. Proc Natl Acad Sci USA 108:6169–6174.

Butler H, Juurlink BHJ (1987): An Atlas for Staging Mammalian and Chick Embryos. Boca Raton, CRC Press.

Brody S (1945): Bioenergetics and Growth: With Special Reference to the Efficiency Complex in Domestic Animals. New York, Reinhold.

Dobbing J (1973): The developing brain: A plea for more critical interspecies extrapolation. Nutr Rep Int 7:401–406.

Dobbing J, Sands J (1979): Comparative aspects of the brain growth spurt. Early Hum Dev 3:79–83.

Elliot MG, Crespi BJ (2008): Placental invasiveness and brain-body allometry in eutherian mammals. J Evol Biol 21:1763–1778.

Holliday MA (1986): Body composition and energy needs during growth; in Falkner F, Tanner JM (eds): Human Growth: A Comprehensive Treatise, 2nd ed. Vol. 2. New York, Plenum Press, New York, pp 117–139

Huggett AG, Widdas WF (1951): The relationship between mammalian foetal weight and conception age. J Physiol 114:306–317.

Kojima T (1951): On the brain of the sperm whale (Physeter catodon L). Sci Rep Whales Res Inst 32:199–218.

Laird AK (1967): Evolution of the human growth curve. Growth 31:345–355.

Martin RD (1981): Relative brain size and basal metabolic rate in terrestrial vertebrates. Nature 293:57–60.

McCutcheon IE, Metcalfe J, Metzenberg AB, Ettinger T (1982): Organ growth in hyperoxic and hypoxic chick embryos. Respir Physiol 50:153–163.

Ming G, Song H (2005): Adult neurogenesis in the mammalian central nervous system. Annu Rev Neurosci 28:223–250.

Mink JW, Blumenschine RJ, Adams DB (1981): Ratio of central nervous system to body metab-

olism in vertebrates: Its constancy and functional basis. Am J Physiol 241:R203–212.

Naumann RK (2015): Even the smallest mammalian brain has yet to reveal its secrets. Brain Behav Evol 85:1–3.

O'Rahilly RR, Müller F (2006): The Embryonic Human Brain: An Atlas Of Developmental Stages. Hoboken, Wiley.

Pagel MD, Harvey PH (1988): How mammals produce large-brained offspring. Evolution 42:948–957.

Pagel MD, Harvey PH (1990): Diversity in the brain sizes of newborn animals: Allometry, energetics, or life history tactics? Bioscience 40:116–122.

Passingham RE (1985): Rates of brain development in mammals including man. Brain Behav Evol 26:167–175.

Renfree MB, Holt AB, Green SW, Carr JP, Cheek DB (1982): Ontogeny of the brain in a marsupial (Macropus eugenii) throughout pouch life. Brain Behav Evol 20:57–71.

Sacher GA, Staffeldt EF (1974): Relation of gestation time to brain weight for placental mammals: Implications for the theory of vertebrate growth. Am Nat 108:593–615.

Seelke AMH, Dooley JC, Krubitzer LA (2013): Differential changes in the cellular composition of the developing marsupial brain. J Comp Neurol 521:2602–2620.

Simmons RA, Gounis AS, Bangalore SA, Ogota ES (1992): Intrauterine growth retardation: Fetal glucose transport is diminished in lung but spared in brain. Pediatr Res 31:59–63.

Workman AD, Charvet CJ, Clancy B, Darlington RB, Finlay BL (2013): Modeling transformations of neurodevelopmental sequences across mammalian species. J Neurosci 33:7368–7383.

SI & Data Source References

Abdul-Karim RW, Bruce NW (1972): The regulatory effect of oestrogens on fetal growth: II. Uterine and placental blood flow in rabbits. J Reprod Fert 30:477–480.

Åström K-E (1967): On the early development of the isocortex in fetal sheep. Prog Brain Res 26:1–59.

Barcroft J (1947): Researches on Pre-natal Life. Hoboken, Blackwell.

Bell AW, Battaglia FC, Meschia G (1987): Relation between metabolic rate and body size in the ovine fetus. J Nutr 117:1181–1186.

Bruce NW, Abdul-Karim RW (1973): Relationships between fetal weight, placental weight and maternal placental circulation in the rabbit at different stages of gestation. J Reprod Fert 32:15–24.

Butler H, Juurlink BHJ (1987): An Atlas for Staging Mammalian and Chick Embryos. Boca Raton, CRC Press.

Cheek DB (1975): Appendix II: Data on normal fetal and postnatal Macaca mulatta. In Cheek DB (ed), Fetal and Postnatal Cellular Growth. Hoboken, Wiley, pp 521–534.

Coppoletta JM, Wolbach SB (1933): Body lengths and organ weights of infants and children: A study of the body length and normal weights of the more important vital organs of the body between birth and twelve years of age. Am J Pathol 9:55–70.

Davison AN, Wajda M (1959): Metabolism of myelin lipids: Estimation and separation of brain lipids in the developing rabbit. J Neurochem 4:353–359.

Dickerson JWT, Dobbing J (1967): Prenatal and postnatal growth and development of the central nervous system of the pig. Proc R Soc Lond B Biol Sci 166:384–395.

Dobbing J, Sands J (1979): Comparative aspects of the brain growth spurt. Early Hum Dev 3:79–83.

Done JT, Hebert CN (1968): The growth of the cerebellum in the foetal pig. Res Vet Sci 9:143–148.

Draper RL (1920): The prenatal growth of the guinea-pig. Anat Rec 18:369–392.

Dwyer CM, Madgwick AJA, Ward SS, Stickland NC (1995): Effect of maternal undernutrition in early gestation on development of fetal myfibres in the guinea-pig. Reprod Fertil Dev 7:1285–1292.

Edson JL, Hudson DG, Hull D (1975): Evidence for increased fatty acid transfer across the placenta during maternal fast in rabbits. Biol Neonate 27:50–55.

Edwards MJ, Wanner RA, Mulley RC (1976): Growth and development of the brain in normal and heat retarded guinea-pigs. Neuropathol Appl Neurobiol 2:439–450.

Frasch MG, Müller T, Wicher C, Weiss C, Löhle M, Schwab K, Schubert H, Nathanielsz PW, Witte OW, Schwab M (2007): Fetal body weight and the development of the control of the cardiovascular system in fetal sheep. J Physiol 579:893–907.

Goedbloed JF (1976): Embryonic and postnatal growth of rat and mouse. IV. Prenatal growth of organs and tissues: age determination, and general growth pattern. Acta Anat 95:8–33.

Guihard-Costa A-M, Ménez F, Delezoide A-L (2002): Organ weights in human fetuses after formalin fixation: Standards by gestational age and body weight. Pediatr Dev Pathol 5:559–578.

Hansen K, Sung CJ, Huang C, Pinar H, Singer DB, Oyer CE (2003): Reference values for second trimester fetal and neonatal organ weights and measurements. Pediatr Dev Pathol 6:160–167.

Hard DL, Anderson LL (1983): Nucleic acid content and growth of fetal brain, liver, and heart during inanitation in pigs. Biol Reprod 29:799–804.

Harel S, Watanabe K, Linke I, Schain RJ (1972): Growth and development of the rabbit brain. Biol Neonate 21:381–399.

Hudson DG, Hull D (1975): Growth of adipose tissue in the fetal rabbit. Biol Neonate 27:71–79.

Jones CT, Parer JT (1983): The effect of alterations in placental blood flow on the growth and nutrient supply to the fetal guinea-pig. J Physiol 343:525–537.

Kerr GR, Allen JR, Scheffler G, Couture J (1974): Fetal and postnatal growth of rhesus monkeys (M. mulatta). J Med Primatol 3:221–235.

Knight JW, Bazer FW, Thatcher WW, Franke DE, Wallace HD (1977): Conceptus development in intact and unilaterally hysterectomized-ovariectomized gilts: Interrelations among hormonal status, placental development, fetal fluids and fetal growth. J Anim Sci 44:620–637.

Lafeber HN, Rolph TP, Jones CT (1984): Studies on the growth of the fetal guinea pig: The effects of ligation of the uterine artery on organ growth and development. J Dev Physiol 6:441–459.

MacDowell EC, Allen E, MacDowell CG (1927): The prenatal growth of the mouse. J Gen Physiol 11:57–70.

Maroun LL, Graem N (2005): Autopsy standards of body parameters and fresh organ weights in

nonmacerated and macerated human fetuses. Pediatr Dev Pathol Off J Soc Pediatr Pathol Paediatr Pathol Soc 8:204–217.

Marrable AW, Ashdown RR (1967): Quantitative observations on pig embryos of known ages. J Agr Sci Camb 69:443–447.

McIntosh GH, Baghurst KI, Potter BJ, Hetzel BS (1979): Foetal brain development in the sheep. Neuropathol Appl Neurobiol 5:103–114.

Myers RE, Hill DE, Holt AB, Scott RE, Mellits ED, Cheek DB (1971): Fetal growth retardation produced by experimental placental insufficiency in the rhesus monkey. I. Body weight, organ size. Biol Neonate 18:379–394.

Myers SA, Sparks JW, Makawski EL, Meschia G, Battaglia FC (1982): Relationship between placental blood flow and placental and fetal size in guinea pig. Am J Physiol 243:H404-409.

Osgerby JC, Wathes DC, Howard D, Gadd TS (2002): The effect of maternal undernutrition on ovine fetal growth. J Endocrinol 173:131–141.

Pasqualani JR, Sumida C, Gelly C, Nguyen BL (1976): Specific [3H]-estradiol binding in the fetal uterus and testis of guinea pig: Quantitative evolution of [3H]-estradiol receptors in the differential fetal tissues (kidney, lung, uterus and testis) during fetal development. J Steroid Biochem 7:1031–1038.

Pond WG, Boleman SL, Fiorotto ML, Ho H, Knabe DA, Mersmann HJ, Savell JW, Su DR (2000): Perinatal ontogeny of brain growth in the domestic pig. Exp Biol Med 223:102–108.

Rattray PV, Robinson DW, Garrett WN, Ashmore RC (1975): Cellular changes in the tissues of lambs during fetal growth. J Anim Sci 40:783–788.

Renfree MB, Holt AB, Green SW, Carr JP, Cheek DB (1982): Ontogeny of the brain in a marsupial (Macropus eugenii) throughout pouch life. Brain Behav Evol 20:57–71.

Richardson C, Hebert CN (1978): Growth rates and patterns of organs and tissues in the ovine foetus. Br Vet J 134:181–189.

Sacher GA, Staffeld EF (1974): Relation of gestation time to brain weight for placental mammals: Implications for the theory of vertebrate growth. Am Nat 108:593–615.

Schneidereit M (1985): Study of fetal organ growth in Wistar rats from day 17 to 21. Lab Anim 19:240–244.

Sikov MR, Thomas JM (1970): Prenatal growth of the rat. Growth 34:1–14.

Singer D, Sung C, Wigglesworth J (1991): Fetal growth and maturation: With standards for body

and organ development. Textb Fetal Perinat Pathol 1:11–15.

Sparks JW, Girard JR, Callikan S, Battaglia FC (1985): Growth of fetal guinea pig: Physical and chemical characteristics. Am J Physiol 248:E132–139.

Taeusch HW, Carson SH, Wang NS, Avery ME (1973): Heroin induction of lung maturation and growth retardation in fetal rabbits. Semin Fetal Neonatal Med 82:869–875.

Thurley DC, Revfeim KJA, Wilson DA (1973): Growth of the Romney sheep foetus. New Zeal J Agr Res 16:111–114.

Tumbleson ME (1973): Brain weight, as a function of age, in miniature swine. Growth 37:13–17.

Ullrey DE, Sprague JI, Becker DE, Miller ER (1965): Growth of the swine fetus. J Anim Sci 24:711–717.

Vallet JL, Freking BA (2006): Changes in fetal organ weights during gestation after selection for ovulation rate and uterine capacity in swine. J Anim Sci 84:2338–2345.

Vidyasagar D, Chernick V (1975): Effect of metopirone on the synthesis of lung surfactant in does and fetal rabbits. Biol Neonate 27:1–16.

Wallace L (1945): The composition of sheep foetuses. J Physiol 104S:33P–34P.

Wilson JG, Fradkin R, Hardman A (1970): Breeding and pregnancy in rhesus monkeys used for teratological testing. Teratology 3:59–71.

Wingert F (1969): Biometrische Analyse der Wachstumsfunktionen von Hirnteilen und Körpergewicht der Albinomaus. J Hirnforschungen 11:133–197.

Workman AD, Charvet CJ, Clancy B, Darlington RB, Finlay BL (2013): Modeling transformations of neurodevelopmental sequences across mammalian species. J Neurosci 33:7368–7383.

Zilversmit DB, Remington M, Hughes LB (1972): Fetal growth and placental permeability in rabbits fed cholesterol. J Nutrition 102:1681–1688.

Chapter 2: Supporting Information

Dataset collection

Data on the weight of fetal brain, body, heart, liver, lung (x2), and kidney (x2), as well as post-conception age in days were collected from published literature. In experimental studies, values were taken from control animals only. When individual observations were not published in the original paper, data were reconstructed from figures using Photoshop CC and are labeled as such in the corresponding tables below. Most observations represent average values as originally published.

Data on neonatal brain and body size in the nine mammals described in this paper are taken from the following sources: human [Sacher & Staffeldt, 1974]; macaque [Kerr et al., 1974]; pig [Ullrey et al., 1965]; sheep [Sacher & Staffeldt, 1974]; rabbit [Edson et al., 1975]; guinea pig [Edwards et al., 1976]; mouse [Wingert, 1969]; rat [Sikov & Thomas, 1970; 21dg average]; wallaby [Renfree et al., 1982]. All other species' data on neonatal brain size, as well as gestation length for all species, is taken from Sacher & Staffeldt [1974] and Harvey & Clutton-Brock [1985]. Age estimates for Carnegie Stage 10 was taken from Butler & Juurlink [1987].

Gompertz & velocity models

For any given species and organ, individual studies differ systematically in age estimation, as reflected in intercept shifts in cube root models below. Accordingly, Gompertz models are best fit to brain growth data using representative fetal and early postnatal datasets rather than all available data. Sources used to fit Gompertz models are listed separately from subsequent cube-root model sources, which were fit to larger numbers of datasets. Gompertz models were fit to fetal, perinatal, and early postnatal data to improve model fit; as such, asymptotes do not reflect adult brain size, and velocity curves are only approximate. The primary function of growth models was to estimate the timing of peak velocity in a non-biased way in order to isolate exponential data for cube-root modeling.

Gompertz models were autofit to brain growth data using nonlinear least squares curve fitting with the nls function in the {stats} package for R. Velocity functions were calculated from the first order derivative of the Gompertz model. Estimates of the age of neurodevelopmental events in available species were taken from models developed from empirical data [Workman et al., 2013] and available on the Translating Time website (translatingtime.net). Neurodevelopmental events were coded as involving neurogenesis, tract formation, or myelination and fit to velocity curves in available species.

Cube Root Models

Brain growth data preceding peak velocity, as calculated from Gompertz autofit functions, were considered exponential and were included in cube root models. In species born earlier than peak velocity, all exponential data (including early postnatal data) were included in this analysis. Whole body growth data includes all fetal data in each species, as body growth peak velocity is always postnatal. Exponential growth data for liver, heart, lungs, and kidneys were isolated by visually inspecting cube-root data, determining a point of growth deceleration, and removing

values older that.

Cube root models were calculated separately by data source for each organ and species to minimize artifacts introduced from differences in age estimation across studies (i.e. intercept shifts; see cube root models below). Exponential data from each study was cube-root transformed, and ordinary least squares (OLS) models were fit predicting cube-root weight in grams from days post-conception. Model parameters were then averaged across available studies to produce a final slope estimate for statistical tests.

Instantaneous growth rate calculation

Data preceding peak velocity, as calculated in Gompertz models, are included for each species. Instantaneous velocities (g/d) were calculated by taking the slope between adjacent data points according to increasing age (i.e. $(mass_2 - mass_1)/(age_2 - age_1)$). As sources differ in post-conceptual age approximation, reflected as intercept shifts along cube-root models, velocities were calculated separately by source. Data was averaged by day post-conception in mouse [Goedbloed, 1976; Wingert, 1969] and rat [Goedbloed, 1976] to allow velocity calculation between time periods.

Instantaneous velocity calculated from raw data regularly indicates unlikely values, such as sudden decreases in velocity (i.e. negative values) or abnormally high or low velocities at a given brain size, often caused by samples over short age intervals (e.g. the smallest brain sizes) (Fig. S3.1C). Negative velocities were removed from the sample. To remove remaining outlier values, ordinary least squares regression models were fit to velocities according to brain size in log-log coordinates for each individual species subsample. Values outside of the 95% confidence interval were removed.

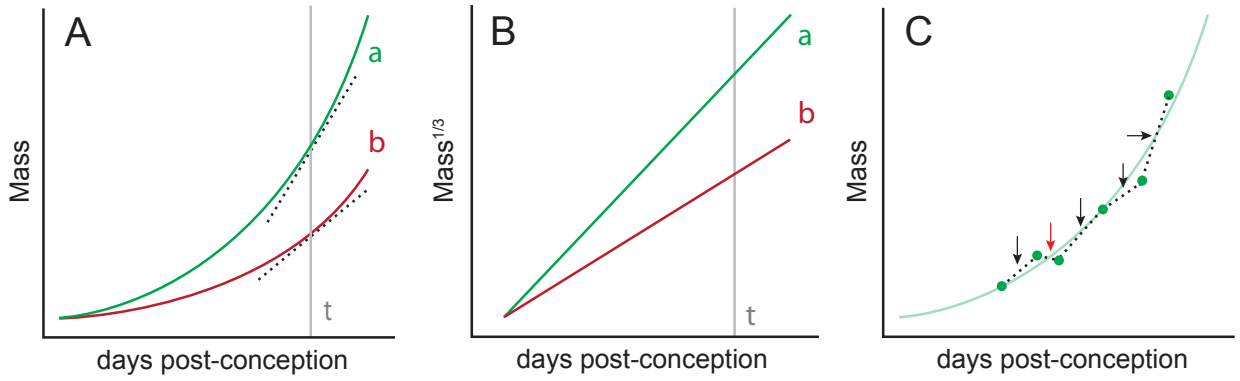

Figure S3.1. Models of exponential growth using a set exponent, traditionally cubic, can be used to compare growth acceleration using a single variable, slope. (A) Two cubic functions with higher (a) and lower (b) coefficients differ in mass size and growth velocity (dotted line) at any given time (t) following an identical onset of exponential growth. (B) Linear models fit to cube-root transformed mass show differences in slope, corresponding to the relative acceleration rate of brain growth in species (a). (C) Instantaneous velocity can also be calculated directly from raw data by taking the slope between two points (dotted lines) and assigning it to average brain mass or age. However, this method produces artifacts (red arrow), particularly in clustered data.

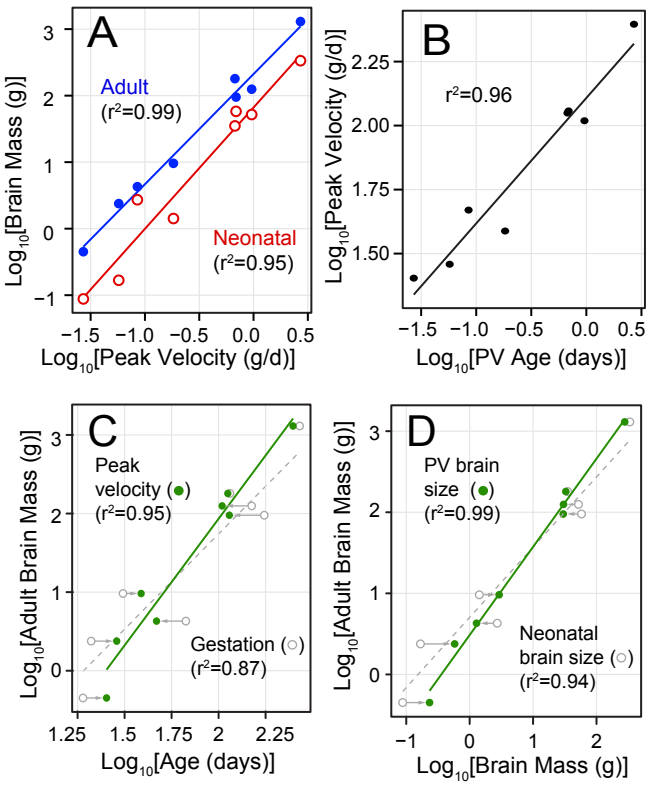

Figure S3.2. (A) Peak brain velocity (g/d) predicts both neonatal (red) and adult (blue) brain size. (B) Age of peak velocity predicts peak velocity. (C) Age of peak velocity is a better predictor of adult brain size than is total gestation length. (D) Brain size at peak velocity is a better predictor of adult brain size than is neonatal brain size.

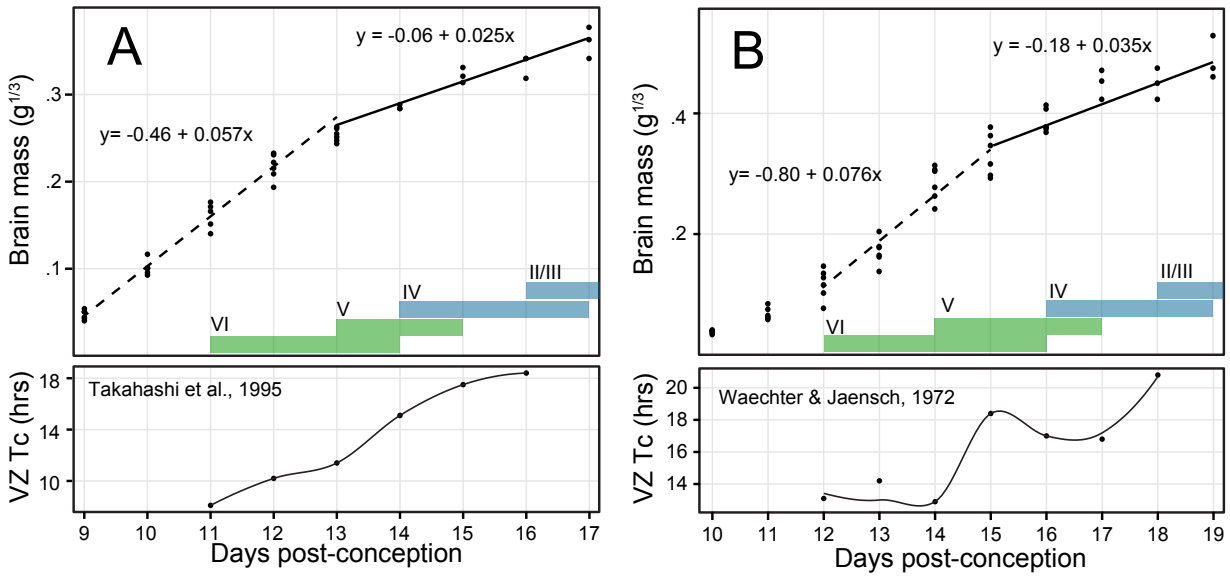

Figure S3.3. Embryonic brain growth in (A) mouse and (B) rat from an exceptional dataset [Goedbloed, 1976] shows more rapid growth rates prior to E13 and E15, respectively. Color bars indicate windows of cortical neurogenesis by layer, taken from neurodevelopmental event models [Workman et al., 2013]. Below, cell cycle duration (Tc) in the ventricular zone (VZ) of each species increases as larger proportions of progenitors enter neurogenic (asymmetric) division. Whole brain growth rates decelerate and cell cycle duration increases sharply around the onset of layer IV neurogenesis, which is thought to coincide with the contraction of the symmetrically dividing progenitor pool [Caviness et al. 1995].

Table S3.1 Organ slope averages

Average slope values from brain (S3.4-S3.14), whole body (table S3.6; figure S3.14) and visceral organ (tables S3.7-S3.10; figures S3.15-S3.18) OLS models predicting $(mass)^{1/3}$ from days post-conception.

	Body	*Brain*	*Liver*	*Heart*	*Lungs*	*Kidneys*
Homo sapiens	0.0654	0.0326	0.0230	0.0128	0.0175	0.0141
Macaca mulatta	0.0648	0.0331	0.0231	0.0114	0.0179	0.0125
Ovis aries	0.1687	0.0387	0.0514	0.0316	0.0552	0.0278
Sus scrofa	0.1027	0.0371	0.0270	0.0200	0.0330	0.0201
Orycto. cuniculus	0.1803	0.0473	0.0917	0.0434	0.0517	0.0493
Cavia porcellus	0.0887	0.0316	0.0296	0.0151	0.0295	0.0194
Mus musculus	0.1019	0.0250	0.0555	0.0157		0.0225
Rattus rattus	0.1616	0.0356	0.0768	0.0335	0.0621	0.0356
Euth. var. (x1000)	**2.1851**	**0.0415**	**0.6896**	**0.1377**	**0.3310**	**0.1494**
Macropus eugenii		0.0123				
Monodelphis dom.		0.0133				
C. virgianus		0.0416				
M. undulates		0.0345				

Table S3.2 Organ variance F tests.

Comparison of variance in average slope values for brain vs. whole body, liver, heart, lungs, and kidneys. Values are given for the whole eutherian sample (n=8).

vs. Brain	*F stat.*	*df*	*p*	
Body	52.62	(7,7)	0.000	***
Liver	16.61	(7,7)	0.002	**
Heart	3.32	(7,7)	0.136	
Lungs	7.97	(6,7)	0.015	*
Kidneys	3.60	(7,7)	0.113	

Table S3.3 Organ slope correlation table

	Total eutherian sample (n=8)					
	Body	*Brain*	*Liver*	*Heart*	*Kidneys*	*Lungs*
Body		0.680	0.876**	0.967***	0.909**	0.961***
Brain	0.483		0.521	0.810*	0.722*	0.596
Liver	0.820*	-0.001		0.890**	0.956***	0.855*
Heart	0.978***	0.593	0.789*		0.960***	0.899**
Kidneys	0.934**	0.291	0.932**	0.930**		0.823*
Lungs	0.986***	0.683	0.939**	0.989***	0.983***	
	Rabbit removed (n=7)					

Table S3.4 Organ slope regression models

EV: Body cube root slope	slope	int.	*t*	*p*	df	r^2	*sig.*
Brain cube root slope	0.094	0.03	2.27	0.064	6	0.46	ns
Rabbit removed	0.052	0.03	1.24	0.272	5	0.23	ns
Liver cube root slope	0.492	-0.01	4.44	0.004	6	0.77	**
Rabbit removed	0.402	0.00	3.21	0.024	5	0.67	*
Heart cube root slope	0.243	-0.01	9.33	0.000	6	0.94	***
Rabbit removed	0.209	0.00	10.56	0.000	5	0.96	***
Lungs cube root slope	0.349	0.00	7.74	0.001	6	0.92	***
Rabbit removed	0.402	-0.01	11.61	0.000	5	0.97	***
Kidneys cube root slope	0.238	0.00	5.33	0.002	6	0.83	**
Rabbit removed	0.176	0.00	5.83	0.012	5	0.87	*

Table S3.5 OLS bivariate regression models

Dependent variable *Explanatory variable*	slope	int.	*t*	*p*	df	r^2	*sig.*
Log_{10}(adult brain [g])							
Log_{10}(peak velocity [g/d])	1.66	2.33	20.20	0.000	6	0.99	***
Log_{10}(gestation [d])	2.42	-3.11	6.20	0.000	6	0.87	***
Log_{10}(PV age [d])	3.22	-4.51	11.17	0.000	6	0.95	***
Log_{10}(neo brain [g])	0.87	0.70	10.01	0.000	6	0.94	***
Log_{10}(PV brain [g])	1.09	0.49	27.87	0.000	6	0.99	***
Log_{10}(neo. brain [g])							
Log_{10}(peak velocity [g/d]) Log_{10}(gestation [d]) Log_{10}(PV age [d])	1.82	1.82	10.50	0.000	6	0.95	***
Log_{10}(Peak velocity [g/d])							
Log_{10}(PV age [d])	0.01	-0.38	12.08	0.000	6	0.96	***
Brain cube root slope							
Placental type (dummy)	0.00	0.04	-0.68	0.524	6	0.07	ns
Relative BMR	0.00	0.04	-1.69	0.142	6	0.32	ns
Altricial/precocial (dummy)	0.00	0.03	0.26	0.801	6	0.01	ns
Neonatal brain/body ratio							
Brain cube root slope	-2.50	0.14	-1.32	0.234	6	0.23	ns
Body cube root slope	-0.55	0.16	-2.90	0.027	6	0.58	*
Allometric RGP slope							
Brain cube root slope	-12.46	1.32	-2.73	0.042	5	0.60	*
(Rabbit removed)	-11.24	1.28	-1.44	0.223	4	0.34	ns
Body cube root slope	-2.10	1.12	-6.09	0.002	5	0.88	**
(Rabbit removed)	-1.89	1.11	-4.59	0.010	4	0.84	*

Fig. S3.4 Human brain growth models

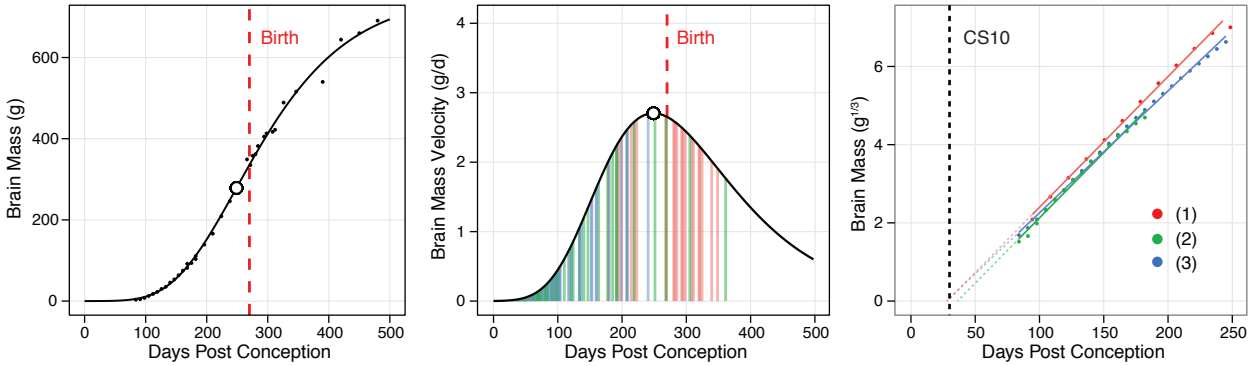

Species	*Homo sapiens*		**Peak velocity**	2.705	g/d
Gestation	270	dpc	**PV age**	248.9	dpc
Carnegie Stage 10:	29	dpc	**PV brain size**	278.7	g

Gompertz model: Singer et al., 1998; Coppoletta & Wolbach, 1933; Hansen et al., 2003

OLS regression: (dpc) predicting (brain mass [g])$^{1/3}$

	Source	*slope*	*y-int.*	*x-int.*	r^2
(1)	Guihard-Costa et al. 2002	0.0334	-0.94	28.2	1.00
(2)	Hansen et al., 2003	0.0333	-1.21	36.2	0.99
(3)	Maroun & Graem, 2005	0.0312	-0.86	27.6	1.00
	Average	**0.0327**	**-1.00**	**30.7**	**n/a**

Fig. S3.5 Rhesus macaque brain growth models

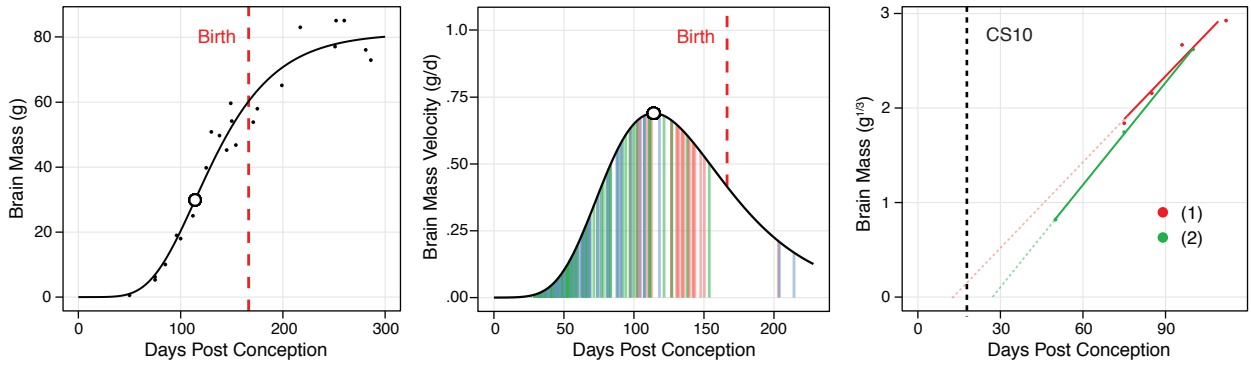

Species	*Macaca mulatta*		**Peak velocity**	0.690	g/d
Gestation	166.5	dpc	**PV age**	114.1	dpc
Carnegie Stage 10:	22	dpc	**PV brain size**	29.90	g

Gompertz model: Cheek, 1975; Kerr et al., 1974

OLS regression: (dpc) predicting (brain mass[g])$^{1/3}$

	Source	*slope*	*y-int.*	*x-int.*	r^2
(1)	Cheek, 1975	0.0303	-0.39	12.8	0.96
(2)	Kerr et al., 1974	0.0360	-0.97	27.0	1.00
	Average	**0.0331**	**-0.68**	**19.9**	**n/a**

Fig. S3.6 Sheep brain growth models

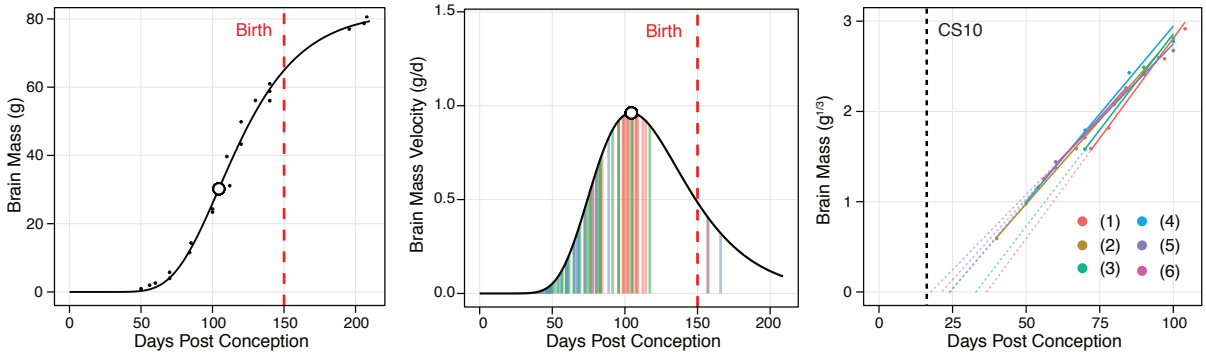

Species	*Ovis aries* (sheep)		**Peak velocity**	0.961	g/d
Gestation	150	dpc	**PV age**	104.45	dpc
Carnegie Stage 10:	16	dpc	**PV brain size**	30.22	g

Gompertz model: Rattray et al, 1975; Wallace, 1945; Richardson & Hebert, 1978; Duncan et al., 2004

		OLS regression: (dpc) predicting (brain mass [g])$^{1/3}$			
	Source	*slope*	*y-int.*	*x-int.*	r^2
(1)	Barcroft, 1946	0.0443	-1.62	36.6	1.00
(2)	McIntosh et al., 1979	0.0371	-0.88	23.7	1.00
(3)	Rattray et al., 1975	0.0426	-1.40	32.8	1.00
(4)	Richardson & Hebert, 1979	0.0390	-0.95	24.4	1.00
(5)	Thurley et al., 1973	0.0333	-0.59	17.6	1.00
(6)	Wallace, 1945	0.0360	-0.76	21.2	1.00
	Average	**0.0387**	**-1.03**	**26.1**	**n/a**

Fig. S3.7 Pig brain growth models

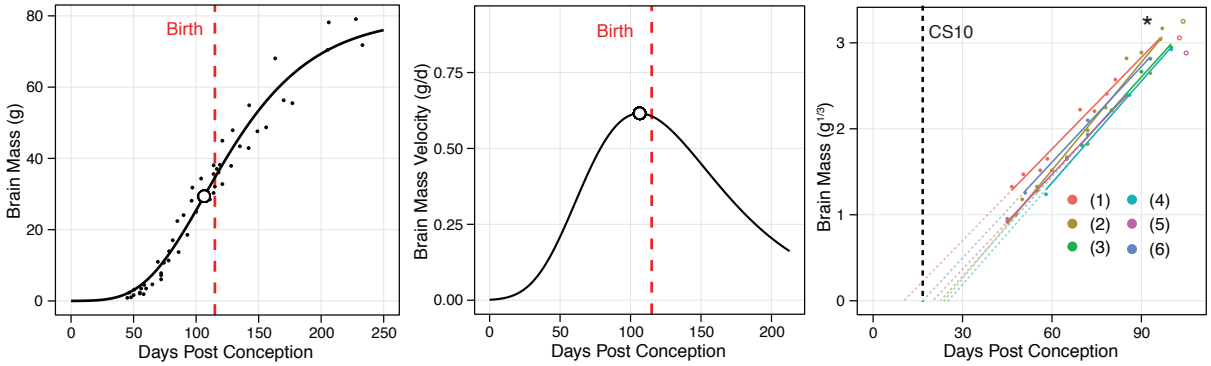

Species	*Sus scrofa* (pig)		**Peak velocity**	0.674	g/d
Gestation	150	dpc	**PV age**	111.98	dpc
Carnegie Stage 10:	16	dpc	**PV brain size**	32.86	g

Gompertz model: Dickerson & Dobbing, 1967; Done & Hebert, 1968; Tumbleson, 1973
* Three decelerated values removed from models

		OLS regression: (dpc) predicting (brain mass [g])$^{1/3}$			
	Source	*slope*	*y-int.*	*x-int.*	r^2
(1)	Dickerson & Dobbing, 1967	0.0334	-0.23	7.0	0.98
(2)	Done & Herbert, 1968	0.0412	-0.95	23.1	0.98
(3)	Pond et al., 2000	0.0386	-0.87	22.6	0.99
(4)	Tumbleson, 1973	0.0394	-0.99	25.2	0.99
(5)	Ullrey et al., 1965	0.0371	-0.62	16.6	1.00
(6)	Vallet & Freking, 2006	0.0331	-0.52	15.8	0.99
	Average	**0.0371**	**-0.70**	**18.4**	**n/a**

Fig. S3.8 Mouse brain growth models

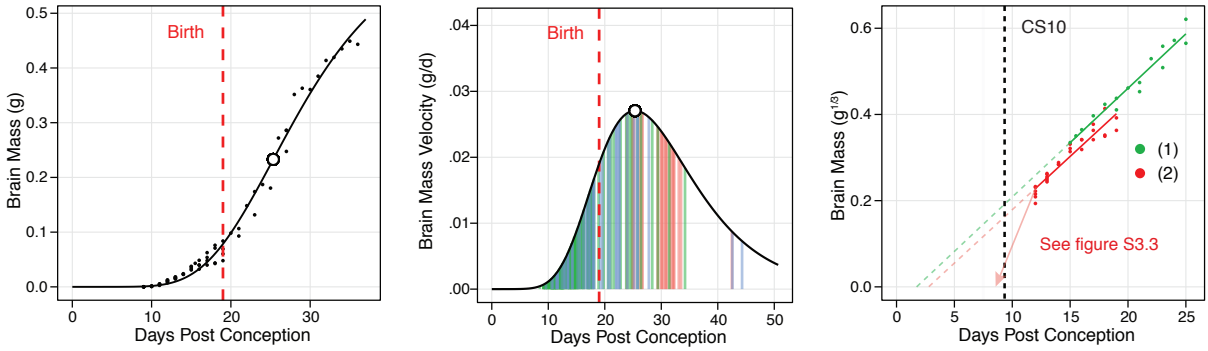

Species	*Mus musculus* (mouse)		**Peak velocity**	0.0271	g/d
Gestation	19	dpc	**PV age**	25.35	dpc
Carnegie Stage 10:	9.5	dpc	**PV brain size**	0.233	g

Gompertz model: Wingert, 1967; Goedbloed, 1976

OLS regression: (dpc) predicting (brain mass [g])$^{1/3}$

	Source	*slope*	*y-int.*	*x-int.*	r^2
(1)	Wingert, 1967	0.0252	-0.04	1.7	0.95
(2)	Goedbloed, 1976	0.0248	-0.07	2.8	0.91
	Average	**0.0250**	**-0.06**	**2.3**	**n/a**

Fig. S3.9 Rat brain growth models

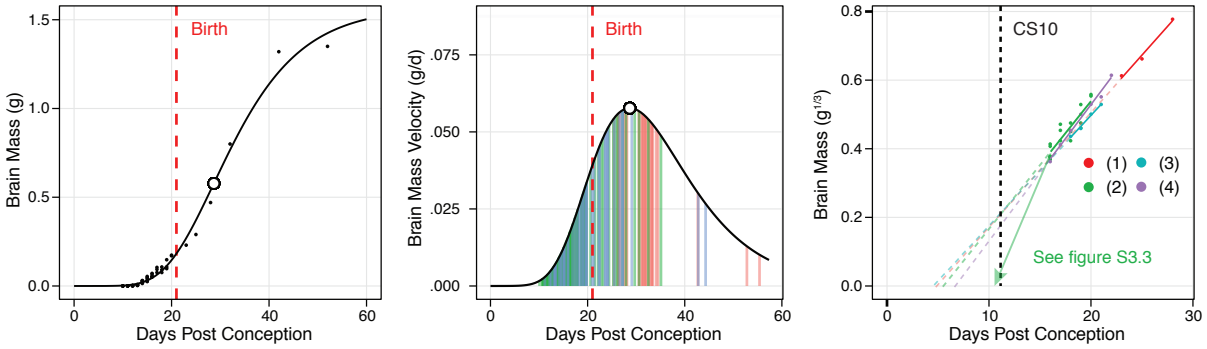

Species	*Rattus rattus* (rat)		**Peak velocity**	0.0574	g/d
Gestation	21	dpc	**PV age**	28.73	dpc
Carnegie Stage 10:	11	dpc	**PV brain size**	0.580	g

Gompertz model: Gille et al., 1996; Goedbloed, 1976

OLS regression: (dpc) predicting (brain mass [g])$^{1/3}$

	Source	*slope*	*y-int.*	*x-int.*	r^2
(1)	Gille et al., 1996	0.0334	-0.16	4.9	0.99
(2)	Goedbloed, 1976	0.0372	-0.21	5.5	0.82
(3)	Schneidereit, 1985	0.0321	-0.14	4.5	0.99
(4)	Sikov & Thomas, 1970	0.0397	-0.26	6.7	0.99
	Average	**0.0356**	**-0.68**	**5.4**	**n/a**

Fig. S3.10 Guinea pig brain growth models

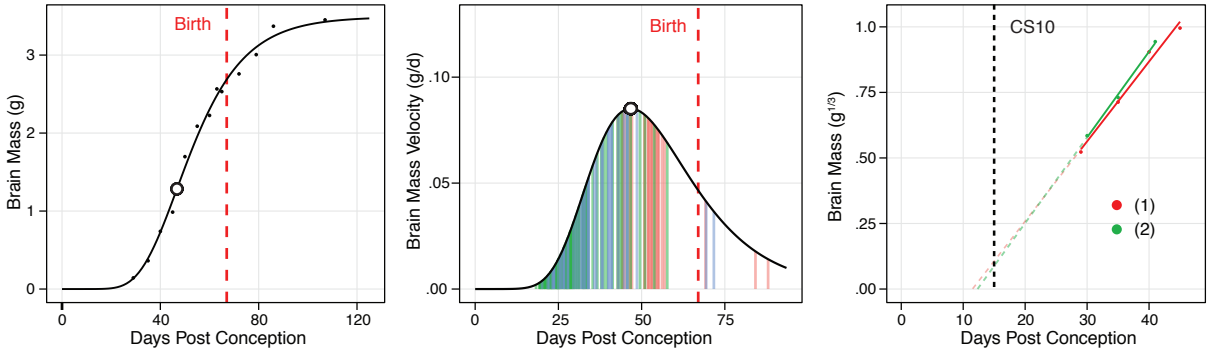

Species	*Cavia porcellus* (guinea pig)		**Peak velocity**	0.0852	g/d
Gestation	67	dpc	**PV age**	46.76	dpc
Carnegie Stage 10:	14.5	dpc	**PV brain size**	1.284	g

Gompertz model: Dobbing & Sands, 1970

		OLS regression: (dpc) predicting (brain mass [g])$^{1/3}$			
	Source	*slope*	*y-int.*	*x-int.*	r^2
(1)	Dobbing & Sands, 1970*	0.0304	-0.35	11.5	0.98
(2)	Edwards et al., 1976	0.0327	-0.40	12.3	1.00
	Average	**0.0316**	**-0.38**	**11.9**	**n/a**

Fig. S3.11 Rabbit brain growth models

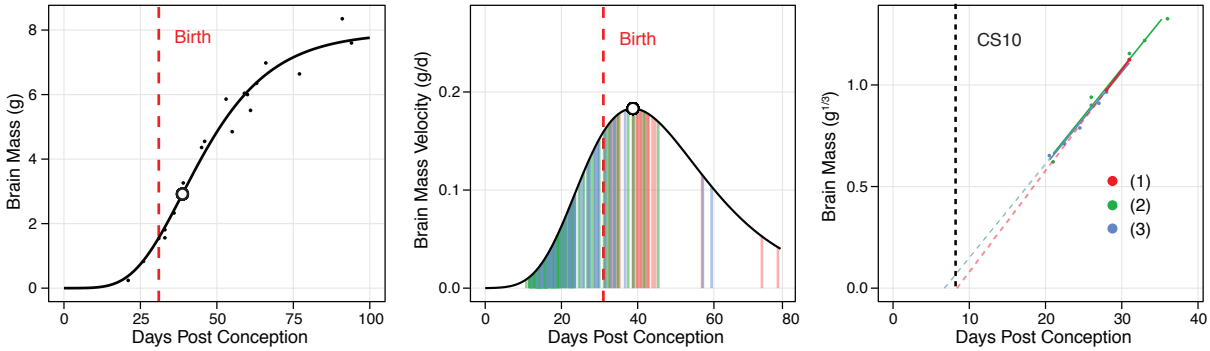

Species	*Oryctolagus cuniculus* (rabbit)		**Peak velocity**	0.183	g/d
Gestation	31	dpc	**PV age**	38.73	dpc
Carnegie Stage 10:	8.5	dpc	**PV brain size**	2.917	g

Gompertz model: Harel et al., 1972; Davison & Wadja, 1959

		OLS regression: (dpc) predicting (brain mass [g])$^{1/3}$			
	Source	*slope*	*y-int.*	*x-int.*	r^2
(1)	Edson et al., 1975	0.0498	-0.42	8.4	0.99
(2)	Harel et al., 1972	0.0465	-0.32	6.8	0.82
(3)	Hudson et al., 1975	0.0457	-0.31	6.7	0.99
	Average	**0.0473**	**-0.35**	**7.3**	**n/a**

Fig. S3.12 Wallaby brain growth models

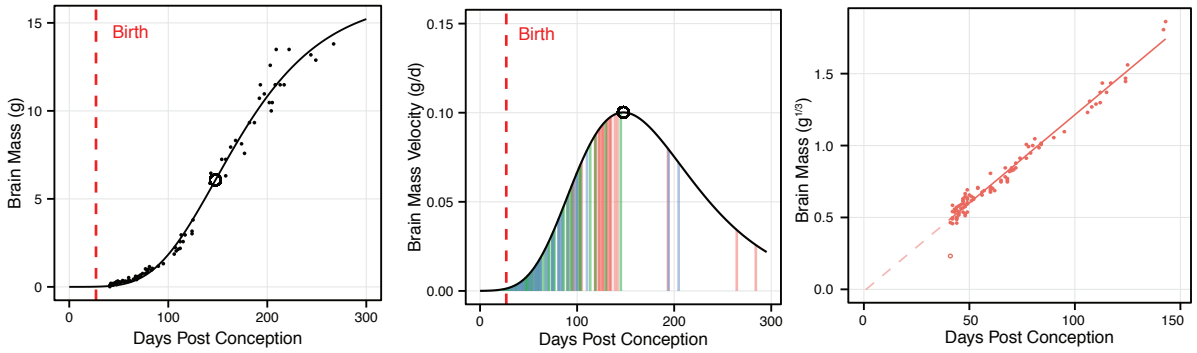

Species	*Macropus eugenii* (wallaby)	**Peak velocity**	0.100	g/d
Gestation	27 dpc	**PV age**	147.64	dpc
Carnegie Stage 10:	unknown	**PV brain size**	6.068	g

Gompertz model: Renfree et al., 1982

		OLS regression: (dpc) predicting (brain mass)$^{1/3}$			
	Source	*slope*	*y-int.*	*x-int.*	r^2
(1)	**Renfree et al., 1982**	**0.0123**	**-0.01**	**0.97**	**0.97**

Fig. S3.13 Bird and opossum brain growth models

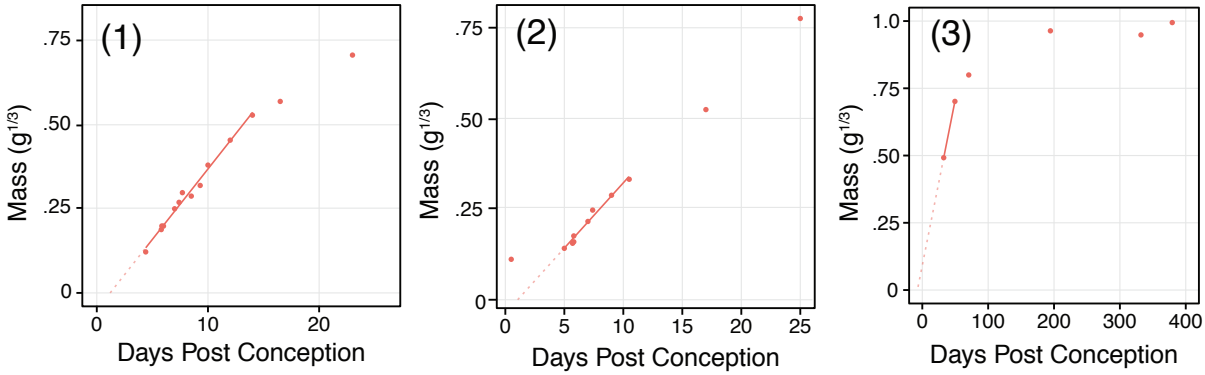

		OLS regression: (dpc) predicting (brain mass)$^{1/3}$			
	Source	*slope*	*y-int.*	*x-int.*	r^2
(1)	**Quail (*C. virgianus*)** Striedter & Charvet, 2008	**0.0416**	**-0.05**	**1.20**	**0.99**
(2)	**Parakeet (*M. undulatus*)** Striedter & Charvet, 2008	**0.0345**	**-0.03**	**0.87**	**0.98**
(3)	**Opossum (*M. domestica*)** Seelke et al., 2013	**0.0133**	**0.06**	**-4.50**	**n/a**

Fig. S3.14 Fetal body growth cube-root regression models

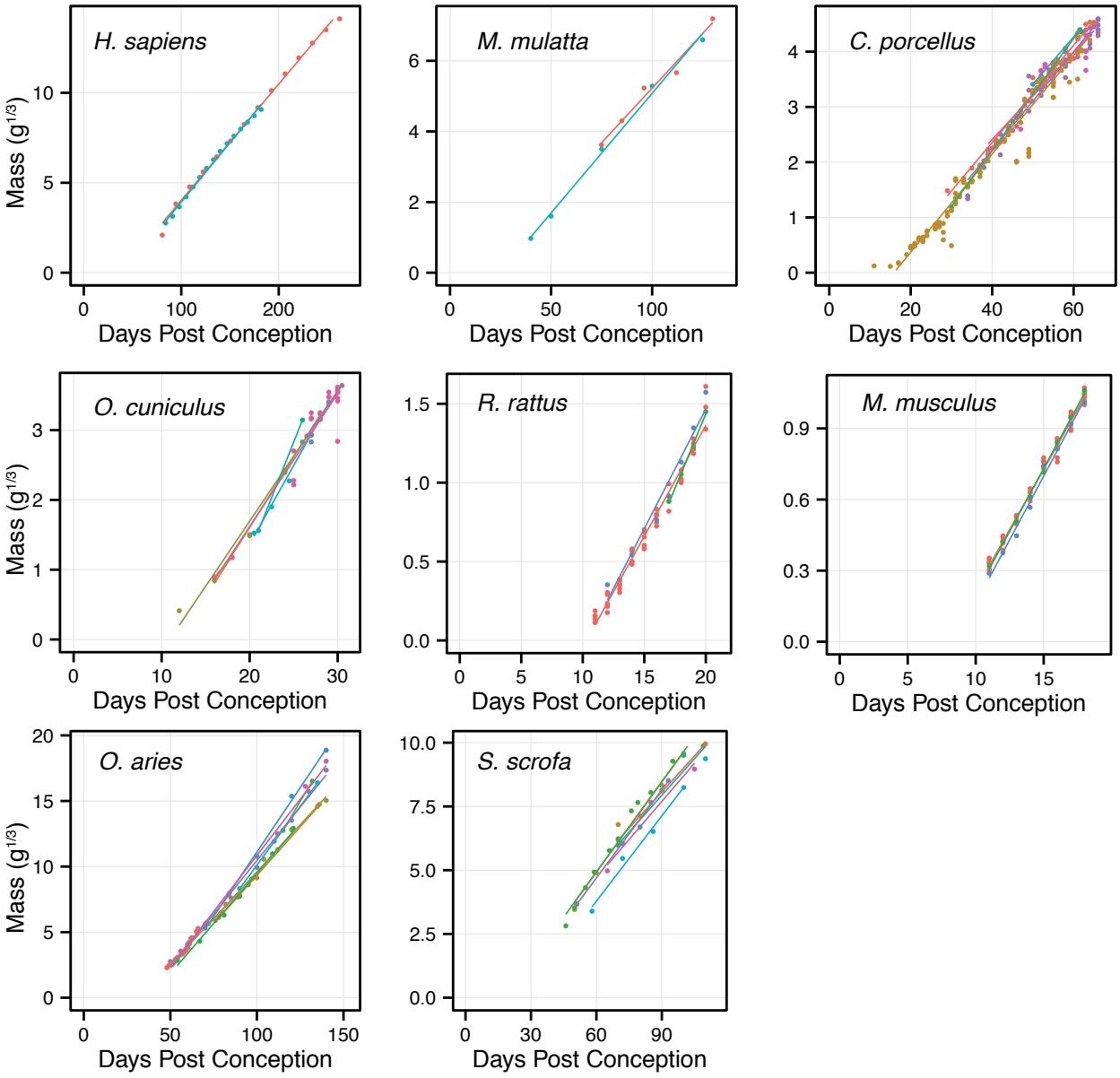

Table S3.6 Fetal body growth cube root models by source

Species	Source	beta	y-int.	x-int.	r^2
H. sapiens	Hansen et al., 2003	0.0661	-2.68	40.6	1.00
	Guihard-Costa et al., 2002	0.0646	-2.44	37.7	1.00
	Average	**0.0654**	**-2.56**	**39.2**	**N/A**
M. mulatta	Kerr et al., 1974	0.0678	-1.70	25.0	1.00
	Cheek, 1975	0.0619	-0.97	15.6	0.98
	Average	**0.0648**	**-1.33**	**20.3**	**N/A**
C. porcellus	Sparks et al., 1985	0.0787	-0.74	9.4	0.88
	Myers et al., 1982	0.0893	-1.36	15.2	0.95
	Lafeber et al., 1984	0.0859	-0.89	10.3	1.00
	Edwards et al., 1976	0.1012	-1.83	18.1	1.00
	Draper, 1920	0.0891	-1.41	15.9	0.96
	Dobbing & Sands, 1970*	0.0879	-1.16	13.2	0.98
	Average	**0.0887**	**-1.23**	**13.7**	**N/A**
O. cuniculus	Abdul-Karim & Bruce, 1972	0.1403	-1.35	9.6	1.00
	Bruce & Abdul-Karim, 1973	0.2013	-2.42	12.0	1.00
	Davison & Wadja, 1959	0.1866	-2.04	10.9	0.99
	Harel et al., 1972**	0.3169	-5.09	16.1	1.00
	Vidyasagar & Chernick, 1975	0.1825	-1.92	10.5	1.00
	Zilversmit et al., 1972	0.1907	-2.19	11.5	0.92
	Average	**0.1803**	**-1.98**	**10.9**	**N/A**
R. rattus	Goedbloed, 1976	0.1452	-1.53	10.5	0.97
	Schneidereit, 1985	0.1882	-2.33	12.4	1.00
	Sikov & Thomas, 1970	0.1515	-1.56	10.3	0.96
	Average	**0.1616**	**-1.80**	**11.1**	**N/A**
M. musculus	Goedbloed, 1976	0.1026	-0.81	7.9	0.99
	MacDowell et al., 1927	0.1027	-0.81	7.9	1.00
	Wingert, 1969	0.1005	-0.81	8.0	0.99
	Average	**0.1019**	**-0.81**	**7.9**	**N/A**
O. aries	Astrom, 1967	0.1389	-4.39	31.7	0.98
	Barcroft, 1946	0.1435	-4.75	33.1	1.00
	Bell et al., 1987	0.1480	-5.47	37.0	1.00
	Frasch et al., 2007	0.2213	-12.69	57.3	1.00
	McIntosh et al., 1979	0.1527	-5.79	37.9	1.00
	Osgerby et al., 2002	0.1793	-7.83	43.7	1.00
	Rattray et al., 1975	0.1964	-8.53	43.4	1.00
	Richardson & Hebert, 1978*	0.1671	-6.32	37.8	1.00
	Wallace, 1945	0.1714	-6.29	36.7	1.00
	Average	**0.1687**	**-6.90**	**39.8**	**N/A**
S. scrofa	Hard & Anderson, 1983	0.0944	-0.43	4.6	1.00
	Knight et al., 1977	0.1090	-1.38	12.6	0.97
	Marrable & Ashdown, 1967	0.1120	-1.63	14.6	0.97
	Pond et al., 2000	0.0961	-0.72	7.4	0.93
	Tumbleson, 1973	0.1029	-2.91	26.1	0.99
	Ullrey et al., 1965	0.1040	-2.21	19.2	1.00
	Vallet & Freking, 2006	0.0997	-1.28	12.8	0.96
	Average	**0.1026**	**-1.18**	**10.5**	**N/A**

* Note: original data in this paper was unavailable, and was reconstructed from plots published as figures.
** Outlier excluded from the average.

Fig. S3.15 Fetal liver growth cube-root regression models

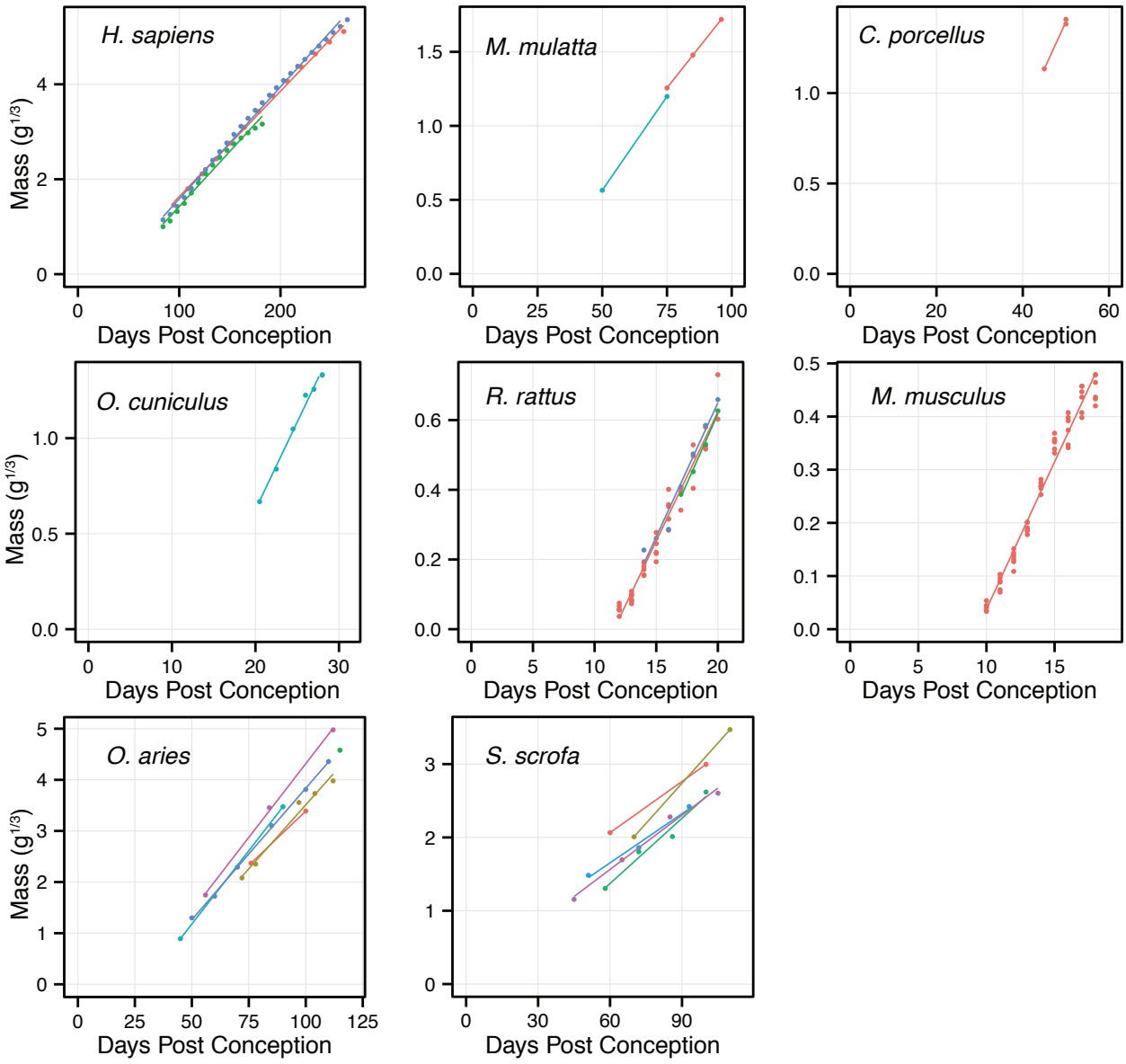

Table S3.7 Fetal liver growth cube root models by source

Species	Source	beta	y-int.	x-int.	r^2
H. sapiens	Guihard-Costa et al., 2002	0.0222	-0.59	26.5	1.00
	Hansen et al., 2003	0.0232	-0.90	38.6	0.99
	Maroun & Graem, 2005	0.0236	-0.77	32.7	1.00
	Average	**0.0230**	**-0.75**	**32.6**	**N/A**
M. mulatta	Cheek, 1975	0.0221	-0.40	18.1	1.00
	Kerr et al., 1974	0.0242	-0.64	26.3	1.00
	Average	**0.0231**	**-0.52**	**22.2**	**N/A**
C. porcellus	**Composite data**[1]	**0.0296**	**-0.15**	**4.9**	**0.94**
O. cuniculus	**Hudson & Hull, 1975**	**0.0917**	**-1.21**	**13.2**	**0.99**
R. rattus	Goedbloed, 1976	0.0741	-0.86	11.6	0.96
	Schneidereit, 1985	0.0796	-0.97	12.2	0.99
	Sikov & Thomas, 1970	0.0768	-0.89	11.6	0.97
	Average	**0.0768**	**-0.91**	**11.8**	**N/A**
M. musculus	**Goedbloed, 1976**	**0.0555**	**-0.52**	**9.3**	**0.97**
O. aries	Bell et al., 1987	0.0425	-0.86	20.2	1.00
	Barcroft, 1946	0.0501	-1.50	29.9	0.99
	Osgerby et al., 2002	0.0574	-1.69	29.5	1.00
	Richardson & Hebert, 1978*	0.0495	-1.18	23.8	1.00
	Wallace, 1945	0.0577	-1.45	25.2	1.00
	Average	**0.0514**	**-1.34**	**25.7**	**N/A**
S. scrofa	Hard & Anderson, 1983	0.0366	-0.55	15.1	1.00
	Hafez et al., 1958	0.0242	0.60	-24.8	1.00
	Tumbleson, 1973	0.0262	-0.16	6.0	0.96
	Ullrey et al., 1965	0.0232	0.26	-11.1	0.99
	Vallet & Freking, 2006*	0.0246	0.09	-3.5	0.99
	Average	**0.0270**	**-0.47**	**-3.7**	**N/A**

1. Data was combined from Jones & Parer, 1983, Lafeber et al., 1984, and Dwyer et al. 1995 to produce this estimate. Data from Jones & Parer was incorrectly listed in the original paper as 26.4g liver at ~34g body size; in this analysis it is corrected to 2.64g liver size at 50dpc, which is consistent with other sources.

* Note: original data in this paper was unavailable, and was reconstructed from plots published as figures.
** Note: Beta values for these studies are not included in the average, as x-intercepts indicate the onset of exponential growth prior to conception.

Fig. S3.16 Fetal heart growth cube-root regression models

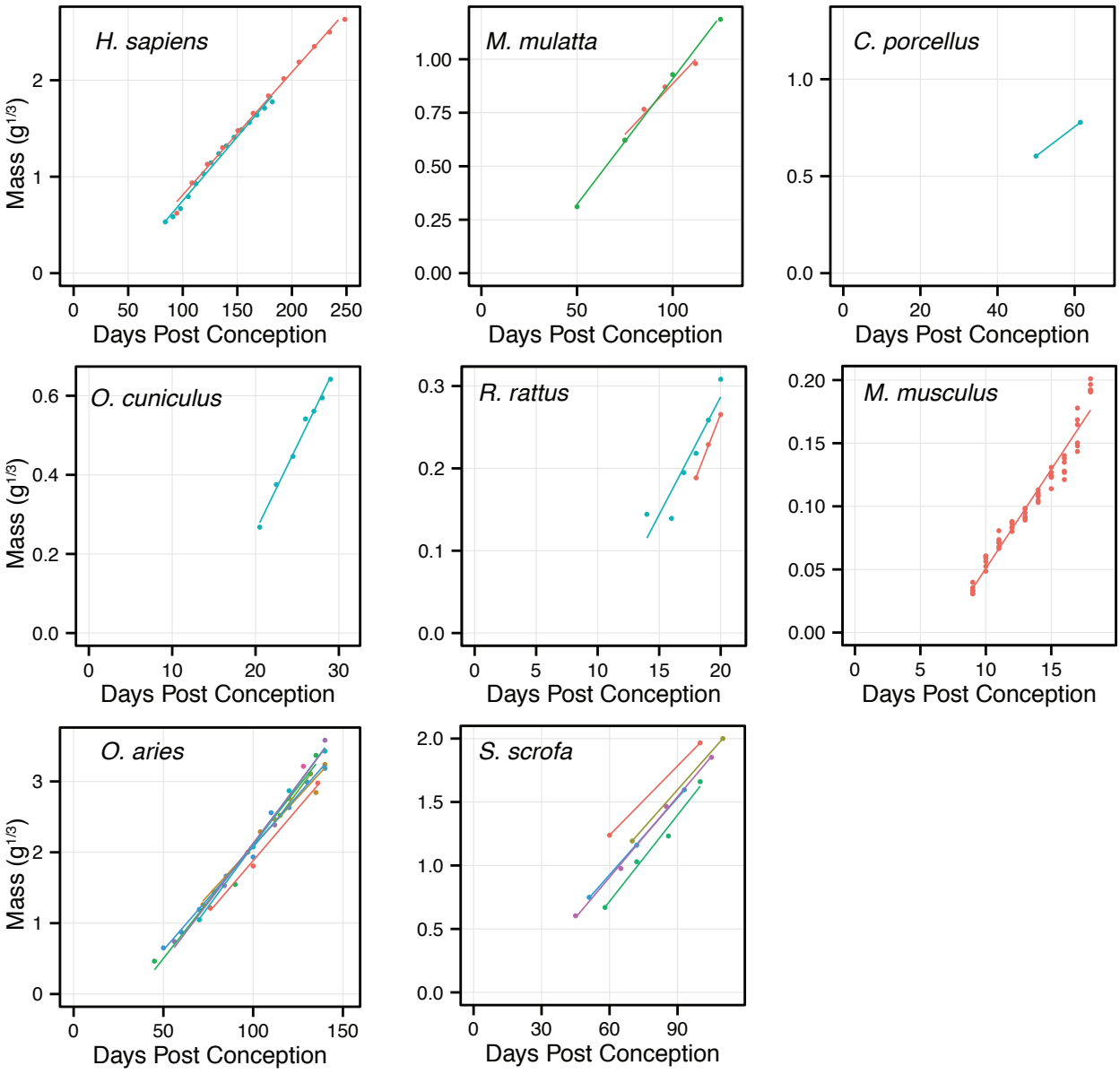

Table S3.8 Fetal heart growth cube root models by source

Species	Source	beta	y-int.	x-int.	r^2
H. sapiens	Guihard-Costa et al., 2002	0.0124	-0.42	33.4	0.99
	Hansen et al., 2003	0.0133	-0.57	43.4	0.99
	Average	**0.0128**	**-0.50**	**38.4**	**N/A**
M. mulatta[1]	Cheek, 1975	0.0110	-0.19	17.5	0.97
	Kerr et al., 1974	0.0117	-0.27	22.6	1.00
	Average	**0.0114**	**-0.23**	**20.0**	**N/A**
C. porcellus	**Lafeber et al., 1984**	**0.0151**	**-0.15**	**10.1**	**1.00**
O. cuniculus	**Hudson & Hull, 1975**	**0.0434**	**-0.61**	**14.1**	**0.99**
R. rattus	Schneidereit, 1985	0.0385	-0.50	13.1	1.00
	Sikov & Thomas, 1970	0.0286	-0.29	10.0	0.88
	Average	**0.0335**	**-0.40**	**11.55**	**N/A**
M. musculus	**Goedbloed, 1976**	**0.0157**	**-0.11**	**6.8**	**0.96**
O. aries	Bell et al., 1987	0.0296	-1.08	36.4	1.00
	Barcroft, 1946	0.0277	-0.68	24.6	0.98
	Frasch et al., 2007	0.0346	-1.45	42.1	1.00
	Osgerby et al., 2002	0.0323	-1.11	34.4	0.98
	Rattray et al., 1975	0.0345	-1.36	39.3	1.00
	Richardson & Hebert, 1978*	0.0292	-0.84	28.7	0.99
	Wallace, 1945	0.0335	-1.22	36.5	0.99
	Average	**0.0316**	**-1.11**	**34.6**	**N/A**
S. scrofa	Hard & Anderson, 1983	0.0202	-0.22	10.8	1.00
	Hafez et al., 1958**	0.0195	0.06	-8.1	1.00
	Tumbleson, 1973	0.0201	-0.46	22.7	0.97
	Ullrey et al., 1965	0.0186	-0.18	9.7	1.00
	Vallet & Freking, 2006	0.0212	-0.36	17.2	1.00
	Average	**0.0200**	**-0.30**	**15.1**	**N/A**

1. Data after 145dpc was excluded as it had already decelerated

* Note: original data in this paper was unavailable, and was reconstructed from plots published as figures.

** Note: Beta value for this study is not included in the average, as x-intercepts indicate the onset of exponential growth prior to conception.

Fig. S3.17 Fetal lung growth cube-root regression models

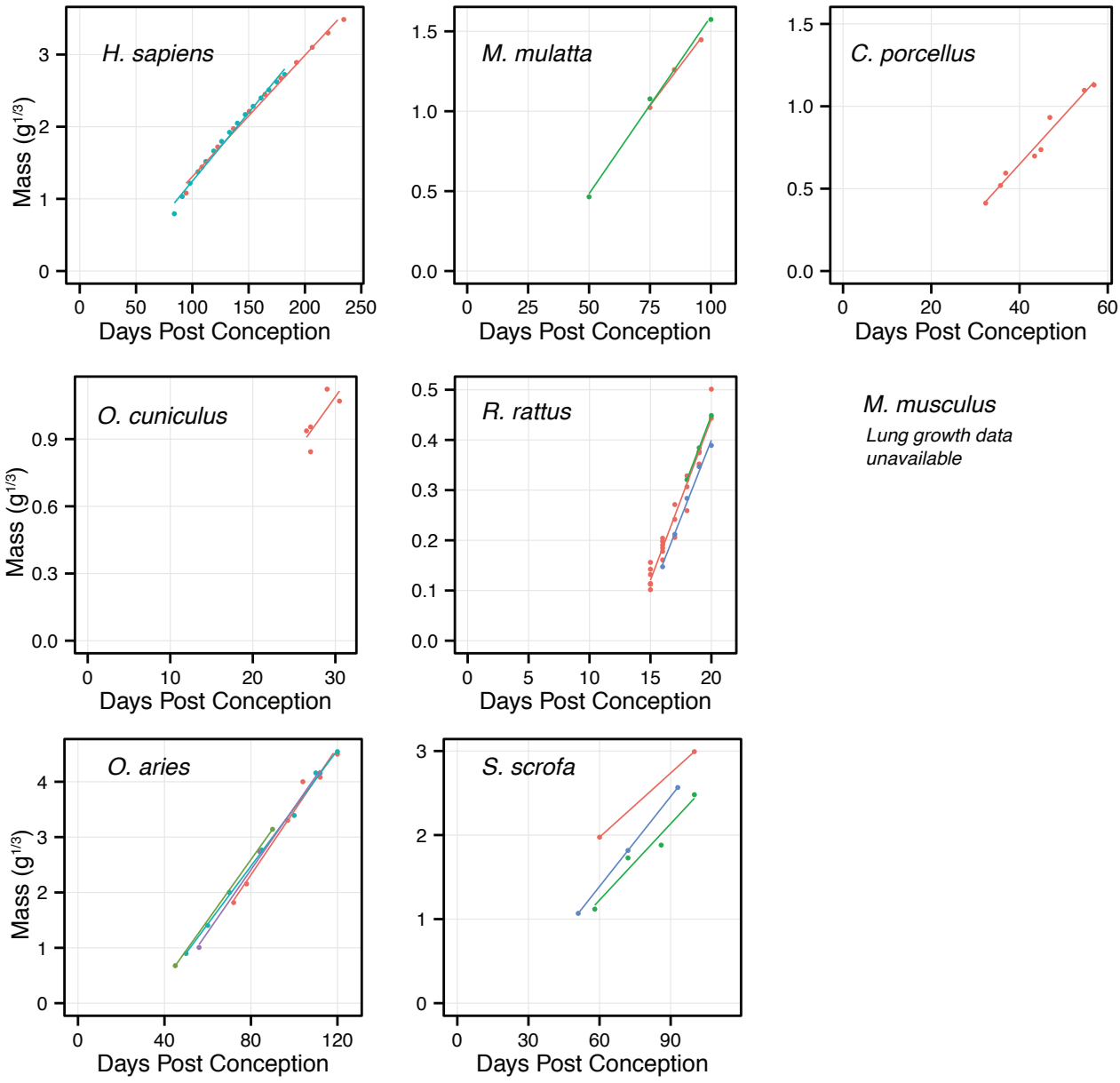

Table S3.9 Fetal lung growth cube root models by source

Species	Source	beta	y-int.	x-int.	r^2
H. sapiens	Guihard-Costa et al., 2002	0.0160	-0.26	16.0	0.99
	Hansen et al., 2003	0.0190	-0.65	34.3	0.99
	Average	**0.0175**	**-0.45**	**25.2**	**N/A**
M. mulatta	Cheek, 1975	0.0169	-0.21	12.6	0.99
	Kerr et al., 1974	0.0189	-0.40	21.4	0.98
	Average	**0.0179**	**-0.56**	**17.0**	**N/A**
C. porcellus	**Pasqualini et al 1976***	**0.0295**	**-0.53**	**18.0**	**0.97**
O. cuniculus	**Composite**[1]	**0.0517**	**-0.46**	**8.9**	**0.62**
R. rattus	Goedbloed, 1976	0.0604	-0.78	12.8	0.96
	Schneidereit, 1985	0.0639	-0.83	13.0	1.00
	Sikov & Thomas, 1970	0.0618	-0.84	13.5	0.99
	Average	**0.0621**	**-0.81**	**13.1**	**N/A**
O. aries	Barcroft, 1946	0.0576	-2.29	39.7	0.98
	Osgerby et al., 2002	0.0548	-1.79	32.6	1.00
	Richardson & Hebert, 1978*	0.0524	-1.71	32.7	1.00
	Wallace, 1945	0.0562	-2.09	37.2	1.00
	Average	**0.0552**	**-1.97**	**35.6**	**N/A**
S. scrofa	Hafez et al., 1958**	0.0255	0.45	-17.6	1.00
	Tumbleson, 1973	0.0303	-0.59	19.5	0.96
	Ullrey et al., 1965	0.0357	-0.75	21.0	1.00
	Average	**0.0330**	**-0.67**	**20.3**	**N/A**

1. Data was combined from Taeusch et al., 1973 and Vidyasagar & Cernick, 1975 to produce this model.

* Note: original data in this paper was unavailable, and was reconstructed from plots published as figures.

** Note: Beta value for this study is not included in the average, as x-intercepts indicate the onset of exponential growth prior to conception.

Fig. S3.18 Fetal kidneys growth cube-root regression models

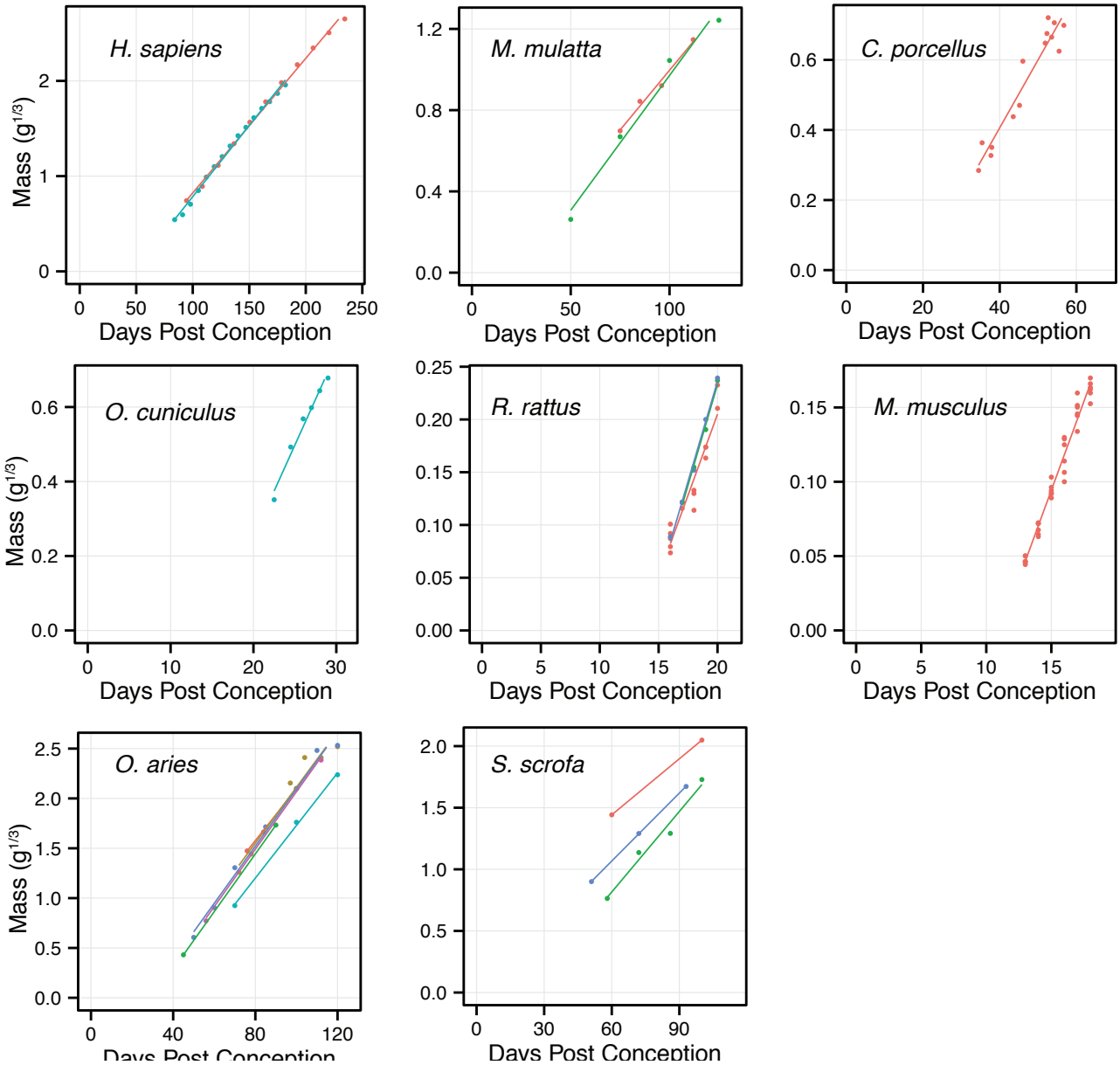

Table S3.10 Fetal kidney growth cube root models by source

Species	Source	beta	y-int.	x-int.	r^2
H. sapiens	Guihard-Costa et al., 2002	0.0133	-0.47	35.4	0.99
	Hansen et al., 2003	0.0150	-0.71	47.5	0.99
	Average	**0.0141**	**-0.59**	**41.5**	**N/A**
M. mulatta	Cheek, 1975	0.0118	-0.18	15.2	0.99
	Kerr et al., 1974	0.0133	-0.36	26.9	0.98
	Average	**0.0125**	**-0.27**	**21.0**	**N/A**
C. porcellus	**Pasqualini et al 1976***	**0.0194**	**-0.37**	**19.0**	**0.92**
O. cuniculus	**Hudson & Hull, 1975**	**0.0493**	**-0.73**	**14.9**	**0.98**
R. rattus	Goedbloed, 1976	0.0307	-0.41	13.3	0.92
	Schneidereit, 1985	0.0382	-0.53	13.9	0.99
	Sikov & Thomas, 1970	0.0379	-0.52	13.8	0.99
	Average	**0.0356**	**-0.49**	**13.7**	**N/A**
M. musculus	**Goedbloed, 1976**	**0.0225**	**-0.24**	**10.7**	**0.97**
O. aries	Bell et al., 1987	0.0259	-0.50	19.1	1.00
	Barcroft, 1946	0.0280	-0.69	24.5	0.94
	Osgerby et al., 2002	0.0289	-0.87	30.1	1.00
	Rattray et al., 1975	0.0264	-0.91	34.5	1.00
	Richardson & Hebert, 1978*	0.0286	-0.77	26.9	0.99
	Wallace, 1945	0.0288	-0.81	28.2	1.00
	Average	**0.0278**	**-0.76**	**27.2**	**N/A**
S. scrofa	Hafez et al., 1958**	0.0152	0.53	-35.1	1.00
	Tumbleson, 1973	0.0218	-0.49	22.6	0.97
	Ullrey et al., 1965	0.0184	-0.04	2.0	1.00
	Average	**0.0201**	**-0.26**	**12.3**	**N/A**

* Note: original data in this paper was unavailable, and was reconstructed from plots published as figures.

** Note: Beta value for this study is not included in the average, as x-intercepts indicate the onset of exponential growth prior to conception.

CHAPTER 4. The embryonic origins of primate encephalization: Allometric and growth analyses of brain and body volume in primate and non-primate embryos.

Abstract

Quantifying differential tissue growth over embryogenesis is necessary to understand how evolution alters developmental programs to generate morphological differences between species. For example, all primates exhibit exceptionally high brain/body proportions across all of fetal development, an allometric difference that begins during embryonic development. This shared alteration to allometric growth is uncorrelated to adult brain size, isocortical proportions, and differences in encephalization between primate radiations, and remains poorly understood despite the fact that encephalization is a defining characteristic of the primate Order. To characterize brain and body growth patterns across embryonic development, 86 whole embryos from diverse primate and non-primate mammalian radiations were digitized using microscopic photography; tissue volumes were reconstructed from area measures over individual slices. Using allometric and exponential models to characterize differential tissue growth, I present preliminary evidence that primate-shared encephalization over fetal development is a consequence of slower prenatal body growth, rather than changes to embryonic brain growth. These findings implicate evolutionary pressures for body size reduction – e.g. as an adaptation to a "fine-branch" arboreal niche – rather than cognitive or behavioral features as the driving force of relative brain size increase at the origin of the primate Order.

Introduction

Encephalization is one of the defining characteristics of the primate Order. On average, primate brains are roughly twice the size we should expect for any given body size; this order-wide degree of encephalization is observed in adults [Von Dongen, 1998], at birth, and across fetal development [Count, 1947; Sacher, 1982; Martin, 1983; Deacon, 1990]. A recent review of prenatal brain/body allometry in twelve primate and sixteen non-primate mammals indicates that primates are already highly encephalized as they transition from embryonic to fetal phases of development [Chapter 2]. This exceptional degree of prenatal encephalization is developmentally and phylogenetically unique, and suggests an "extraordinary evolutionary event" [Sacher, 1982] occurred in one of primates' last common ancestors to increase brain or decrease body size, beginning during embryonic development. However, despite having first been reported nearly seventy years ago [Count, 1947], the developmental origins of primate prenatal encephalization have eluded anatomical characterization or explanation.

While encephalization has frequently been used to describe evolutionary changes to brain size, there are several reasons to suspect that body size changes also play an important role. Phylogenetic analyses indicate that changes to both brain and body size have affected the evolution of encephalization across mammalian radiations [Smaers et al., 2012]. Primates share a suite of adaptations associated with occupying an arboreal niche, such as forward-facing eyes for stereoscopic vision and grasping limbs. Deacon [1990] has argued that postcranial body reduction may have evolved to allow early primates to carry their young or to accommodate arboreal forms of

locomotion. Consistent with primates' slow life histories [Charnov & Berrigan, 1993; Pontzer et al., 2014] and postnatal growth rates [Vinicius, 2005], both human and macaque exhibit exceptionally slow body and visceral organ growth rates during prenatal development when compared with a range of other eutherian mammals [Chapter 3]. By contrast, primate brain growth rates fall within the range of other eutherians. This suggests the possibility that shared primate encephalization across prenatal development reflects decelerated body growth rates beginning in the embryonic period.

However, primates also exhibit relatively large isocortices that deviate from allometric expectations according to brain size [Stephan et al., 1981; Barton & Harvey, 2000]. This grade shift in isocortical proportions is most pronounced in anthropoid primates (which regularly exhibit isocortices 9-10x the size of non-primate mammals with similarly-sized non-isocortical brains) but is also observed in prosimians to a lesser degree. This shared primate "isocorticalization" is a strong candidate for mosaic evolution [Barton & Harvey, 2000], as it deviates from the range of variation proposed under the developmental constraint hypothesis of brain region scaling [Finlay & Darlington, 1995]. This increase in isocortical proportions is an attractive alternative candidate for primate prenatal encephalization, but is complicated by several factors. First, primate isocorticalization comes at the expense of a variety of limbic structures, such as the olfactory cortex, hippocampus, and olfactory bulbs [Finlay & Darlington, 1995; Reep et al., 2007], which are reduced in primates relative to allometric expectations. Reep et al., [2007] have suggested this "push-pull" relationship between the relative size of limbic and isocortical structures in primates may reflect shifting genetic boundaries within the secondary prosencephalon [see Rubenstein et al., 1994; Puelles & Rubenstein, 2003]. Thus, isocortical proportions in primates may not produce any clear shift in prenatal brain/body allometric trajectories, and could instead simply extend the duration of neurodevelopment . This possibility is further advanced by unremarkable brain growth rates in primates relative to other mammals [Chapter 3].

The emergence of primate encephalization during prenatal development has never been characterized due in large part to the difficulty of studying relative growth in very small embryos. However, reconstruction of whole embryo and organ volumes from sectioned tissue by the Cavalieri [1635] method have previously been used to characterize relative and absolute growth in mouse and rat [Goedbloed, 1976] as well as quail and parakeet [Striedter & Charvet, 2008]. This study examines embryonic brain and body growth across the second half of embryonic development (Carnegie Stages 12-23) and in early fetal development across a sample of available primate and non-primate mammalian embryos. Our goal is to provide the first anatomical characterization of how and when primate encephalization emerges during early development.

Allometric vs. growth models. Fetal brain/body growth is approximately linear in log-log coordinates (but see Count, [1947]; Chapter 2), indicating that relative brain size over this period remains constant (isometry) or changes in regular ways (positive or negative allometry). Accordingly, fetal allometric growth can be modeled using linear functions (Chapter 2). However, brain/body proportions during embryonic development fluctuate considerably [Goedbloed, 1976; see below], producing deviations from linearity in log-log plots and changing brain/body proportions over time or developmental stages (Fig. 4.1A). Brain and body growth over time during this period are both exponential; accordingly, deviations from linear allometric growth must be consequences of changes to exponential growth rates in either brain or body.

Increases in allometric proportions (Fig. 4.1A, green dashed lines) may be caused by

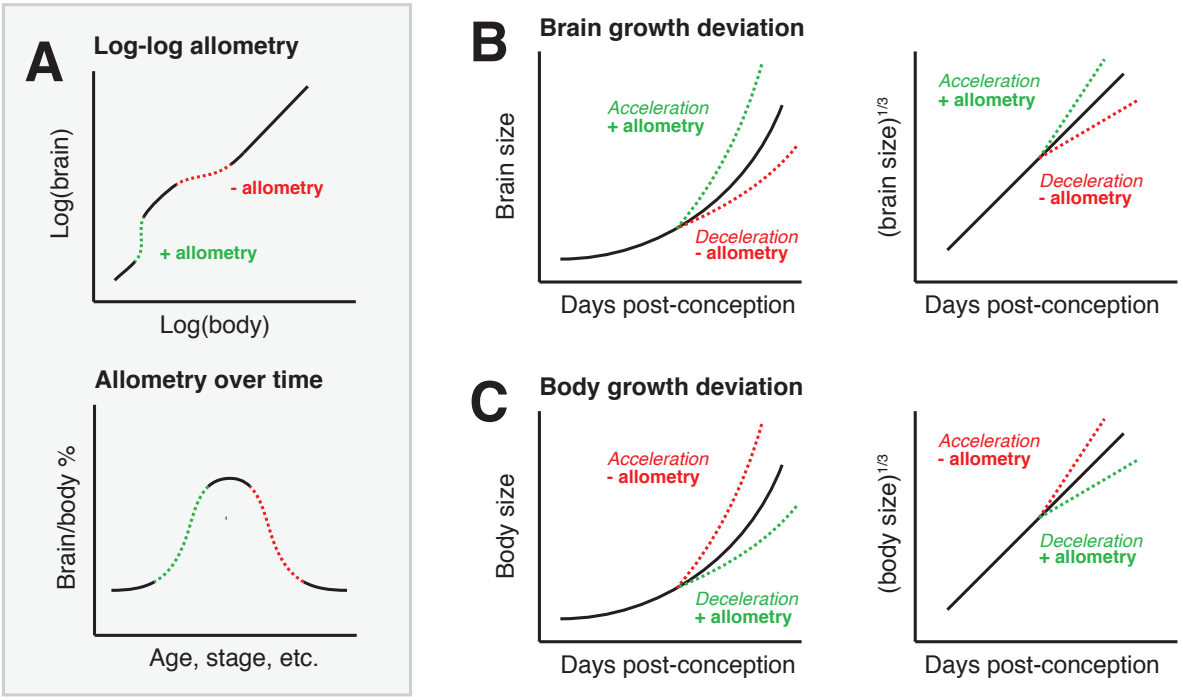

Figure 4.1. Models of brain and body growth over embryonic development, highlighting potential sources of deviation from linear growth in log-log coordinates. (A) Increases in log-log allometric growth (green dashed line) correspond to increases in brain/body proportions over age post-conception or developmental stage (e.g. Carnegie stage). Decreases in log-log allometric growth (red dashed line) correspond to decreases in brain/body proportions. (B, C) Potential changes to exponential brain and body growth, in both mass/time and linearized cube-root mass/time, causing these allometric changes. Increased allometry (green) may be caused by either brain growth acceleration (B) or body growth deceleration (C). Decreased allometry (red) may be caused by either brain growth deceleration (B) or body growth acceleration (C).

either accelerations in the exponential growth of brain tissue (Fig. 4.1B) or by decreases in the exponential growth of the whole embryo (Fig. 4.1C). Correspondingly, decreases in allometric proportions (Fig 4.1A, red dashed lines) may be caused by either decelerations in exponential brain growth (Fig. 4.1B) or by accelerations in exponential growth of the whole embryo (Fig. 4.1C). Because allometric growth plots contain no information about what causes the underlying shift, distinguishing between these possibilities requires additional methods of comparing exponential growth rates across species (e.g. cube-root modeling [Huggett & Widdas, 1951; Chapter 3]).

Materials & Methods

Histology and reconstruction. Data was collected by macro- and microscopic photography of embryos sectioned for histology. Embryological slides were digitized at the American Museum of Natural History, the National Museum for Health and Medicine, the Duke Comparative Embryology Collection (DUCEC), the Kathleen Smith Collection, the Museum für Naturkunde, and the Cornell Embryo Collection. Image sets provided by the Virtual Human Embryo, eMAP project, and the Theunissen lab were also analyzed. Images were acquired at serial intervals along

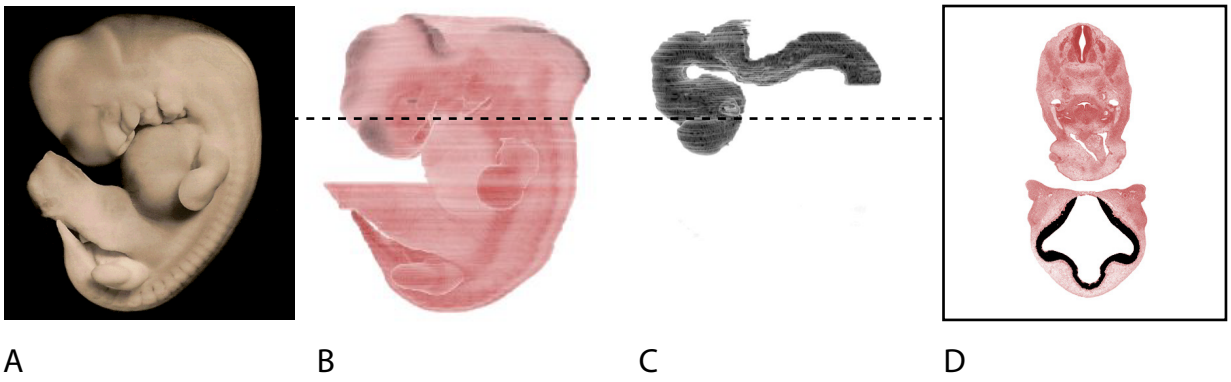

Figure 4.2. Methods for reconstruction of whole embryos from sectioned material prepared for histology. (A) Photograph of a Carnegie Stage 16 human embryo prior to sectioning. (B) Lateral view of the reconstructed 3D embryo produced by stacking 275 individual slices. (C) The embryonic brain isolated via image analysis. (D) A transverse slice with brain tissue marked in black, sampled from the level of the dotted line. Photograph and histology sets taken from the Virtual Human Embryo project.

the axis of dissection for the entire embryo. Acquisition frequency differs by dissection axis, but ranges from 80-350 images per embryo.

Image processing. Processing includes image stitching and isolation of embryonic issue (Photoshop CC), registration of adjacent sections (ImageJ: StackReg), and 3D imaging (ImageJ: 3DViewer). Tissue boundaries were delineated with reference to embryonic atlases and outlined in Photoshop CC (Fig. 4.2). Umbilical tissue was removed by tracing the ventral wall of the torso, retaining visceral organs. Area estimation follows Weibel's [1963] method of using projections and a point-lattice to estimate section area, using pixels instead of a point-lattice.

Volumetric reconstruction. Structure volumes are reconstructed via the Cavalieri method [Cavalieri, 1635], which multiplies sample depth by slice area along the axis of dissection. Variants of this method have been used to study interbrain allometry in adult [Stephan et al., 1981] and embryonic brains [Striedter & Charvet, 2008], as well as whole embryos and embryonic organs [Goedbloed 1976]. Sample depth was calculated by multiplying dissection depth by acquisition frequency. Absolute tissue volume estimates are complicated by the effects of shrinkage in preparation for histology (i.e. fixation and sectioning). Reconstructed volumes were corrected to account for tissue shrinkage using the correction factor in Goedbloed [1976] of 0.40 (the volume ratio of reconstructed to original embryonic tissue). This correction factor is similar to that found in Striedter & Charvet [2008]. Allometric analyses can partially mitigate this effect, though it is likely that fixation affects tissue populations differently. As such, absolute volumes and allometric proportions reported here should be treated with the same caution as previous studies employing these techniques [e.g. Goedbloed, 1967; Stephan et al., 1981; Striedter & Charvet, 2008].

Staging and age estimation. In species for which embryonic staging is available, each embryo was assigned a Carnegie Stage according to a combination of total length, external morphology, and age in days post-conception.

Total sample. A total of 86 embryos were analyzed in this study, and are combined with averaged

data on mouse and rat from Goedbloed [1976]. Embryos were selected to maximize temporal distribution across stages of embryonic development and according to availability in the relevant collections. Primate species include *Homo sapiens* (n=12), *Macaca mulatta* (n=1), *Macaca fascicularis* (n=4), *Presbytis melalophos* (n=1), *Nasalis larvatus* (n=1), *Tarsius* sp. (n=3), *Microcebus myoxinus* (n=12), and *Galagoides demidovii* (n=4). Non-primate species include *Felis catus* (n=8), *Canis familiaris* (n=1), *Equus ferus* (n=1), *Bos taurus* (n=9), *Sus scrofa* (n=5), *Centetes ecandatus* (n=1), *Hemicentetes* sp. (n=3), *Ovis aries* (n=8), and *Tupaia javanica* (n=5).

Growth modeling. The sample of embryos presented here represents the first data of its kind in most of the species considered. However, both allometric and growth models are limited by several constraints of this dataset. First, in species for which only a few embryos are available or in which embryos are not distributed over developmental stages, complete characterization of embryonic growth patterns cannot be fully determined. Second, as few embryos in this collection have a known age post-conception, growth models over time (cf. Fig 4.1B, 4.1C) can only be applied to species for which estimates of embryonic staging vs. age are available. Finally, variation in allometric proportions and total mass are considerable across embryonic stages [Goedbloed, 1976], and in fact were a motivating factor in the development of the Carnegie Staging system [O'Rahilly & Muller, 1987]; the limited embryos in this sample cannot possibly capture this variation, but remain useful to characterize broad growth patterns in the species presented.

In order to facilitate comparisons with fetal allometric growth analyses (Chapter 2), log-log brain/body growth is modeled over embryonic development in the present dataset, with average fetal regression models for primate and non-primate mammals superimposed. However, as whole body size is variable across species relative to embryonic stages [Butler & Juurlink, 1987], relative brain size is also plotted according to embryonic stages; intercept values from fetal models (i.e. predicted relative brain size at 1g body size; Chapter 2) are similarly superimposed. Relative brain size vs. Carnegie Stage for individual species is plotted separately to allow visual inspection of species trends; this analysis is presented only for species in which sample size is sufficient to describe trends over developmental time.

Finally, in order to distinguish between brain and body growth acceleration or deceleration as the cause of allometric shifts (Fig. 4.1), cube-root models of estimated mass over age post-conception is presented in a limited subsample for which reliable age post-conception is available: *Homo sapiens, Mus musculus, Rattus rattus, and Felis catus*. Cube-root regression models are compared using analysis of covariance (ANCOVA) to test for slope differences. This analysis is applied to later phases of embryonic development, during which most non-primate mammals decrease in allometric proportions (a decrease not observed in primates; see below).

Results

Embryonic allometry. Log-transformed brain and body size are presented in Figure 4.3B for both primates (blue) and non-primate mammals (red); later fetal allometric data are shown in Fig. 4.3A for reference (see Chapter 2). In order to examine individual species' transitions across this period, relative brain size over embryonic stages (Carnegie Staging) is shown in Fig. 4.3C (primates) and Fig. 4.3D (non-primates). Ranges of relative brain size over later fetal development (Fig. 4.3A) for primates (P) and non-primates (NP) are shown to the right of both plots to provide context for later fetal growth trends.

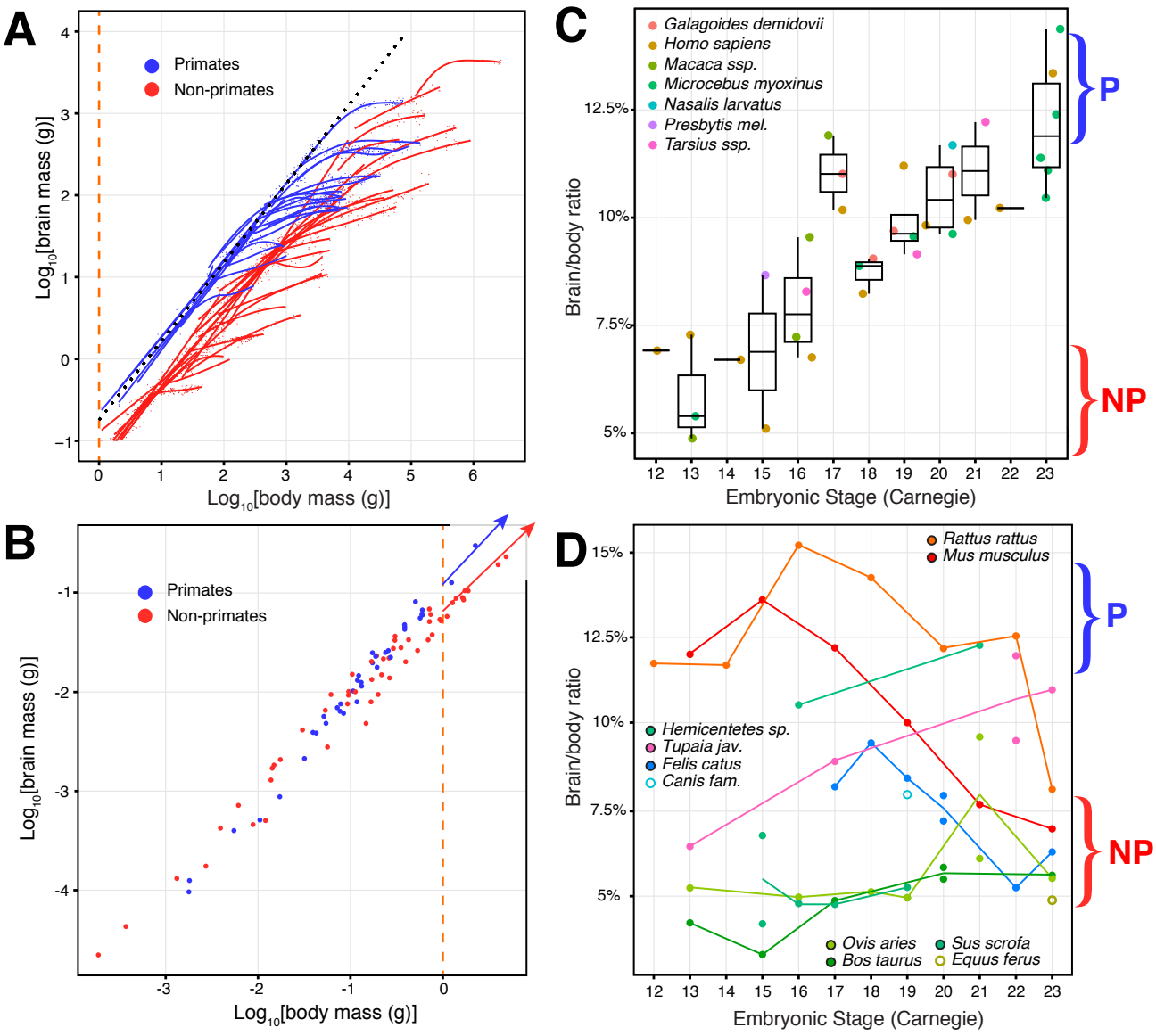

Figure 4.3. Embryonic and fetal brain/body allometric growth. (A) Log-log whole ontogenetic trajectories for primate (blue) and non-primate mammals (red) across fetal and postnatal development. The intercept is shown as a dashed orange line. (B) Log-log brain/body growth of the embryos analyzed in this study. Again, the intercept (1g body size) is shown as a dashed orange line. Average fetal regression models for primates and non-primates are shown in the upper right corner. (C) Relative brain size across Carnegie Stages 12-23 of embryonic development in the primate subsample. Relative brain size increases between CS 15 and CS17 in primates, entering fetal development within the range of values during fetal development [P]. (D) Relative brain size across Carnegie Stages 12-23 of embryonic development in the non-primate subsample. Mouse, rat, tree shrew, tenrec, and cat all exhibit high allometric portions over this period, while values for ungulates (sheep, pig, and ox) remain relatively low. Among the available sample, most species show gradual decreases ending within the range of non-primate fetal values [NP] observed later in development.

Primate relative brain size increases over embryonic development, beginning approximately at Carnegie Stage 16, to reach the ~12-14% proportions that will predominate throughout the rest of fetal development. The timing of this increase coincides with estimates of progenitor proliferation in the telencephalon in both human and macaque (described as the "ballooning" of the telencephalic vesicle [Rakic & Kornack, 2001]). For example, neurodevelopmental event models predict the appearance of the post-proliferative zone of the medial pallium at 42d in human (CS17) and 38d in macaque (CS19), with the onset of cortical neurogenesis beginning shortly thereafter (layer I emergence: 51d in human [CS21], 43d in macaque [CS21])[Workman et al., 2013; Butler & Juurlink, 1987]. This high relative brain size is retained in primates across later fetal development (Chapter 2).

Non-primate mammals exhibit considerably more variability in allometric proportions across embryonic development. Mouse (*Mus musculus*) and rat (*Rattus rattus*)[Goedbloed, 1976] exhibit high allometric proportions across earlier stages of embryogenesis following neurulation (CS8/9); only in later stages do they decrease to enter the non-primate range of fetal proportions. Neurogenic onset is earlier in these species in relation to Carnegie Stages (post-proliferative zone of the medial pallium appears at 11d in mouse [CS13]; 14d in rat [CS14]; [Workman et al., 2013]). Cat (*Felis catus*) also reach a peak relative brain side coinciding with this event (23d [CS18]) but decrease in relative brain size thereafter as neurogenesis commences. Tree shrew (*Tupaia*) and tenrec (*Hemicentetes*) also exhibit relatively high proportions over later embryonic development; measures in ungulates remain low throughout the embryonic period. Full characterization of allometric growth in several of these species is limited by data availability. Most non-primate species exit embryonic development within the range of relative brain size observed across fetal development in all non-primate mammals.

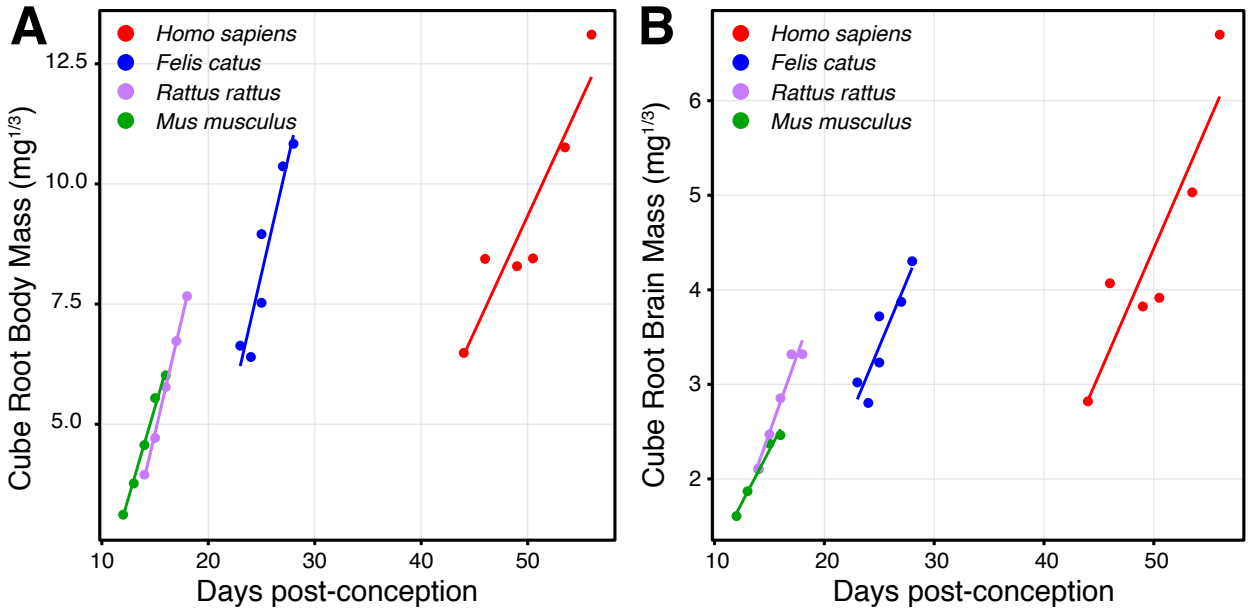

Figure 4.4. Cube root models of brain and body growth over later stages of embryonic development. This subsample of embryos traces the period of time when allometric proportions decrease in mouse, rat, and cat while remaining fairly constant in human. (A) Body mass slope in human is approximately half that of cat, mouse, or rat over this period. (B) Brain mass slope is relatively constant across all four species.

In the broadest terms, this analysis demonstrates that primates are not unique in attaining high relative brain size over embryonic development; however, primates alone retain this high brain/body proportion into fetal development, while most non-primate species exhibit a sharp decrease in relative brain size over the later stages of embryogenesis.

Cube root modeling of brain and body growth. Cube root models of brain and body size over days post-conception are shown in Fig. 4.4. The human body coefficient (0.421) is lower that of cat (0.962), mouse (0.755), and rat (0.945); in ANCOVA tests, the difference between human and cat reaches the level of significance ($p= 0.032$), but not mouse ($p= 0.092$) or rat ($p= 0.063$). By contrast, the human brain coefficient (0.225) is lower to those of cat (0.278) and rat (0.326), and slightly higher than mouse (0.209); no test reaches significance, and p values for the interaction terms are considerably higher (cat, $p=0.689$; mouse, $p=0.896$; rat, $p= 0.564$).

Discussion

This paper presents the first allometric brain/body data during embryonic development in a comparative dataset of primate and non-primate mammals. As previously reported for mouse and rat [Goedbloed, 1976], allometric proportions over embryonic development deviate from the approximately linear trends observed over later fetal development [i.e. the "rapid growth phase"; Renfree et al., 1982]. These deviations are distributed over different body masses and embryonic stages in different species, reflecting differences in embryo sizes at similar developmental events [Butler & Juurlink, 1987] and differences in neurodevelopment vs. embryonic stages, which largely track postcranial somatic morphology.

Origins of primate prenatal encephalization. Primates are not unique in achieving high brain/body proportions during embryonic development – unambiguously high proportions are also observed in mouse, rat, cat, tree shrew, and tenrec specimens over this period (Fig. 4.3D). However, primates alone retain these high proportions into fetal development, producing relatively large brains (~12% [Sacher, 1982]) for the remainder of the "rapid growth phase" [Renfree et al., 1982] of fetal development (Fig 4.3C). Allometric decreases in later stages of embryonic development are clearly shown in mouse, rat, and cat; while tree shrew embryos in this study suggest a similar growth trajectory to primates, their conformity with non-primate trends at birth (Chapter 2) suggest they also decrease in allometric proportions in a manner common to other non-primate mammals.

Cube root models of brain and body growth over age post-conception (Fig. 4.4) applied to later embryonic stages – those periods when allometric proportions decrease in non-primates but remain high in primates – suggest that slow somatic growth accounts for primates' retention of high brain/body proportions in later embryonic and subsequent fetal development. Human body growth acceleration over this period (measured from cube-root slope; see Chapter 3) is much lower than mouse, rat, or cat, while brain growth coefficients largely overlap. While ANCOVA tests of this trend produce ambiguous results due to the limited sample sizes in this study, body slope differences produce p-values below 0.10, while difference in brain growth slopes are far from significant (all p-values >0.5). This is consistent with the slow primate fetal growth rates observed in later fetal stages of development, and with the relative constancy of eutherian brain growth rates (Chapter 3).

It remains possible that changes to brain growth rates during embryonic development play an important role in changing allometric proportions. The most clear evidence for this comes from Goedbloed's [1976] analysis of rat and mouse growth, which shows decelerated brain growth around the onset of neurogenesis from progenitor pools (Fig. S3.3). This effect can only be detected in datasets larger than those examined here. Larger samples of embryos of known age post-conception will be needed to test if similar alterations to brain growth rates accompany the onset of neurogenesis in other species, and whether primates deviate meaningfully patterns of non-primate mammalian brain growth rates.

Limitations and future directions. Embryos analyzed in this study were selected to maximize the number of species represented, as well as their distribution over developmental time (i.e. Carnegie Stages). This emphasis requires a trade-off wherein most stages are represented by only one embryo in a given species, making it difficult to capture variability within species at any given stage, and severely limiting the interpretation of growth models (e.g. cube-root models). Embryo digitization and analysis was also limited to specimens that are available in the collections and museums studied. Finally, assigning ages post-conception to embryos for which this information is unavailable – a necessary step in growth modeling – is only possible in species for which embryonic staging systems have been developed.

Systems of embryonic staging (e.g. the Carnegie system) attempt to classify embryos according to major events common to embryogenesis in diverse species, such as gastrulation and neurulation. This is an essential contribution to comparative embryology, as species differ in both absolute size and age post-conception at which these major events take place [Butler & Juurlink, 1987]. However, staging necessarily overlooks important differences in the growth and development of individual organs and tissues that are central to the emergence of phenotypes later in ontogeny (i.e. heterochrony [Gould, 1977]) by assigning a stage to the whole embryo. Recent work on neurodevelopmental event modeling [Workman et al., 2013] is a good example of how comparative ontogeny might be better understood according to the development of individual organs. Additional work of this type should help to clarify how differential tissue growth and development generate adult phenotypes.

Future research will focus on collecting and analyzing additional embryos in such as way as to overcome these limitations. Increasing the number of embryos within species at given stages will help to characterize the variability in growth patterns that has been well documented in more comprehensive studies of mouse and rat [Goedbloed, 1976]. Similarly, expanding the representation of embryos across stages of development and diverse species will be necessary to examine the emergence of species-unique patterns of growth. While this study has focused on gross brain/body proportions in order to study the emergence of primate encephalization, the datasets collected will be useful to studying early visceral organ growth patterns, as well as the early parcellation of embryonic brain vesicles and their derivatives.

Conclusions

Shared primate encephalization over prenatal development emerges during later stages of embryogenesis. The data presented here suggests this novel feature of primate allometric growth – generating highly encephalized neonates and adults later in ontogeny – is a consequence of slow somatic growth beginning in later stages of embryonic development. Over comparable periods of

development, non-primate mammals exhibit faster somatic growth rates, but similar brain growth rates.

This study provides developmental evidence that the increase in relative brain size at the origin of the primate Order may have resulted from evolutionary pressure to decrease body size, rather than increase brain size [Sacher, 1982; Deacon, 1990]. This is consistent with primates' slow life histories and the relative constancy of exponential brain growth rates irrespective of absolute size or isocortical proportions (Chapter 3). This implies that increased relative brain size shared among primates may have evolved as an adaptation to arboreal locomotion, such as the navigation of a "fine-branch niche" [Cartmill, 1972], rather than as a consequence of selective pressure for improved cognitive or behavioral features.

References

Barton RA, Harvey PH (2000): Mosaic evolution of brain structure in mammals. Nature 405:1055–1058.

Butler H, Juurlink BHJ (1987): An Atlas for Staging Mammalian and Chick Embryos. Boca Raton, CRC Press.

Cartmill M (1972): Arboreal adaptations and the origin of the order Primates. In Tuttle R (ed): The Functional and Evolutionary Biology of Primates. Chicago, Adeline, pp 97–122.

Cavalieri B. 1635. Geometria Indivisibilius Continuorum. Typis Clementis Bonoiae. Reprinted in 1966 as Geometris degli Indivisibili. Torino Union Tipografico-Editrice, Torinese.

Charnov EL, Berrigan D (1993): Why do female primates have such long lifespans and so few babies? or Life in the slow lane. Evol Anthrol 1:191–194.

Count EW (1947): Brain and body weight in man: their antecedents in growth and evolution. Ann N Y Acad Sci 46:993–1122.

Deacon TW (1990): Problems of ontogeny and phylogeny in brain-size evolution. Int J Primatol 11:237–282.

Finlay BL, Darlington RB (1995): Linked regularities in the development and evolution of mammalian brains. Science 268:1578–1584.

Goedbloed JF (1976): Embryonic and postnatal growth of rat and mouse. IV. Prenatal growth of organs and tissues: age determination, and general growth pattern. Acta Anat 95:8–33.

Gould SJ (1977): Ontogeny and Phylogeny. Cambridge, Harvard University Press.

Huggett AG, Widdas WF (1951): The relationship between mammalian foetal weight and conception age. J Physiol 114:306–317.

Martin RD (1983): Human Brain Evolution in an Ecological Context. New York, American Museum of Natural History.

O'Rahilly RR, Müller F (2006): The Embryonic Human Brain: An Atlas Of Developmental Stages. Hoboken, Wiley.

Pontzer H, Raichlen DA, Gordon AD, Schroepfer-Walker KK. Hare B, O'Neill MC, Muldoon KM, Dunsworth HM, Wood BM, Isler K, Burkart J, Irwin M, Schumaker RW, Lonsdorf EV, Ross SR (2014): Primate energy expenditure and life history. Proc Natl Acad Sci USA 111:1433–1437.

Puelles L, Rubenstein LR (2003): Forebrain gene expression domains and the evolving prosomeric model. Trends Neurosci 26: 469–476.

Rakic R, Kornack DR (2001): Neocortical expansion and elaboration during primate evolution: A view from neuroembryology. In Falk D, Gibson DR (eds.): Evolutionary Anatomy of the Primate Cerebral Cortex. Cambridge, Cambridge University Press, pp 30–56.

Reep RL, Finlay BL, Darlington RB (2007): The limbic system in mammalian evolution. Brain Behav Evol 70:57–70.

Renfree MB, Holt AB, Green SW, Carr JP, Cheek DB (1982): Ontogeny of the brain in a marsupial (Macropus eugenii) throughout pouch life. Brain Behav Evol 20:57–71.

Sacher GA (1982): The role of brain maturation in the evolution of the primates; in Armstrong E, Falk D (eds): Primate Brain Evolution. New York, Springer, pp 97–112.

Smaers JB, Dechmann DKN, Goswami A, Soligo C, Safi K (2012): Comparative analyses of evolutionary rates reveal different pathways to encephalization in bats, carnivorans, and primates. Proc Natl Acad Sci USA 109:18006–18011.

Stephan H, Frahm H, Baron G (1981): New and revised data on volumes of brain structures in insectivores and primates. Folia Primatol 35:1–29.

Striedter GF (2005): Principles of Brain Evolution. Sunderland, Sinauer Associates.

Striedter GF, Charvet CJ (2008): Developmental origins of species differences in telencephalon and tectum size: morphometric comparisons between a parakeet (Melopsittacus undulates) and a quail (Colinus virgianus). J Comp Neurol 507:1663–1675.

van Dongen P (1998): Brain size in vertebrates; in Nieuwenhuys R, ten Donkelaar HJ, Nicholson C (eds): The Central Nervous System of Vertebrates. New York, Springer, pp 2099–2131.

Vinicius L (2005): Human encephalization and developmental timing. J Hum Evol 49:762–776.

Weibel, EW (1963): Morphometry of the Human Lung. Berlin, Springer-Verlag.

Workman AD, Charvet CJ, Clancy B, Darlington RB, Finlay BL (2013): Modeling transformations of neurodevelopmental sequences across mammalian species. J Neurosci 33:7368–7383.

CHAPTER 5. Concluding Remarks

Despite differences in adult encephalization between primate radiations, all primates share a uniquely high degree of encephalization across fetal development (Chapter 2). Primate prenatal encephalization can be traced back to early embryonic development, as shown by the increased intercept in primate rapid growth phase regression models relative to other mammalian species. Primates also exhibit relatively high allometric slopes across fetal development (approximately isometric), while most non-primate mammals exhibit negative allometry (with several exceptions; Chapter 2). Anthropoid primates overlap in allometric growth patterns over fetal development, and are unrelated to either grade shifts in encephalization or whole brain size. Neonatal data indicates that prosimians share this high fetal allometric proportion with other primate radiations; limited data in tree shrews indicate they follow the lower trend of non-primate mammals. Other highly encephalized species (e.g. dolphins) conform to the non-primate trend as well, suggesting a novel alteration to embryonic development unique to the primate Order, and responsible for their shared encephalization patterns relative to glires.

Several lines of evidence suggest that changes to body growth are responsible for this primate-shared shift. Fetal brain growth acceleration is not exceptional in primates, but body growth is decelerated [Sacher & Staffeldt, 1974; Chapter 3]; as such, primates' high fetal allometric slopes are likely a consequence of exceptionally slow fetal body growth (Chapter 2, 3). While primates exhibit a shared increase in isocortical proportions over "insectivores" [Stephan et al., 1981; Barton & Harvey, 2000], anthropoid neonatal values overlap with those of prosimians along the primate-shared regression line, suggesting that isocortical proportions do not selectively increase the allometric intercept. Finally, evidence from embryonic allometry and growth modeling suggests that during late embryonic development, primates alone retain high brain/body proportions – a period of time during which body growth acceleration is already lower than that of rat, mouse, and cat (Chapter 4).

Theories that fetal brain growth is constrained by resource availability via physiological variables, such as maternal metabolism [Martin, 1981] or placental morphology [Elliot & Crespi, 2008], are not supported by the data presented here. Regular differences in birth timing relative to allometric (Chapter 2) and sigmoid brain growth plots (Chapter 3) are described, and help account for the observed variation in neonatal brain size across mammals [Sacher & Staffeldt, 1974]. However, the surprisingly low amount of variation observed in brain growth acceleration relative to other organs among eutherian mammals (Chapter 3) could suggest a preferential allocation of resources to neurodevelopment over other organs. Additional research into embryonic organ allometry will be necessary to clarify how evolution alters early growth patterns to generate diverse morphological phenotypes later in mammalian ontogeny.

References

Barton RA, Harvey PH (2000): Mosaic evolution of brain structure in mammals. Nature 405:1055–1058.

Elliot MG, Crespi BJ (2008): Placental invasiveness and brain-body allometry in eutherian mammals. J Evol Biol 21:1763–1778.

Martin RD (1981): Relative brain size and basal metabolic rate in terrestrial vertebrates. Nature 293:57–60.

Sacher GA, Staffeldt EF (1974): Relation of gestation time to brain weight for placental mammals: Implications for the theory of vertebrate growth. Am Nat 108:593–615.

Stephan H, Frahm H, Baron G (1981): New and revised data on volumes of brain structures in insectivores and primates. Folia Primatol 35:1–29.